Archive

OPERATIONAL ISSUES INVOLVING USE OF SUPPLEMENTARY COOLING TOWERS TO MEET STREAM TEMPERATURE STANDARDS WITH APPLICATION TO THE BROWNS FERRY NUCLEAR PLANT

by

Keith D. Stolzenbach, Stuart A. Freudberg
Peter Ostrowski and John A. Rhodes

Energy Laboratory Report No. MIT-EL 79-036
January 1979

COO-4114-7

OPERATIONAL ISSUES INVOLVING USE OF SUPPLEMENTARY COOLING TOWERS TO MEET STREAM TEMPERATURE STANDARDS WITH APPLICATION TO THE BROWNS FERRY NUCLEAR PLANT

by

Keith D. Stolzenbach

Stuart A. Freudberg

Peter Ostrowski

and

John A. Rhodes

Energy Laboratory
and
Ralph M. Parsons Laboratory
for
Water Resources and Hydrodynamics
Department of Civil Engineering

Massachusetts Institute of Technology
Cambridge, Massachusetts 02139

Prepared under the support of
Environmental Control Technology Division
Office of the Assistant Secretary for Environment
U.S. Department of Energy

Contract No. EY-76-S-02-4114.A001

Energy Laboratory Report No. MIT-EL 79-036

January 1979

ABSTRACT

A mixed mode cooling system is one which operates in either the open, closed, or helper (once-through but with the use of the cooling towers) modes. Such systems may be particularly economical where the need for supplementary cooling to meet environmental constraints on induced water temperature changes is seasonal or dependent upon other transient factors such as streamflow. The issues involved in the use of mixed mode systems include the design of the open cycle and closed cycle portions of the cooling system, the specification of the environmental standard to be met, and the monitoring system and associated decision rules used to determine when mode changes are necessary. These issues have been examined in the context of a case study of TVA's Browns Ferry Nuclear Plant which utilizes the large quantity of site specific data reflecting conditions both with and without plant operation. The most important findings of this study are: (1) The natural temperature differences in the Tennessee River are of the same order of magnitude (5°F) as the maximum allowed induced temperature increase. (2) Predictive estimates based on local hydrological and meteorological data are capable of accounting for 40% of the observed natural variability. (3) Available algorithms for plant induced temperature increases provide estimates within 1°F of observed values except during periods of strong stratification. (4) A mixed mode system experiences only 10% of the capacity losses experienced by a totally closed system. (5) The capacity loss is relatively more sensitive to the environmental standard than to changes in cooling system design. (6) About one third of the capacity loss incurred using the mixed mode system is the result of natural temperature variations. This unnecessary loss may be halved by the use of predictive estimates for natural temperature differences.

ACKNOWLEDGMENTS

This report is part of an interdisciplinary effort by the MIT Energy Laboratory to examine issues of power plant cooling system design and operation under environmental constraints. The effort has involved participation by researchers in the R.M. Parsons Laboratory for Water Resources and Hydrodynamics of the Civil Engineering Department and the Heat Transfer Laboratory of the Mechanical Engineering Department. Financial support for this research effort has been provided by the Division of Environmental Control Technology, U.S. Dept. of Energy, under Contract No. EY-76-S-02-4114.A001. The assistance of Dr. William Mott, Dr. Myron Gottlieb and Mr. Charles Grua of DOE/ECT is gratefully acknowledged.

Reports published under this sponsorship include:

"Computer Optimization of Dry and Wet/Dry Cooling Tower Systems for Large Fossil and Nuclear Plants," by Choi, M., and Glicksman, L.R., MIT Energy Laboratory Report No. MIT-EL 79-034, February 1979.

"Computer Optimization of the MIT Advanced Wet/Dry Cooling Tower Concept for Power Plants," by Choi, M., and Glicksman, L.R., MIT Energy Laboratory Report No. MIT-EL 79-035, September 1979.

"Operational Issues Involving Use of Supplementary Cooling Towers to Meet Stream Temperature Standards with Application to the Browns Ferry Nuclear Plant," by Stolzenbach, K.D., Freudberg, S.A., Ostrowski, P., and Rhodes, J.A., MIT Energy Laboratory Report No. MIT-EL 79-036, January 1979.

"An Environmental and Economic Comparison of Cooling System Designs for Steam-Electric Power Plants," by Najjar, K.F., Shaw, J.J., Adams, E.E., Jirka, G.H., and Harleman, D.R.F., MIT Energy Laboratory Report No. MIT-EL 79-037, January 1979.

"Economic Implications of Open versus Closed Cycle Cooling for New Steam-Electric Power Plants: A National and Regional Survey," by Shaw, J.J., Adams, E.E., Barbera, R.J., Arntzen, B.C., and Harleman, D.R.F., MIT Energy Laboratory Report No. MIT-EL 79-038, September 1979.

"Mathematical Predictive Models for Cooling Ponds and Lakes," Part B: User's Manual and Applications of MITEMP by Octavio, K.H., Watanabe, M., Adams, E.E., Jirka, G.H., Helfrich, K.R., and Harleman, D.R.F.; and Part C: A Transient Analytical Model for Shallow Cooling Ponds, by Adams, E.E., and Koussis, A., MIT Energy Laboratory Report No. MIT-EL 79-039, December 1979.

"Summary Report of Waste Heat Management in the Electric Power Industry: Issues of Energy Conservation and Station Operation under Environmental Constraints," by Adams, E.E., and Harleman, D.R.F., MIT Energy Laboratory Report No. MIT-EL 79-040, December 1979.

Site specific data collected at the Browns Ferry Nuclear Plant site was provided by the Water Systems Development Branch, Division of Water Management, of the Tennessee Valley Authority. The study would not have been possible without the cooperation of Mr. Ely Driver, Dr. William Waldrop, Mr. Christopher Ungate, and Mr. Charles W. Almquist of TVA.

TABLE OF CONTENTS

OPERATIONAL ISSUES INVOLVING USE OF SUPPLEMENTARY COOLING TOWERS TO MEET STREAM TEMPERATURE STANDARDS WITH APPLICATION TO THE BROWNS FERRY NUCLEAR PLANT

I. Introduction

The basic motivation for this study has been the need to assess the energy consumption consequences of environmental regulations applied to waste heat discharges from steam electric power plants. This report describes the results of an investigation focussing solely on the operation of mixed mode systems e.g. the real time choice of supplementary cooling mode (open, helper, or closed) to be used to meet a given constraint on induced temperatures in the receiving water body.

The investigation of mixed mode operation has been conducted in the context of a case study involving TVA's Browns Ferry Nuclear Plant. The use of a specific example has provided the opportunity to produce quantitative results associated with actual combinations of environmental and plant design parameters. However, it should be noted that in performing this study it was both necessary and advisable to make a number of assumptions which are not based on actual conditions at Browns Ferry. Accordingly, the results of this investigation are in no way intended to represent past or future actual operation of the Browns Ferry Nuclear Plant by the Tennessee Valley Authority.

The remainder of the report is divided into five sections.

First, the most important general details of the case study problem are outlined, e.g., the characteristics of the Browns Ferry Plant site and design and the associated environmental constraints on waste heat discharges. Following this section, a semi-empirical model for predicting natural temperature differences is presented. The next section describes a model for simulating the river temperature changes due to natural and plant induced causes, for selecting the necessary plant cooling mode, and for calculating the associated energy consumption by the plant. The simulation model is then used to compare a year of plant operation as a function of the following:

- choice of temperature monitor location
- spatial and temporal averaging of temperature monitor values
- correction of monitor values for computed natural temperature differences
- changes in environmental standard
- changes in plant design

The results of this sensitivity study are presented in terms of plant output as a function of time and in terms of total energy requirements. Finally, the plant simulation model and the natural temperature difference model are applied to a year during which the Browns Ferry Nuclear Plant has been operating. This application provided a direct evaluation of the validity of the simulation model results.

The most important findings of this study are the following:

1. The Tennessee River in the vicinity of the Browns Ferry Nuclear Plant (Wheeler Reservoir) exhibits significant variability in water temperature over a wide range of space and time scales.

The difference between temperatures measured upstream and downstream from the plant during a pre-operational period are the same order of magnitude (5°F) as the maximum induced temperature increase permitted by the regulatory standard.

2. A predictive model for the upstream - downstream natural temperature differences is capable of accounting for 40% of the observed variability. This estimate, which is based upon local hydrological and meteorological data, primarily addresses the temperature changes occurring over periods of days to months rather than diurnal variations which are found to be quite random in nature.

3. The plant simulation model provided a good estimate of the induced river temperature rise (within 1°F) except for periods when the upstream temperature monitors were affected by seasonal stratifications not accounted for in the natural temperature model which was used to isolate the plant induced effect from the naturally occurring temperature differences.

4. The simulation study of capacity losses resulting from the necessity to use cooling towers to meet the specified environmental temperature standard indicates the following:

   (a) A mixed mode cooling system experiences only 10% of the capacity losses experienced by a totally closed system.

   (b) The capacity loss is sensitive to the specified limit on induced temperature increases. A decrease in the allowable river temperature increase from 5°F to 3°F produced a 300% increase in lost capacity. Compared to the influence of

environmental standard, changes in plant design, such as cooling tower size or open cycle diffuser mixing, have significantly less influence on plant capacity losses.

(c) About one third of the capacity loss incurred using a mixed mode system is the result of natural temperature variations that are interpreted as plant induced effects by the monitoring system. This unnecessary loss may be cut in half by the use of the predictive model for natural temperature variations. Further reduction may be obtained by spatial and temporal averaging of temperature monitor measurements.

II. Description of the Browns Ferry Nuclear Power Station Case Study

The Browns Ferry Nuclear Power Station consists of three identical General Electric Co. Boiling Water Reactors (BWR), each with a nameplate rating of 1152 megawatts electric (MWe), and a net rating of 1067 MWe. The station is located on an 840 acre site in Limestone County in northern Alabama on the north bank of the Wheeler Reservoir at Tennessee River Mile 294 (TRM 294). This is approximately 10 miles northwest of Decatur, Alabama and 10 miles southwest of Athens, Alabama. (See Fig. 2.1).

2.1 Wheeler Reservoir

Wheeler Reservoir, along which Browns Ferry is located, was constructed by TVA for electric power generation, flood control and navigation, sport and commercial fishing, industrial water supply, and public water supply. The hydraulic regime of Wheeler Reservoir is controlled by the operation of 2 dams: Guntersville, located upstream of Browns Ferry at TRM 349, and Wheeler, located downstream of Browns Ferry at TRM 274.9. These dams, constructed in the 1930's are operated primarily for hydroelectric power production and secondarily for flood control. The long term average flow at Wheeler Dam is 49,000 cfs; its drainage area is 29,590 sq. miles, and it was designed to generate 356.4 MWe. Upstream at Guntersville Dam, the long term average flow is about 40,000 cfs, the drainage area is 24,250 sq. mi. and the hydrostation there is capable of generating 97.2 MWe. The elevation in the predominantly flat pool portion of Wheeler Reservoir is normally 556.3 ft., although this varies by several feet throughout the year, as a

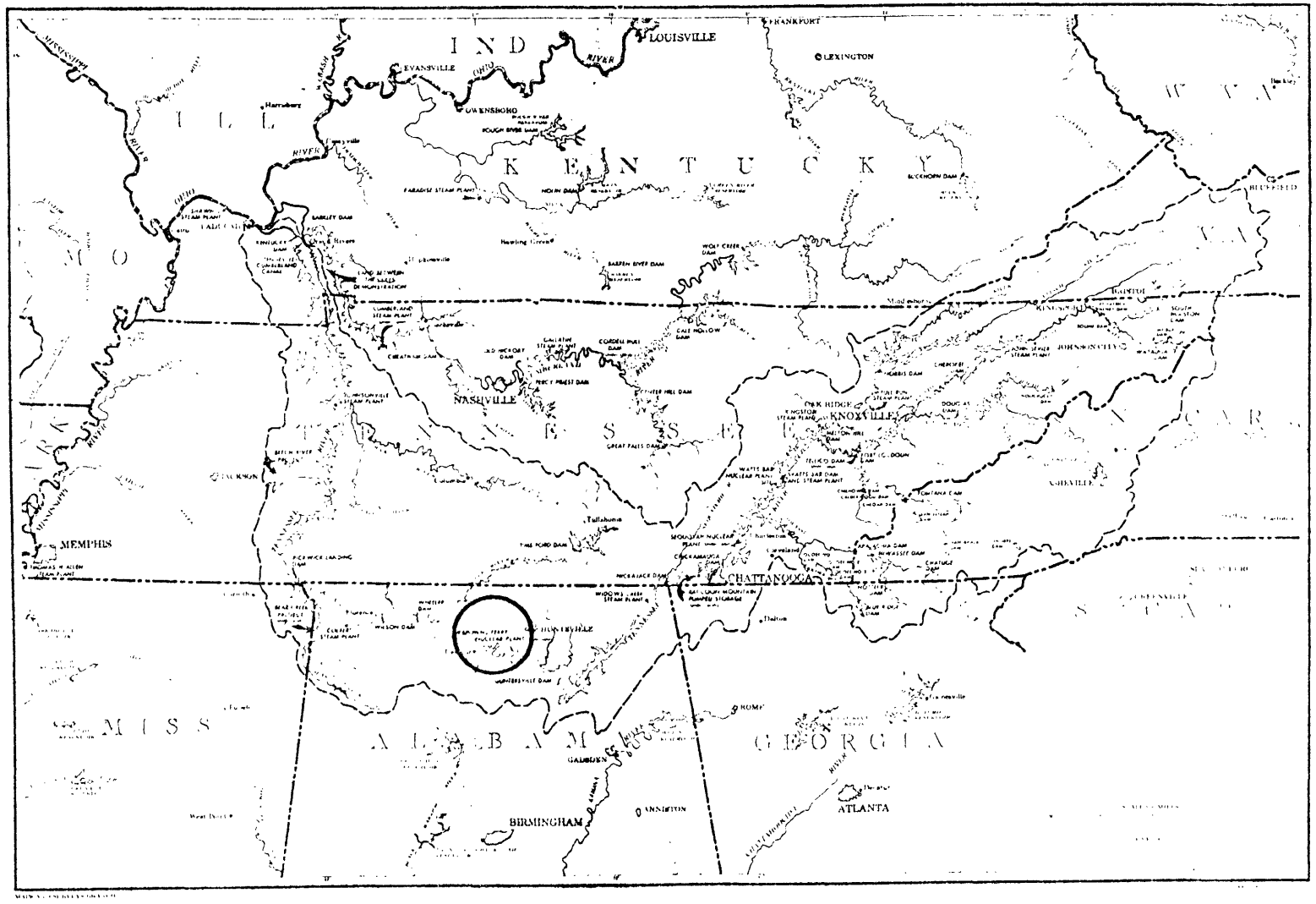

Figure 2.1 Map Showing Location of Browns Ferry Nuclear Plant Station

function of flood control and power production constraints.

2.2 The Cooling System

Browns Ferry Station was originally designed to operate in an "open-cycle" cooling mode, pumping cooling water from the Tennessee River through the condensers at a rate of 4410 cubic feet per second (cfs) for all three units, and then returning it back to the river at an elevated temperature. The temperature of the discharge from the condensers is approximately 25° hotter than the river intake temperature, which corresponds to a net heat rejection rate (for all three units) of 2.467×10^{10} BTU/hr, and thus a plant efficiency of about 30.7%. The discharge in open mode is passed through a submerged multiport diffuser system which consists of three perforated, corrugated galvanized steel pipes laid in parallel across the bottom of the main river channel a short distance downstream from the plant (see Fig. 2.2). The operation of the diffuser has been studied extensively (Harleman, 1968); its main purpose is to facilitate better mixing of the plant's thermal discharge with the river.

The Tennessee River cross-section at this point (TRM 294) consists of navigation channels dredged to a 30-foot depth and approximately 1800 feet laterally across, which is bordered by shallow overbank areas that vary from 2 to 10 feet in depth and 2000 to 6000 feet in width. Although the main channel at this point contains only 1/3 of the total river width, through it passes approximately 65% of the flow (AEC, 1971).

Due to the implementation of the more stringent Alabama water temperature standards, TVA decided in 1971 to spend $59,000,000 and

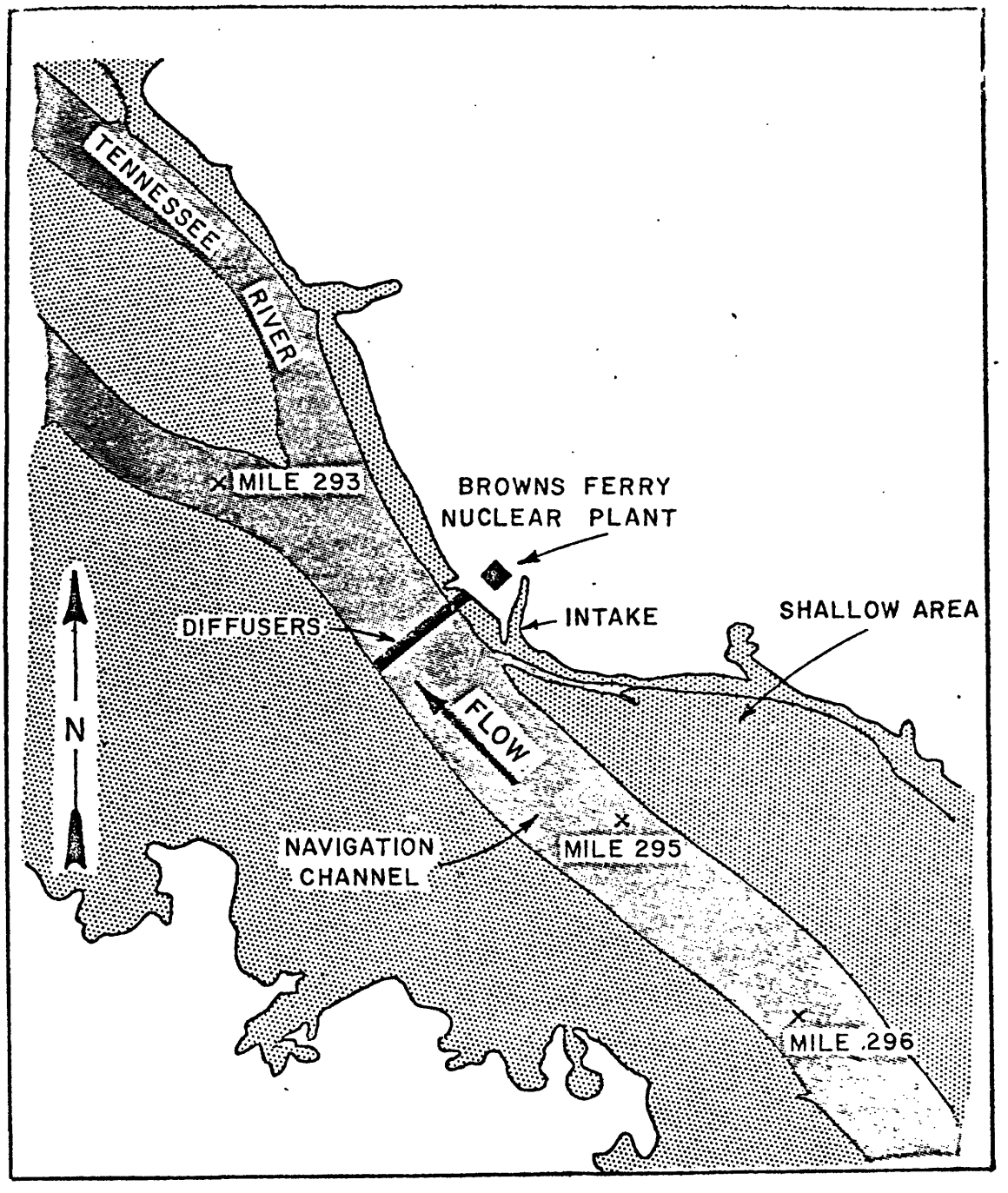

Figure 2.2 Location of Diffuser In Tennessee River
Near Browns Ferry Nuclear Plant Station

construct 6 mechanical draft cooling towers. To increase their versatility, the cooling towers were designed to operate in two modes: "helper-mode" and "closed-cycle mode." In the helper mode, condenser cooling water passes through the towers, is cooled down to within several degrees fahrenheit of the wet bulb temperature, and returned to the river. The discharge rate for helper mode is 3675 cfs. As a general rule, the discharge temperature using helper mode is less than that of open mode, although this may not be the case during times of high wet bulb temperature. In closed-cycle mode, only 110 cfs are released to the river - the so-called "blowdown" - and the remainder of the flow is circulated through the cooling towers and then back into the intake channel. Makeup water needed for the unit due to evaporative losses in this mode is approximately 220 cfs. The option of three cooling modes (open, helper, and closed-cycle) make the cooling system at Browns Ferry unique among power stations. A schematic of the condenser cooling modes is given in Fig. 2.3.

2.3 Temperature Data Collected in Wheeler Reservoir

Because of the presence of the Browns Ferry Station, extensive water temperature records have been collected documenting conditions in Wheeler Reservoir since 1968. At present, there are 12 stations located along the river at which temperature data is collected at least every hour. In addition the temperature is measured at Guntersville and Wheeler Dams. The location of the sampling stations is depicted in Fig. 2.4. At the monitors closest to Browns Ferry (these are labelled Station 1, 9, 10 and 11) and at the furthest upstream monitor (Station 6), temperature data is collected every 15 minutes.

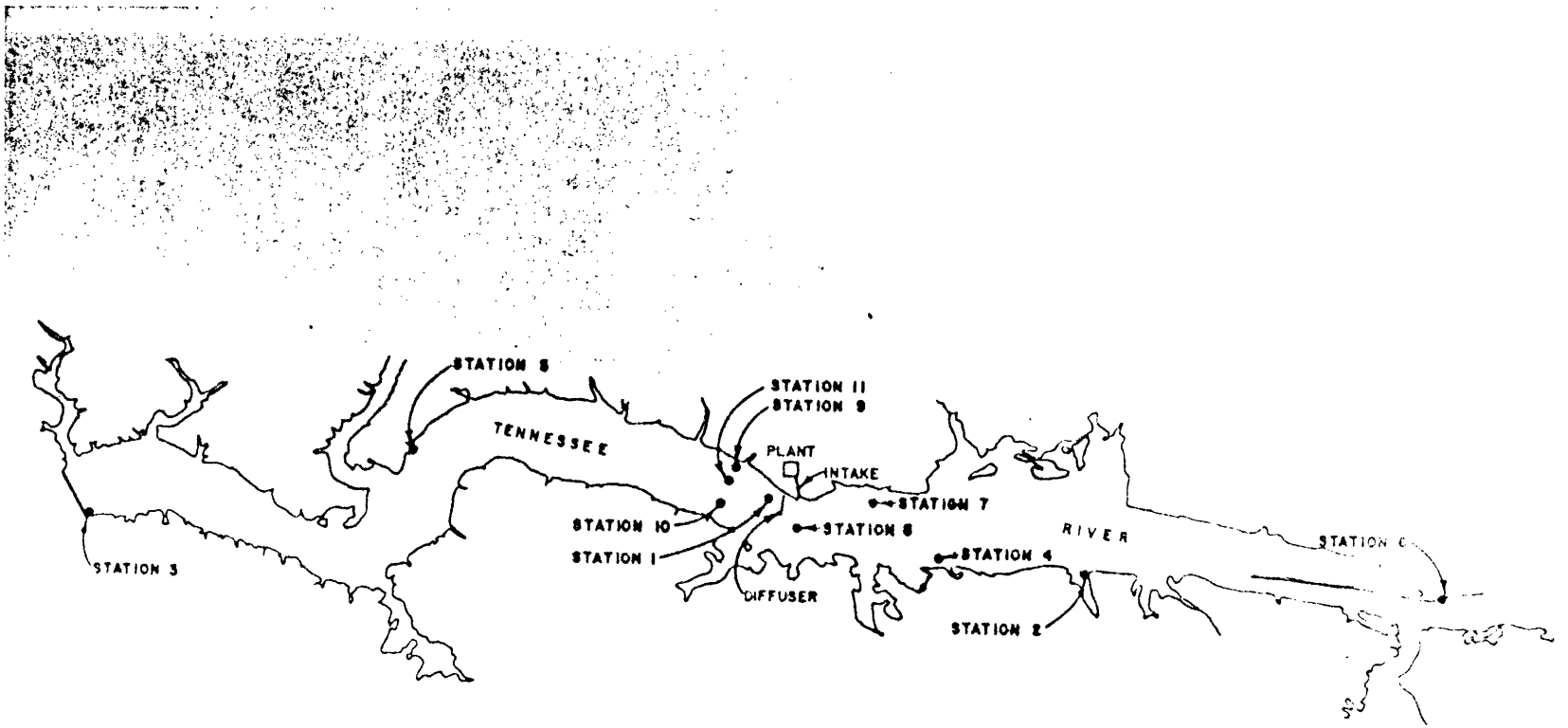

Figure 2.4 Browns Ferry Nuclear Power Station: Location of Temperature Monitors in Wheeler Reservoir

Each of the stations has a vertical string of sensors covering the total water depth. Some of the sensors are located at a fixed height relative to the river bottom, and others are attached to floating moorings so that the reference height is the water surface, which fluctuates during the year by several feet. The measurements are considered to be accurate to ±0.3°F (TVA, 1974).

The means of data collection is via telemetry from the monitor which is initiated by a signal sent from a meteorological station located at Browns Ferry, All the data is punched onto paper tape and each week this tape is retrieved and the data copies to magnetic tape which may then be processed.

The actual data used for analysis in this study was contained on a magnetic tape obtained from the Water Systems Development Branch of TVA in Norris, Tennessee. The period of record is from April 1, 1975 through March 31, 1976. During this time Browns Ferry Power Station was not operating due to the fire of March 22, 1975. Thus the record is essentially of pre-operational or "natural" conditions in the reservoir without the plant's influence.

III. Modeling the National Temperature Difference in Wheeler Reservoir

This section will present a one-dimensional (longitudinal) model for predicting the naturally occuring difference between temperatures in Wheeler Reservoir upstream and downstream from the Browns Ferry Nuclear Plant. This one dimensional approach essentially neglects a variety of natural temperature variations that are known to be more complex resulting in vertical and lateral temperature gradients as well as longitudinal differences. A more complete discussion of these phenomena may be found in Freudberg (1977).

The one-dimensional model was developed using temperature data from monitor #6 (upstream) and monitor #1 (downstream) for the study year described in the previous section. These predictions are also used for the simulation studies (presented in section 5.0 of this report) in which the downstream temperature measurement is defined using stations 9, 10 or 11. Because of the close proximity of these monitors, it is not expected that the error incurred in basing natural temperature difference on Station 1 will be large.

3.1 One-Dimensional Formulation

The basic 1-dimensional convective diffusion equation is given by

$$\frac{\partial TA}{\partial t} + \frac{\partial (QT)}{\partial x} = \frac{\partial}{\partial x}\left(AE \frac{\partial T}{\partial x}\right) + \frac{\phi_n(t)B(x)}{\rho c} \qquad (3.1\text{-}1)$$

where: T is the cross-sectional average temperature

A is the cross-sectional area

t is time

x is the longitudinal position from the upstream station

E is a diffusion coefficient

$\phi_n(t)$ is the net heat flux, a function of time

B(x) is the width, variable with distance along the river

ρ is the density of water, assumed constant

and c is the heat capacity of water, assumed constant.

If it is assumed that the cross-sectional area is constant along the reach from Station 6 to Station 1, that the width is also constant, (their values are given by means) and that the flow does not vary as a function of distance but may vary as a function of time, then equation 3.1-1 becomes, upon dividing through by A:

$$\frac{\partial T}{\partial t} + u \frac{\partial T}{\partial x} = \frac{\partial}{\partial x}\left(E \frac{\partial T}{\partial x}\right) + \frac{\phi_n(t)}{\rho c h} \qquad (3.1\text{-}2)$$

where u is the cross-section average velocity, given by Q/A, and h is the average depth, given by B/A.

If E is taken as a constant dispersion coefficient, and for scaling purposes $\phi_n(t)$ is replaced by $-K(T-T_E)$ or $-K\Delta T_E$ and then the 4th term is rewritten so that $k = K/\rho c$ is substituted, equation 3.1-2 becomes:

$$\frac{\partial T}{\partial t} + u\frac{\partial T}{\partial x} = E\frac{\partial^2 T}{\partial x^2} - \frac{k\Delta T_E}{h} \qquad (3.1\text{-}3)$$

If the temperature is scaled by T', the time by θ, the velocity by V, and the x-coordinate by L, then the scaled parameters corresponding to each term of equation 3.1-3 are:

$$\frac{T'}{\theta}, \qquad V\frac{T'}{L}, \qquad \frac{ET'}{L^2}, \qquad k\frac{\Delta T_E}{h} \qquad (3.1\text{-}4)$$

If each parameter above is divided through by VT'/L to produce non-dimensional parameters, then this results in:

$$\underset{①}{\left[\frac{L}{V\theta}\right]} \qquad \underset{②}{\left[1\right]} \qquad \underset{③}{\left[\frac{E}{VL}\right]} \qquad \underset{④}{\left[\frac{kL\Delta T_E}{VhT'}\right]} \qquad (3.1\text{-}5)$$

Besides the balance between the 2nd and 4th parameters, in equation 3.1-5, what other terms need be retained? $[\frac{L}{V\Theta}]$ would have a value on the order of 1 if the distance between Station 6 and 1, 85000 ft, were used for L, an average velocity of 0.5 ft/sec were used for V, and Θ were about 2 days. Since the time scale of interest for the natural ΔT is on the order of 2 days, this term must be retained.

The third parameter scales the dispersion coefficient. Using the

same values as above for V and L, E would have to be approximately 40,000 ft^2/sec to make this parameter about 1. Almquist (1977) states that for the Tennessee River, a value an order of magnitude lower of 1000 ft^2/sec is probably a good estimate. Therefore, using the value 1000 ft^2/sec, [E/VL] has a value <<1, and therefore the dispersion term shall be neglected. So the 1-D equation becomes (returning to the original formulation of the heat term),

$$\frac{\partial T}{\partial t} + u \frac{\partial T}{\partial x} = \frac{\phi_n(t)}{\rho c h} \tag{3.1-6}$$

The left hand side of equation 3.1-6 represents the changes in the temperature of a parcel of water as it travels downstream from Station 6 to Station 1. In Lagrangian coordinates, this may be written as a material derivative:

$$\frac{DT}{Dt} = \frac{\phi_n(t)}{\rho c h} \tag{3.1-7}$$

Integrating this equation over time for the parcel yields:

$$T_d(t) = T_u(t-\Delta t) = \int_{t-\Delta t}^{t} \frac{\phi_n(t)}{\rho c h}\, dt \tag{3.1-8}$$

where T_d is the temperature of the downstream monitor (Station 1), and T_u is the temperature of the upstream monitor (Station 6).

A moment's thought concerning equation 3.1-8 indicates

its physical foundation. If equation 3.1-8 is rewritten as

$$T_d(t) = T_u(t-\Delta t) + \frac{1}{\rho c h} \int_{t-\Delta t}^{t} \phi_n(t)dt \qquad (3.1\text{-}9)$$

then it is seen that the downstream temperature at time t is a result of the water parcel's temperature when it was at the upstream monitor Δt earlier plus the integrated net heat flux over Δt the parcel received during its journey downstream. The correct definition for this Δt is the travel time for the parcel to move from Station 6 to Station 1. Δt is thus determined from:

$$\int_{t-\Delta t}^{t} u dt = L \qquad (3.1\text{-}10)$$

where L is the distance between upstream and downstream sections. Utilizing the assumptions that the area is a constant between monitors, and that Q, the flow, is a function of time only, equation 3.1-10 becomes:

$$\frac{1}{A} \int_{t-\Delta t}^{t} Q(t)dt = L \qquad (3.1\text{-}11)$$

Thus, it is seen that Δt is itself a function of time.

For the natural ΔT at time t defined by:

$$\Delta T(t) = T_d(t) - T_u(t) \qquad (3.1\text{-}12)$$

equation 3.1-9 combined with 3.1-12 yields:

$$\Delta T(t) = \frac{1}{\rho c h} \int_{t-\Delta t}^{t} \phi_n(t)\, dt - \left[T_u(t) - T_u(t-\Delta t) \right] \qquad (3.1\text{-}13)$$

Thus, the temperature difference between the two stations consists of two effects: the net heat input over Δt and the change in temperature at the upstream monitor during Δt. Equation 3.1-13 represents the desired formulation for the 1-dimensional model.

3.2 Input Data

There are many aspects which make up the natural ΔT. The time scale of many of the more random events are hourly, whereas the 1-dimensional (1-D) influences are felt over longer time periods on the order of a day. Therefore, it was decided to use the 1-D model to fit a 2-day running average of the natural ΔT, which was expected to have more 1-D character. A plot of the natural ΔT after a 49-hour running average was made (49 hours was used so that a symmetric averaging interval occurred) is given in Fig. 3.1. From this signal, "storm cycles" may be observed which appear as wide temperature swings persisting up to a week that are believed to be associated with the weather patterns. Also visible, though less clearly, is the weak annual cycle.

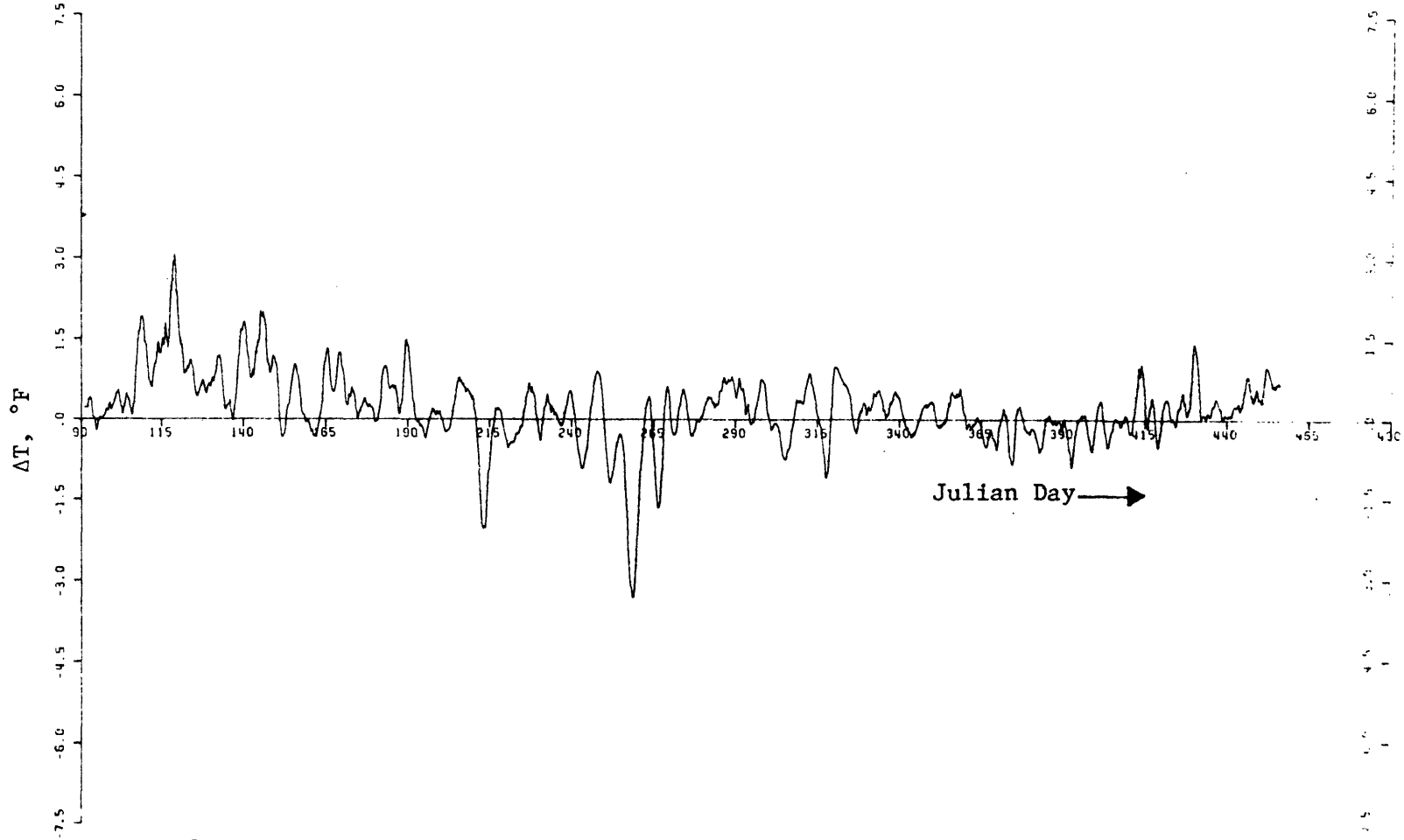

Figure 3.1 Forty-Nine Hour Running Average of Measured Natural ΔT, April 1, 1975 to March 31, 1976

To apply equation 3.1-13, tables of flow, measured upstream temperature, and computation of net heat flux are required. In addition, values for the area, A, and depth, h, must be specified. Since only for certain locations are measurements for A and h available, there is some leeway with their values, and these two parameters were used to tune the model within physically reasonable limits. The means of producing a best fit is described briefly below where the actual results are presented.

The net heat flux was computed using the methods outlined by Ryan (1971). Table 3.1 summarizes the input needed. The actual equations used to compute the net flux are given in Appendix A.

TABLE 3.1

DATA REQUIRED TO COMPUTE NET FLUX

1. Air Temperature
2. Relative Humidity
3. Wind Speed
4. Air Pressure
5. Solar Flux
6. Atmospheric Flux

Necessary inputs to apply equation 3.1-13 are (all 49-hour running averages of) the flow, station 6 bottom temperature, and meteorological inputs measured at Huntsville, Alabama (30 miles from Browns Ferry). For these computations, values of cloud cover and air temperature measured at Huntsville were used.

The period of record for this data is April 1975 through December 1975. Only 3/4 of the year is shown because the flow and meteorological data happened to be available from January 1975 to December 1975 and the natural temperature measurements which were not available until April 1975 as the plant operated until then. The data record of 6598 points is still quite sufficient for applying and testing the 1-D model. The upstream monitor at Station 6 at the bottom was used as the upstream temperature ($T_u(t)$) in equation 3.1-13 as this location is less susceptible to diurnal effects and it is believed to be closer to the cross-sectional temperature.

The choice of depth and cross-sectional area to use was made after several iteratations with the model. The values chosen were h = 12.5 feet and A = 50,000 ft^2, values which are physically reasonable in light of the measured cross-sectional data. The criteria used to choose these values was when the best agreement was obtained between monthly averages of the model prediction and monthly averages of the measured ΔT at the 5-foot depth and bottom monitors. The best

monthly averages of the model prediction and monthly averages of the measured ΔT at the 5-foot depth and bottom monitors. The best result, using h = 12.5 feet and A = 50,000 ft^2 is plotted in Figure 3.2. As is seen, the model is a reasonable fit on a monthly basis. Fig. 3.2 is somewhat misleading however, because neither the top nor bottom measured ΔT values actually are true cross-sectional averages, and due to the monthly averaging scale, the ability of the model to fit the storm cycles is obscured.

The ability of the 1-D model to fit the 49-hour averaged data is dramatically illustrated in Figure 3.3. As is seen the model prediction is a very credible fit of the peaks and valleys of the measured ΔT, although this fit is somewhat worse in the fall and winter. It is suspected that the model fit is better in the spring and summer than the fall or early winter because the valley-wide longitudinal driving force is much smaller in the latter portions of the year, (Freudberg, 1977). In addition, the nature of the river is fundamentally different during heating periods than during cooling periods. Stratification, although weak, occurs particularly in the spring when the river begins to warm. Further, the seasonal heat-up is a relatively steady process which induces very little turbulence as it acts. The flow is not particularly disrupted from its usual 1-dimensional course by density effects. On the other hand, the cool-down in the fall is a far more complex process. Unlike the spring

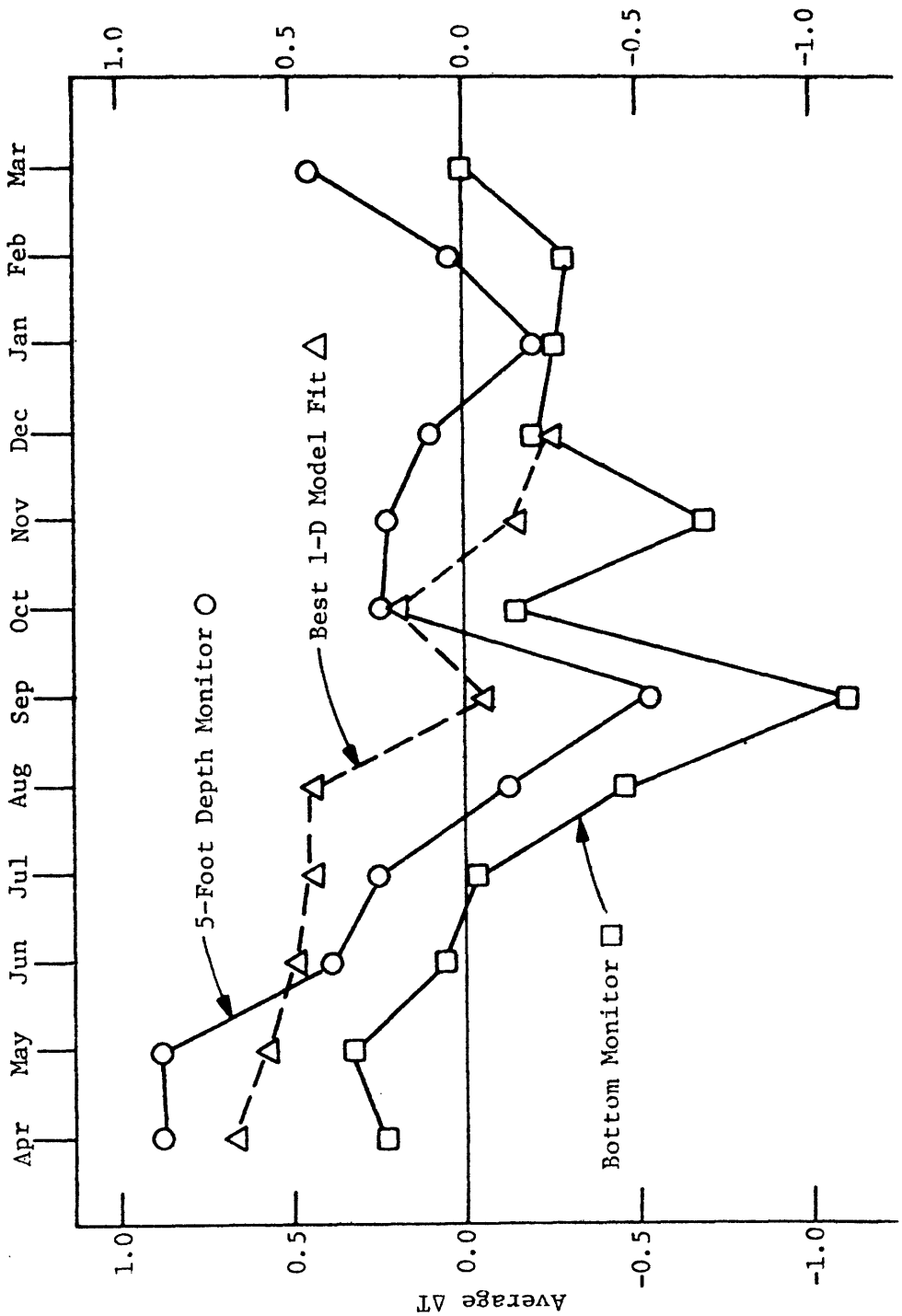

Figure 3.2 Monthly Average Comparison of 1-D Model Fit with h=12.5 Feet and A=50,000 ft^2 to Measured Data at 5-Foot and Bottom Monitor

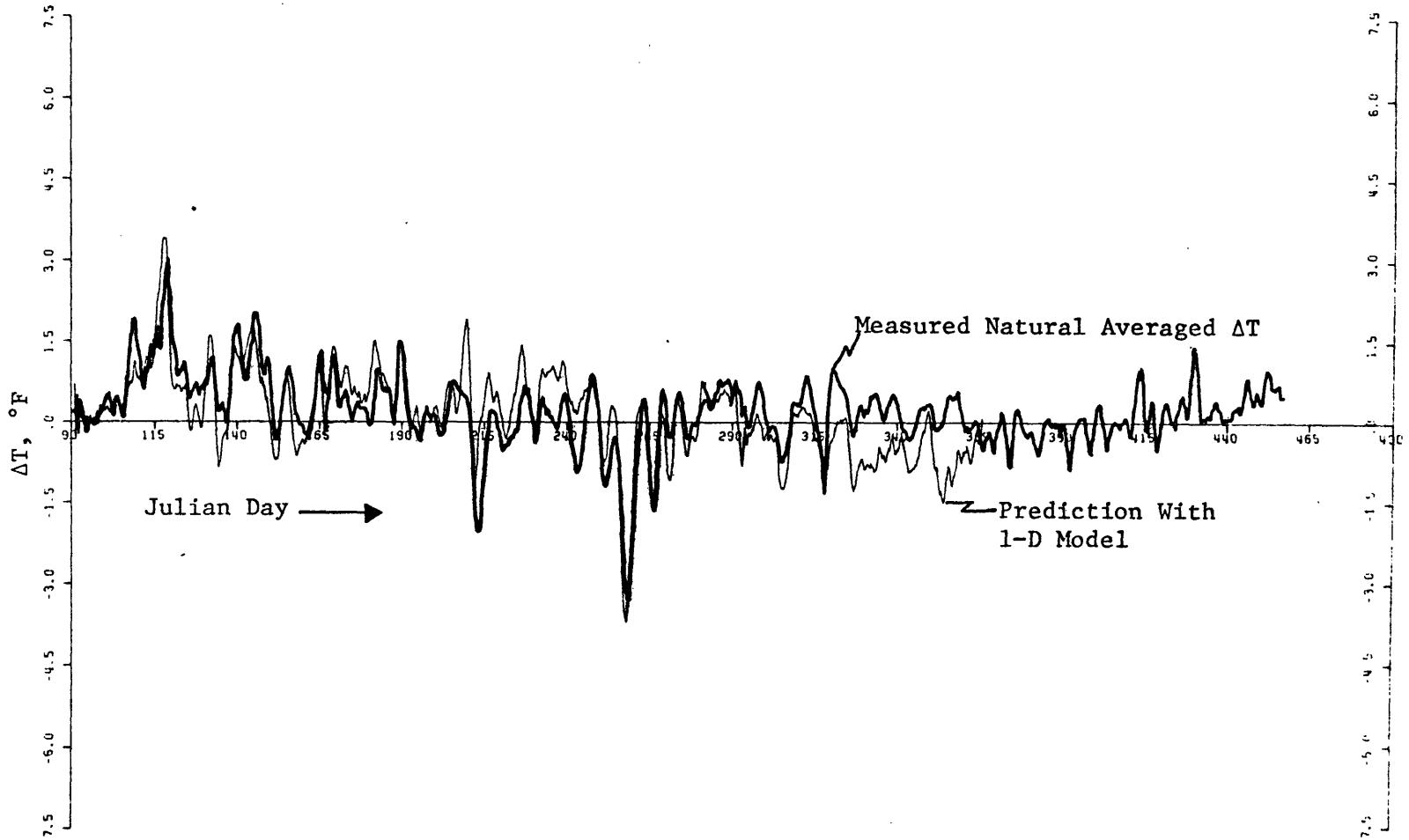

Figure 3.3 Comparison of Measured Hourly Averaged Natural ΔT With Prediction Using 1-D Model With h = 12.5 ft. and A = 50,000 ft^2

when the warmed, bouyant surface water tends to remain at the surface, the cooled surface water in the fall sinks down due to its greater density and thus non-one-dimensional mixing takes place. Thus the 1-D model produces a better result during periods when the river flow itself is generally one-dimensional, the water body is more homogenous, and no complex mixing process is taking place.

The statistics of the mean and variance for the measured data and the 1-D model are presented below, for the period April 1975 - Dec. 1975.

TABLE 3.2 Comparison of Statistics of 1-D Model and Measured Natural ΔT

	MEASURED DATA	1-D MODEL
MEAN	0.26	0.14
VARIANCE	0.53	0.69

These values show that the model is close to the measurements, although there is clearly some error. In Fig. 3.4, a time series plot of this residual obtained via subtracting the 1-D model fit from the data is given. This residual series has a mean of 0.12°F and a variance of $0.34°F^2$. Thus the variance of the data has been reduced roughly 40% using the 1-D model.

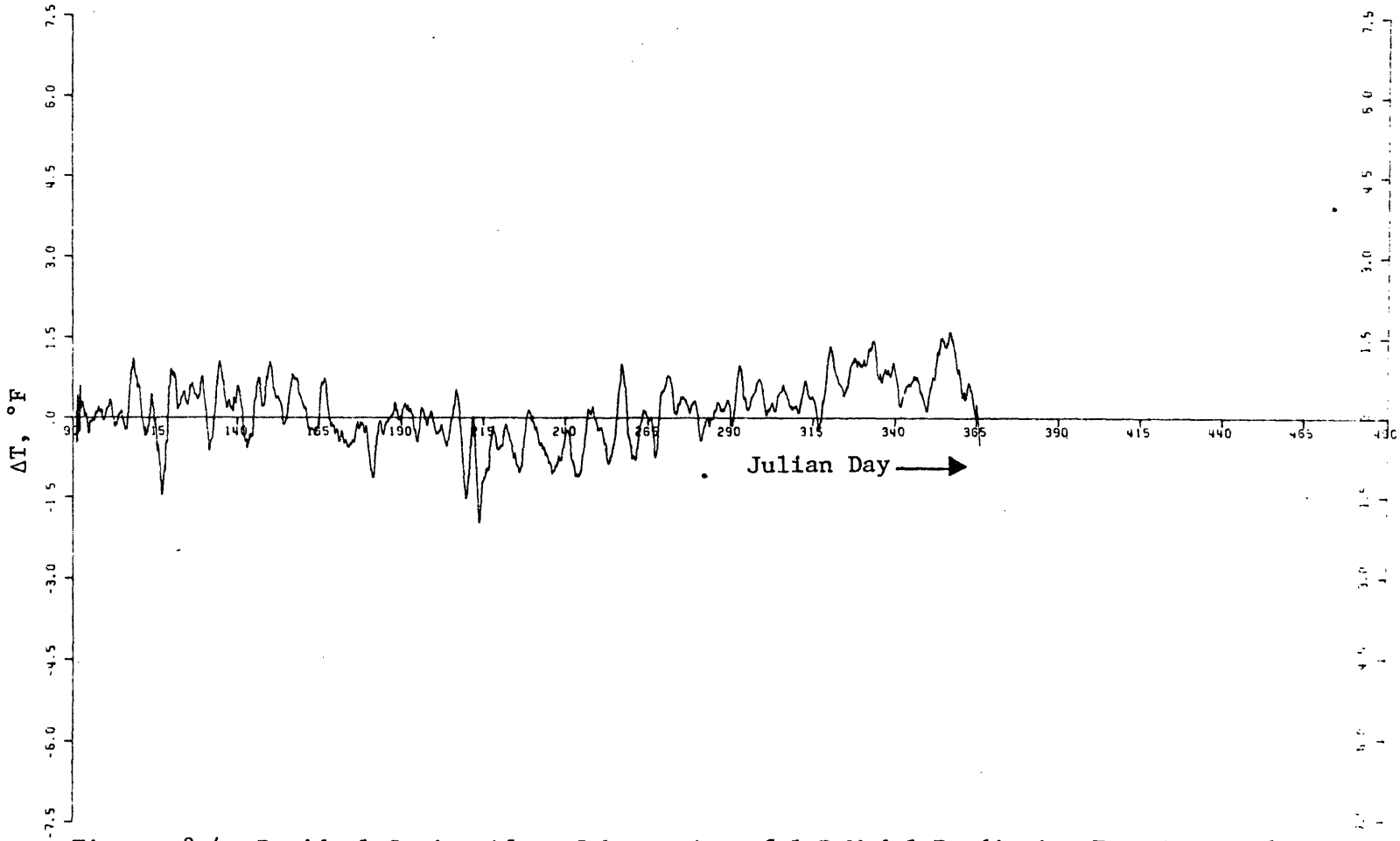

Figure 3.4 Residual Series After Subtraction of 1-D Model Prediction From Measured Averaged Natural ΔT

IV. Simulation of Plant Operation

This section describes a simulation routine developed for the purpose of investigating a year of plant operation at an hourly time scale for a variety of different conditions. The results of the simulation are presented in the next section. Also, because of the complexity of some of the algorithms used to describe the plant operation, diffuser mixing, etc., only the general logic of the simulation program will be presented here.

4.1 Main Simulation Cycles

The logic governing the overall simulation is shown in flow chart form in Figure 4.1. As indicated in the figure, the simulation routine assumes the following quantities are known for the last hour of the period of simulation:

1. Releases from the upstream (Guntersville) and downstream (Wheeler) dams
2. Browns Ferry Plant Target Load
3. Wet bulb air temperature
4. Upstream and downstream natural water temperature
5. The estimated natural temperature difference between upstream and downstream

From the above quantities the simulation program computes for each hour the cooling mode needed to meet the applicable temperature standard. A plant efficiency algorithm is then used to compute the actual power output for each hour.

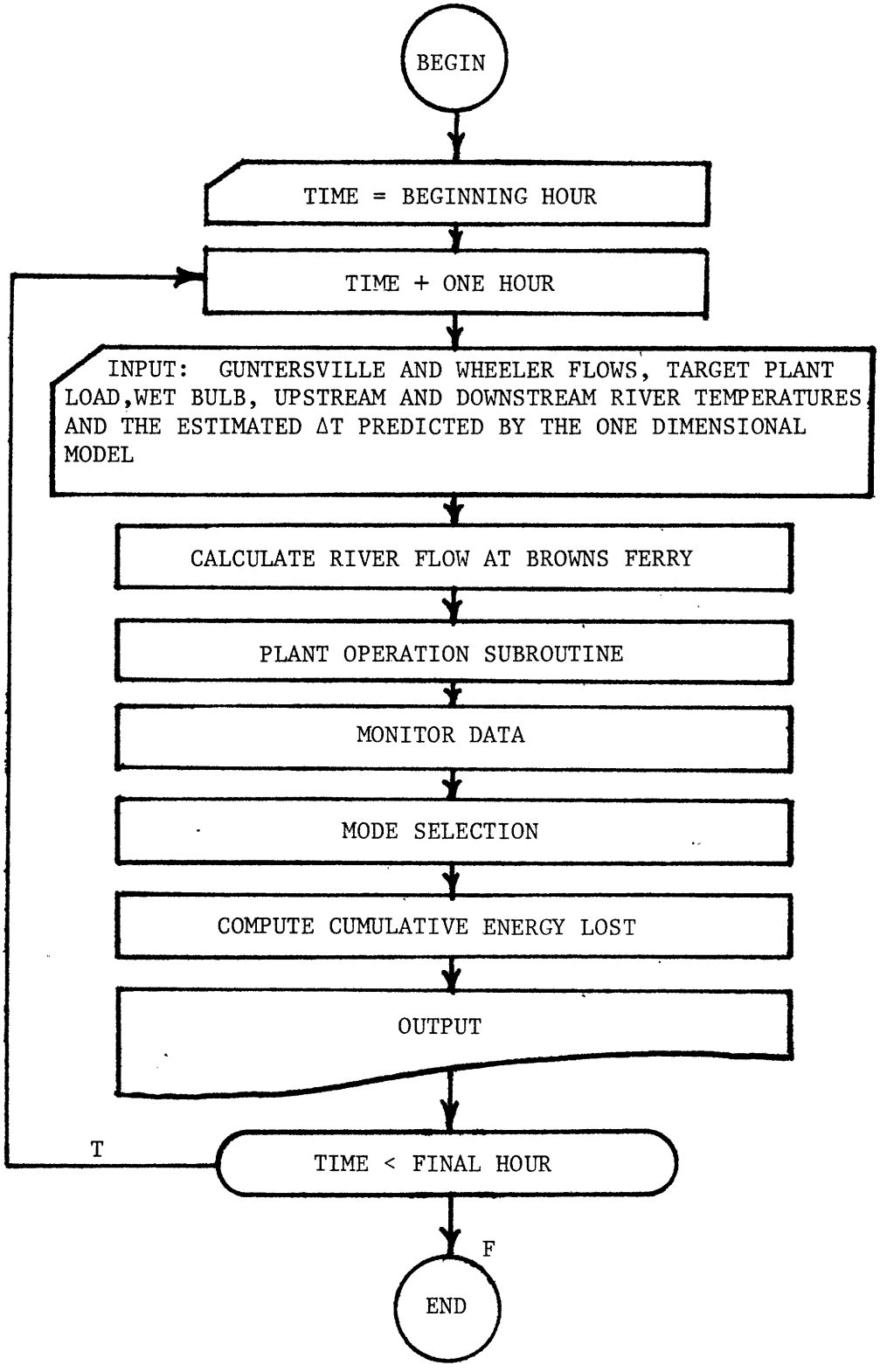

Figure 4.1 Overall Logic Diagram for Simulation of Plant Operation

4.2 Simulation Subroutines

The following section describes the individual algorithms that are used in the simulation routine.

4.2.1 Input

Hourly values of river flows at Guntersville and Wheeler dams; wet bulb temperatures; upstream and downstream temperatures; and when desired the one dimensional models estimates of the natural temperature difference between upstream and downstream monitors, are supplied to the program.

4.2.2 Browns Ferry Flow

The river flow at Browns Ferry is calculated with a two term equation utilizing flow values at Guntersville dam five hours previous to the time of calculation, and flow at Wheeler dam two hours previous. The flow was then time averaged using a fraction (R) of the present flow calculation added to the fraction (1-R) of the previous hours flow calculation. With the diffuser performance a function of flow and using the simple two term model for flow without time averaging causes the plant induced temperature fluctuations to be instantly and strongly respondant to flow variations. We know in reality the induced temperature is not so highly sensitive to flow and the inclusion of time averaging of flows at this point is a means to smooth the induced temperatures response to flow.

4.2.3 Plant Subroutine

The subroutine simulating plant operation is executed three

times per hour to include three possible modes of operation, open, helper and closed. (see Figures 4.2)

Condenser Intake Temperatures: For open and helper modes condenser intake temperatures are approximated by the upstream river temperature. Closed mode iteration is used until the temperature rise across the condensers is equal to the temperature drop across the cooling towers. At this point the condenser intake temperature is approximated by the cooling towers cold side temperature.

Actual Plant Load and Condenser Hot Side Temperature: Actual plant load is a function of the target plant load (held constant at 3300 MWe for the three units considered here), water temperatures, and the mode of operation. The condenser hot side temperature is a function of the actual plant load, the intake temperature and the condenser flow rate (constant within a given mode). However, the ratio of actual plant load to target plant load is a function of the actual plant load and condenser hot side temperature. Hence, iteration is used alternatingly computing the condenser hot side temperature and the actual plant load until both values converge to a final value (for a given intake temperature and mode of operation). An additional 56 MWe is subtracted from the actual plant load in helper and closed modes to account for the operation of the cooling towers pumps. (see Figure 4.3)

Cooling Tower Performance: The temperature drop across the cooling towers is calculated using a fitted polynomial with tower intake temperature and wet bulb temperature as arguments.

Discharge Temperatures: In open mode the condenser hot side

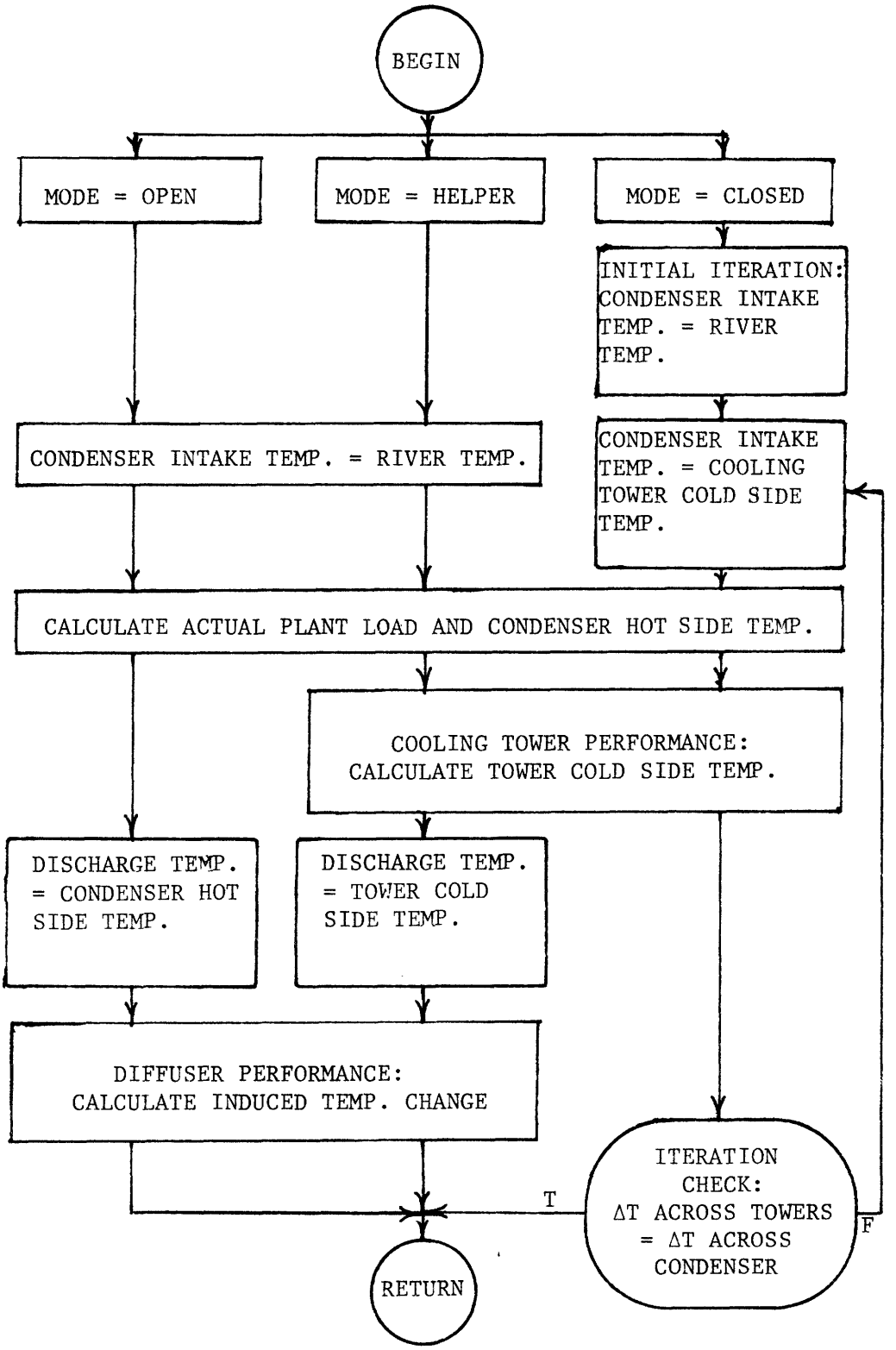

Figure 4.2 Flow Chart for Plant Subroutine

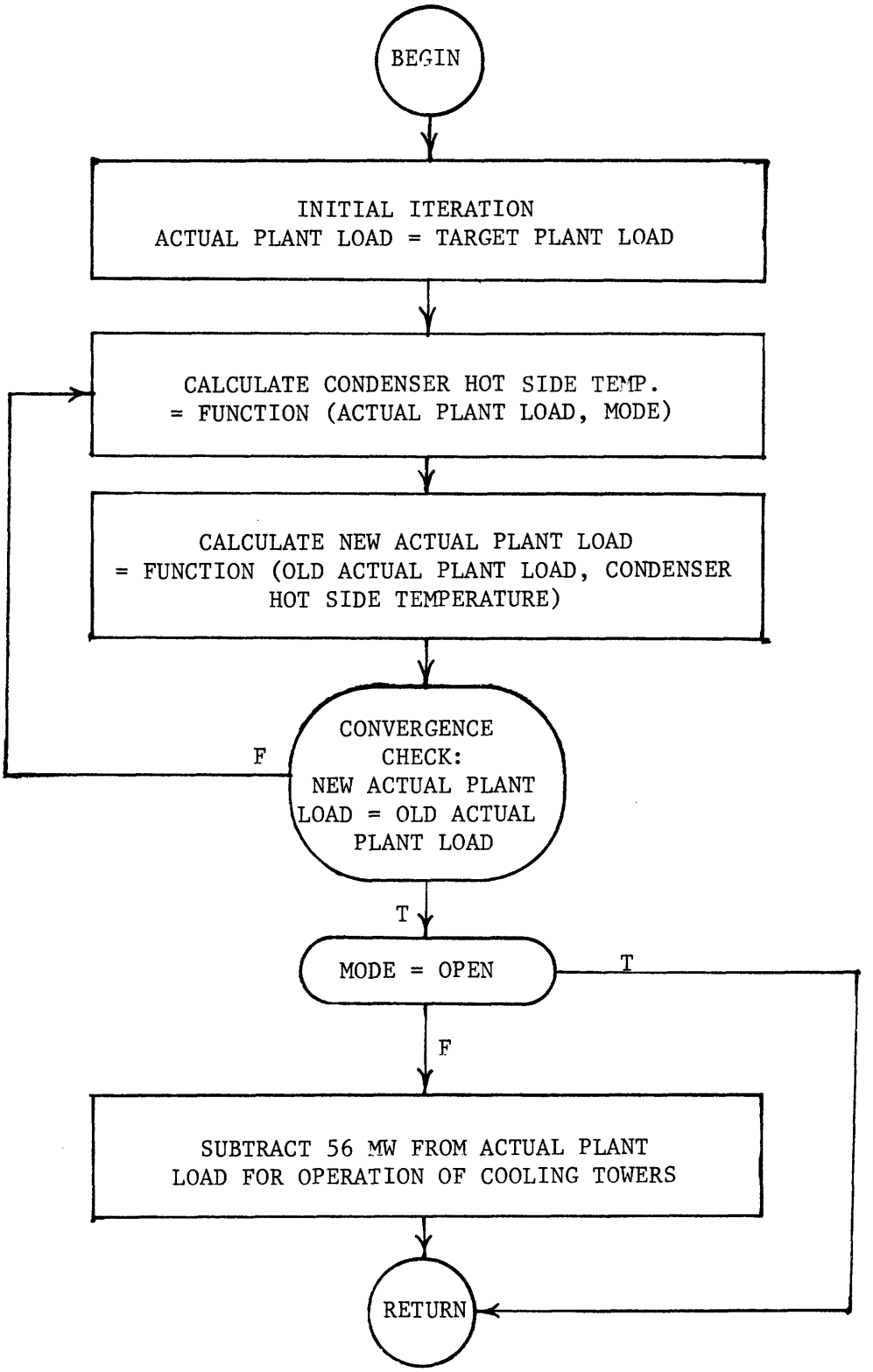

Figure 4.3 Flow Chart of Actual Plant Load and Condenser Hot Side Temperature Algorithm

temperature at the open mode flow rate of 4410 ft^3/sec for the three units is discharged. Helper mode makes use of one pass through the cooling towers and discharges the resulting tower cold side temperature at the helper flow rate of 3675 ft^3/sec to the river.

Induced River Temperature: The induced river temperature is a function of river flow and temperature, discharge flow and temperature, and diffuser performance. The diffuser performance is described by curves fitting the three multiport bottom diffusers in place at Browns Ferry. Complete mixing in higher river flows and the recirculation around the diffuser in lower flows are modeled.

4.2.4 Running Averages

If spatial or temporal averages of temperature monitor values are desired they are performed after the plant subroutine by operating on the observed upstream and downstream temperatures, and the calculated plant induced river temperatures.

4.2.5 Best Mode

The best mode of operation is selected on the basis of the time averaged or unaveraged temperatures depending on the objective of the particular run. In selecting the mode, power production is maximized within the constraints of a maximum downstream river temperature and a maximum change in temperature between the upstream and downstream monitors. This change in temperature is taken as the natural temperature difference given by the upstream and downstream monitors plus the calculated plant induced temperature change. When the ΔT estimated by the one-dimensional model is included, it is subtracted giving the total

ΔT=natural measured ΔT + calculated induced ΔT - 1-D model's estimated ΔT.

4.2.6 Cumulative Energy Lost

The hourly reduced power output caused by the plants compliance to the river temperature standards is accumulated for the years operation. This gives a measure of the energy lost in comparison to operating entirely in open mode.

4.2.7 Output

Output from the program includes the calculated Browns Ferry flow; induced ΔT and actual power output for each mode of operation every hour, the condenser hot side temperature in closed mode, the optimum mode within the temperature constraints, and the cumulative hourly power lost by operating in the constrained modes rather than in open mode.

4.3 Source of Performance

The condenser heat rejection curve and the power reduction curve used in the actual plant load calculation; the cooling tower performance curves; and the diffuser performance curves describing the mixing of thermal discharge with the river were obtained from and at one point used by TVA for the Browns Ferry Plant.

V RESULTS OF COMPUTER SIMULATION OF PLANT OPERATION

A number of sensitivity studies of plant operation were carried out with the model described in Section IV. Sensitivity analysis considered monitor location, spatial averaging of monitors, time averaging of monitors, and changes in environmental standards or plant design. The following subsections describe the results of these studies along with the methods used to display the results and the basis for result evaluation.

5.1 An Explanation of the Forms Used to Display Results of Computer Simulation

The results of the computer evaluations for the sensitivity analyses are presented in three ways: 1) a graph of the power output of the plant in the best mode of operation, 2) a sorted display of how many hours the plant had a reduced power output due to running in either helper or closed mode and 3) the total cumulative output power loss for the period of observation.

5.1.1 Power Output of the Plant in Best Mode of Operation

It is assumed that the plant would like to operate at full power, 3300 MWe, at all times during the year. Some loss of power results when higher water temperatures reaching the condenser cause a loss of thermal efficiency in the plant. When river water temperatures reach certain levels it is necessary to use a helper or closed mode of operation to meet thermal standards. These other modes of operation require a significant amount of energy over and above the losses due

to thermal efficiencies. The results of the sensitivity analyses are graphically displayed as the power output of the plant in megawatts electric (MWe) for each hour of the observation period (grouped by Julian days).

The change in output for the plant often shows up as long spikes due to the switching between various modes of operation in response to changing river temperatures. Figure 5.1 contains three separate graphs showing what the power output of the plant would be if it were run entirely in each mode of operation for the entire period. Each graph of the power output of the plant in best mode can be thought of as a mixture of these curves. The graphs take into account the thermal inefficiency caused by higher river temperatures. Figure 5.2 displays a typical evaluation result identifying basic items that are common to most of the results. This includes the range of each mode of operation, seasonal periods, and constant open cycle operations.

5.1.2 Sorted Power Losses

The power values determined from the plant output in best mode graphs were subtracted from the power of the plant if it was in open mode. These values of power losses, due to running the plant in helper or closed modes, were sorted and displayed versus the number of hours these values of power loss occurred. Figure 5.3 shows a typical example of a sorted power loss evaluation and points out the ranges of open and closed modes of operation as well as some common factors in some of the results.

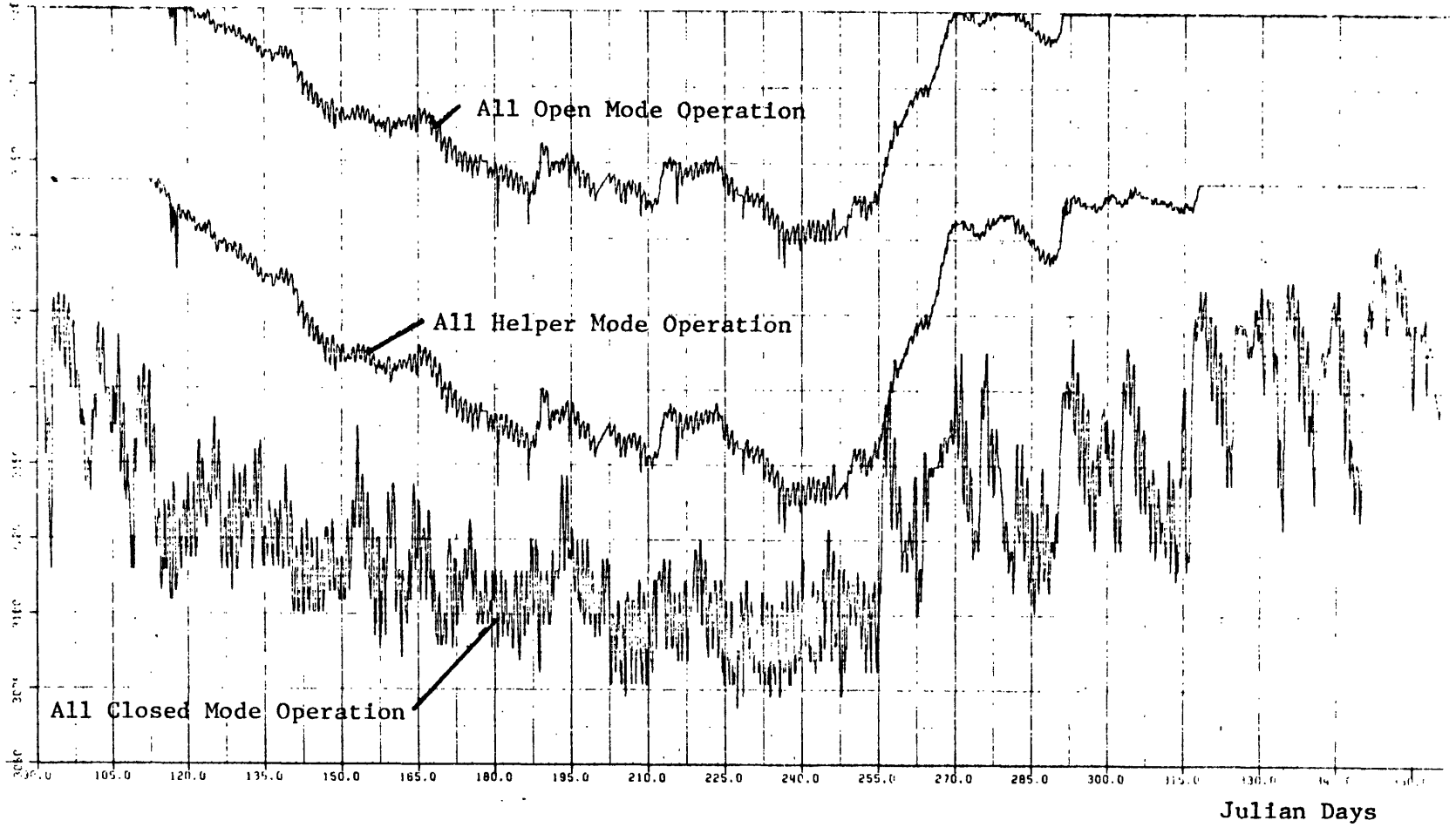

Figure 5.1 Power Output of Plant Under Three Separate Modes Of Operation

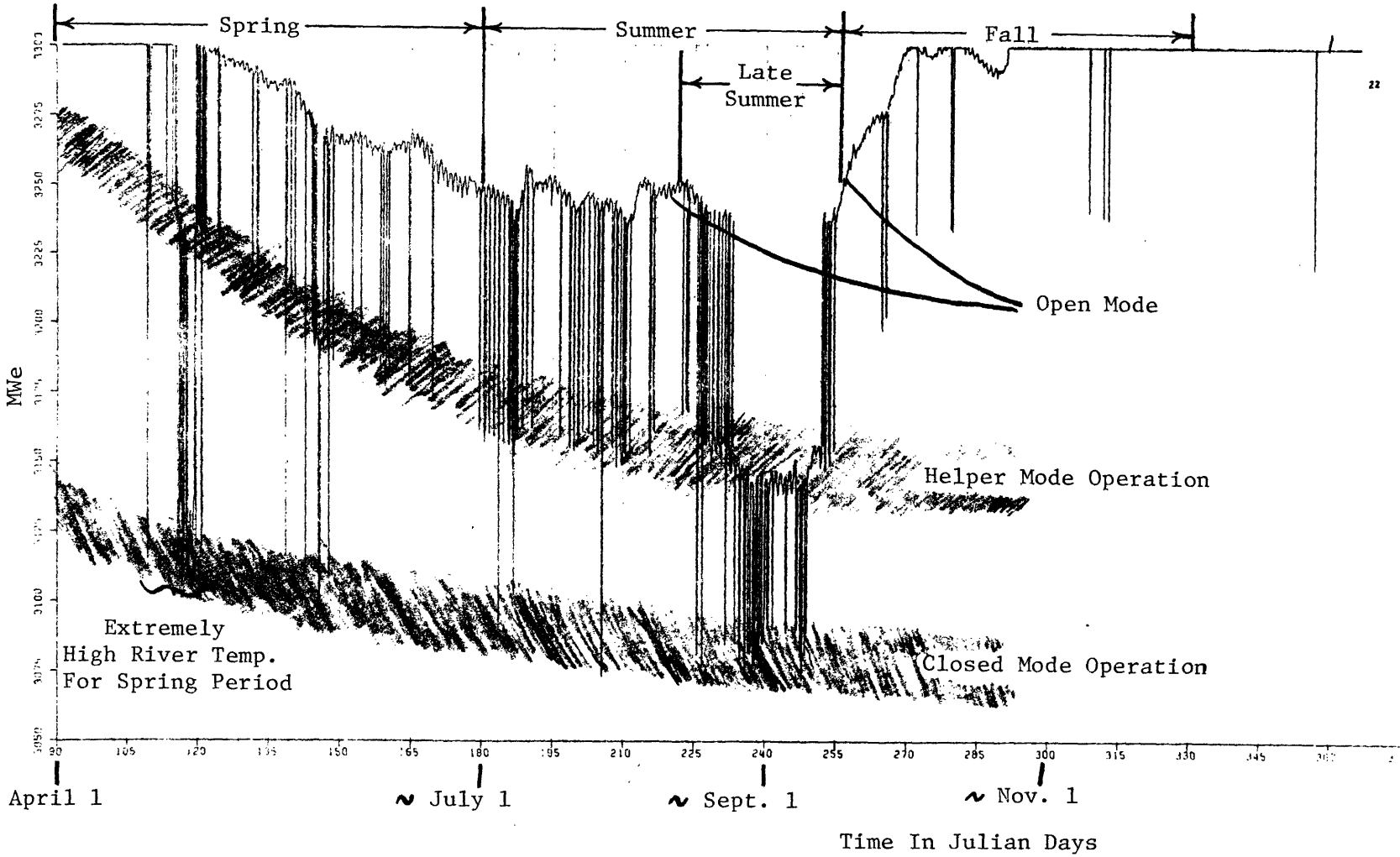

Figure 5.2 Typical Evaluation Result for Power Output of the Plant in Best Mode of Operation

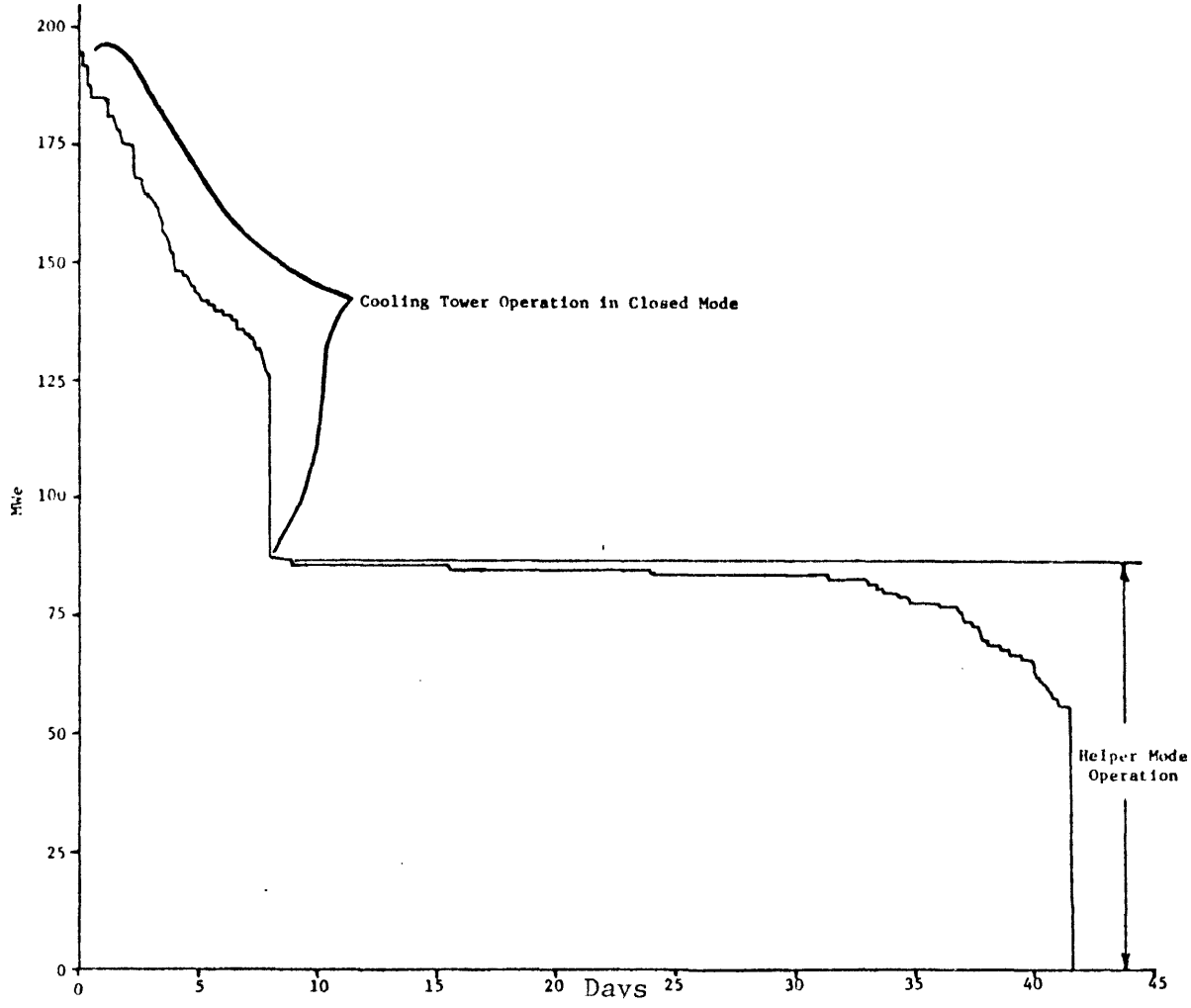

Figure 5.3 Typical Example of Sorted Power Loss Evaluation - Power Output Losses Shown are Those Above Open Mode Operation

5.1.3 Cumulative Hourly Power Losses

Finally, the power losses, due to running the plant in helper or closed mode, during the entire observation period were totaled and are reported as the cumulative hourly power lost in megawatt hours. These values do not consider the thermal inefficiencies of running the plant (i.e. open mode losses have been kept out of the total). Comparing the cumulative hourly power losses provides a good quick method of comparing the results of each sensitivity analysis.

5.2 Base Cases

Two base cases are used in comparing the results of the sensitivity analyses. Data available from the plant consisted of temperature readings at upstream station 6 and downstream stations 1,9,10 & 11 as shown in Figure 5.4. Evaluations were done comparing the individual downstream stations. Station 9 showed the largest cumulative power losses for all the downstream stations, hence, this case was chosen as a basis for comparison. Figures 5.5 and 5.6 show the base power output in best mode graph and the sorted power losses curve, respectively for Base Case A.

Base Case B used the idealized case where the natural upstream temperature is considered equal to the natural downstream temperature. In this case all the effect on the change in temperature in the river between these two points its plant induced. This base case can be thought of as the lowest possible power losses since this only includes the effects of river temperatures on the thermal efficiency of the plant. Figures 5.7 and 5.6 show the power output in best mode plot and sorted power losses.

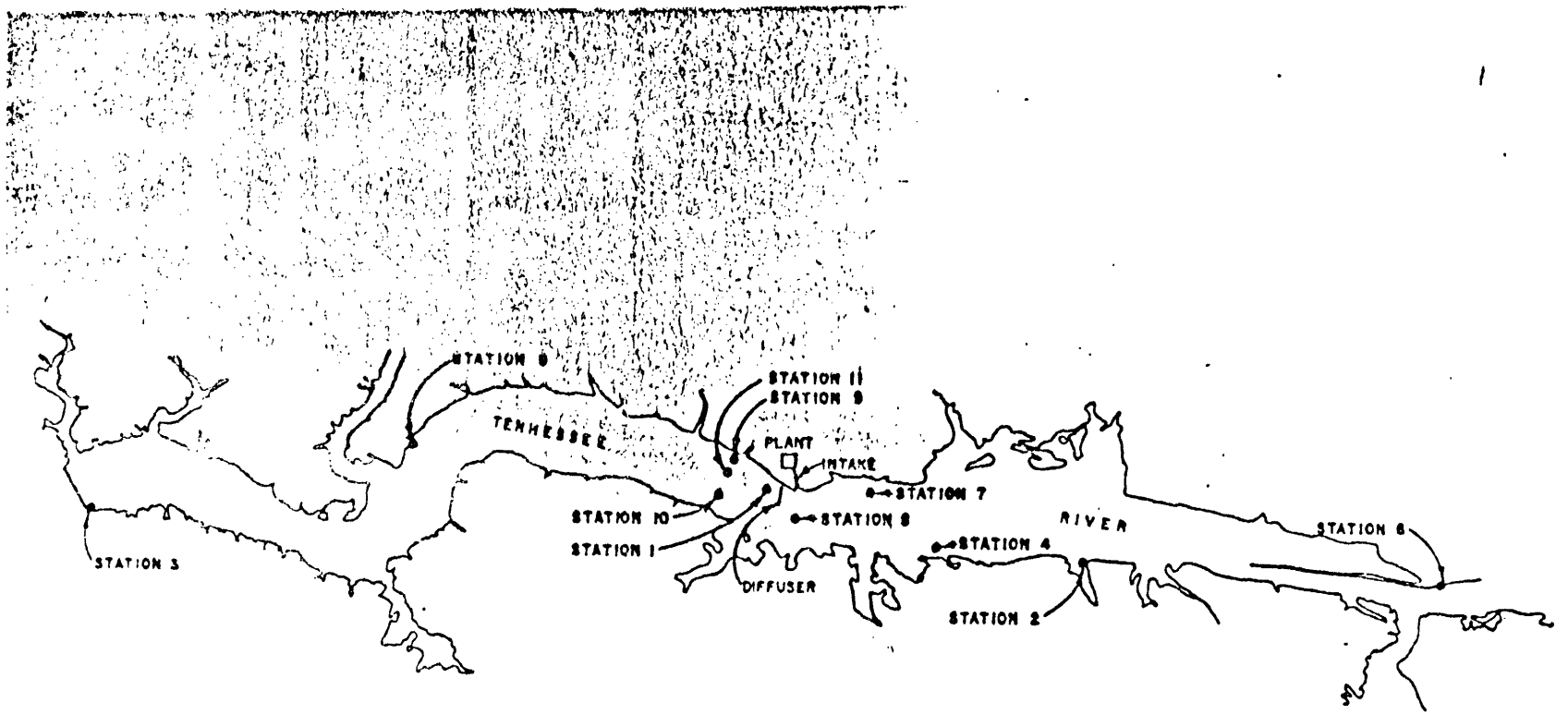

Figure 5.4 BROWNS FERRY NUCLEAR PLANT
WATER TEMPERATURE STATIONS

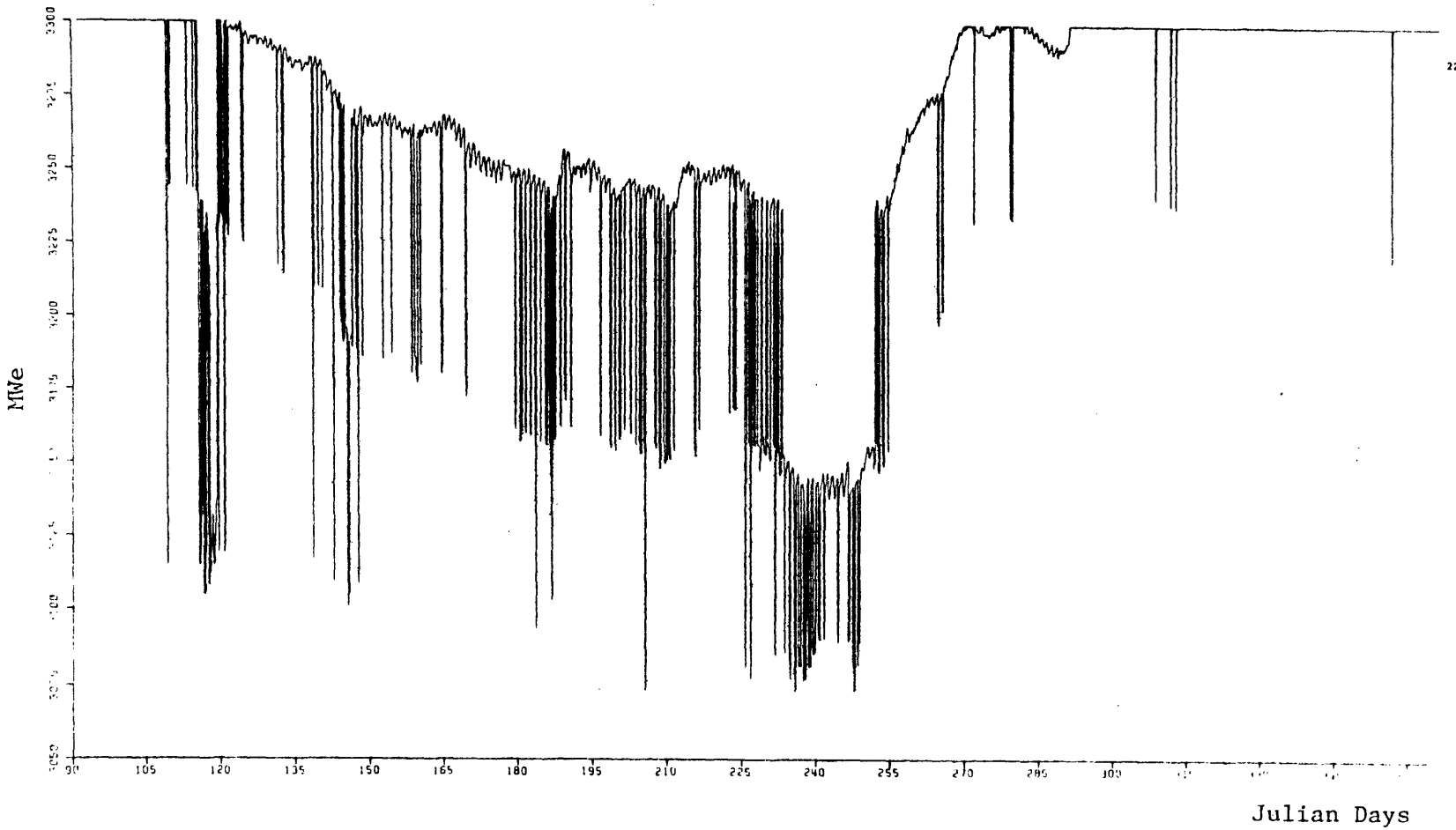

Figure 5.5 Base Case A Power Output in Best Mode (Downstream Station 9)

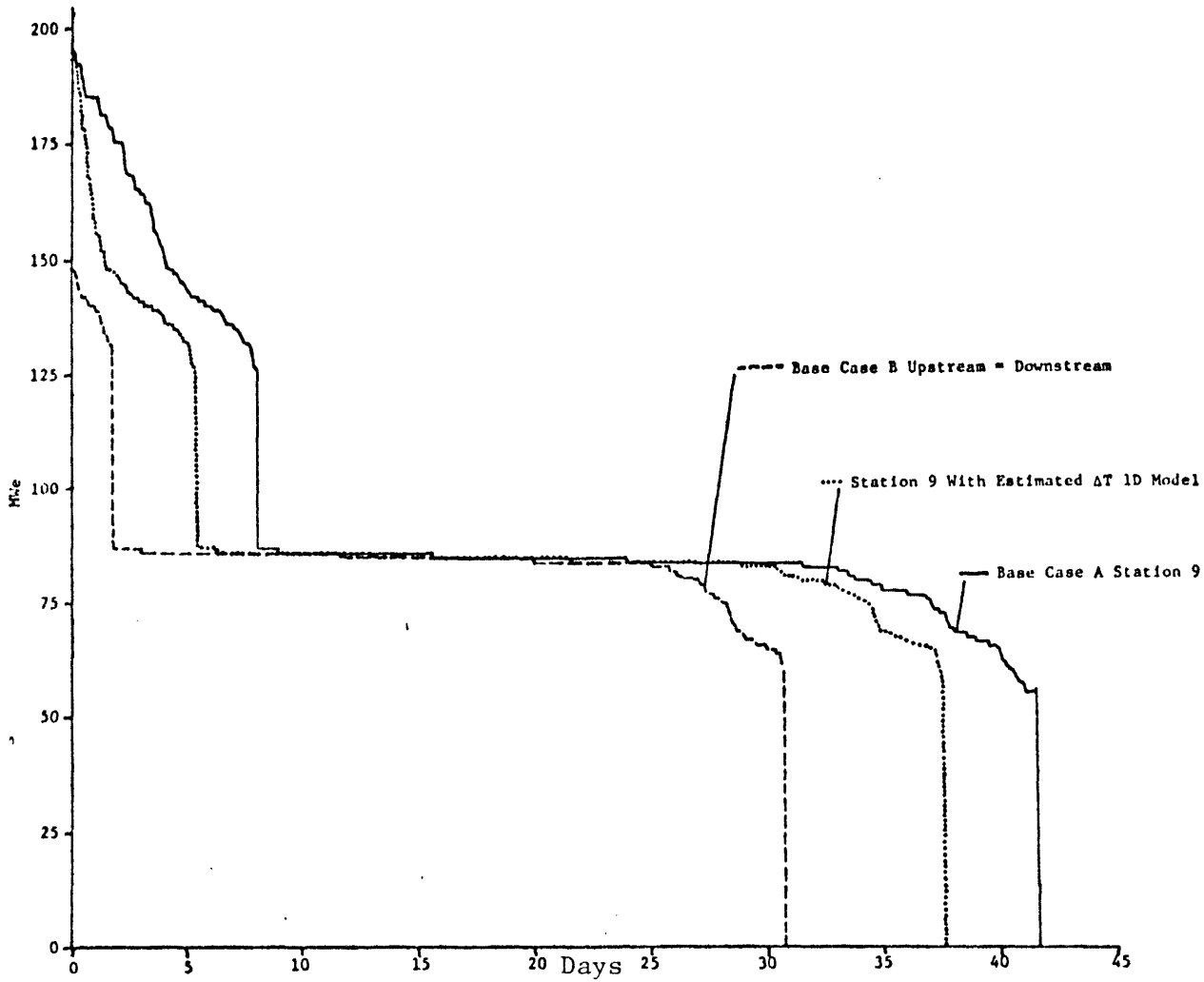

Figure 5.6 Sorted Power Losses Base Cases

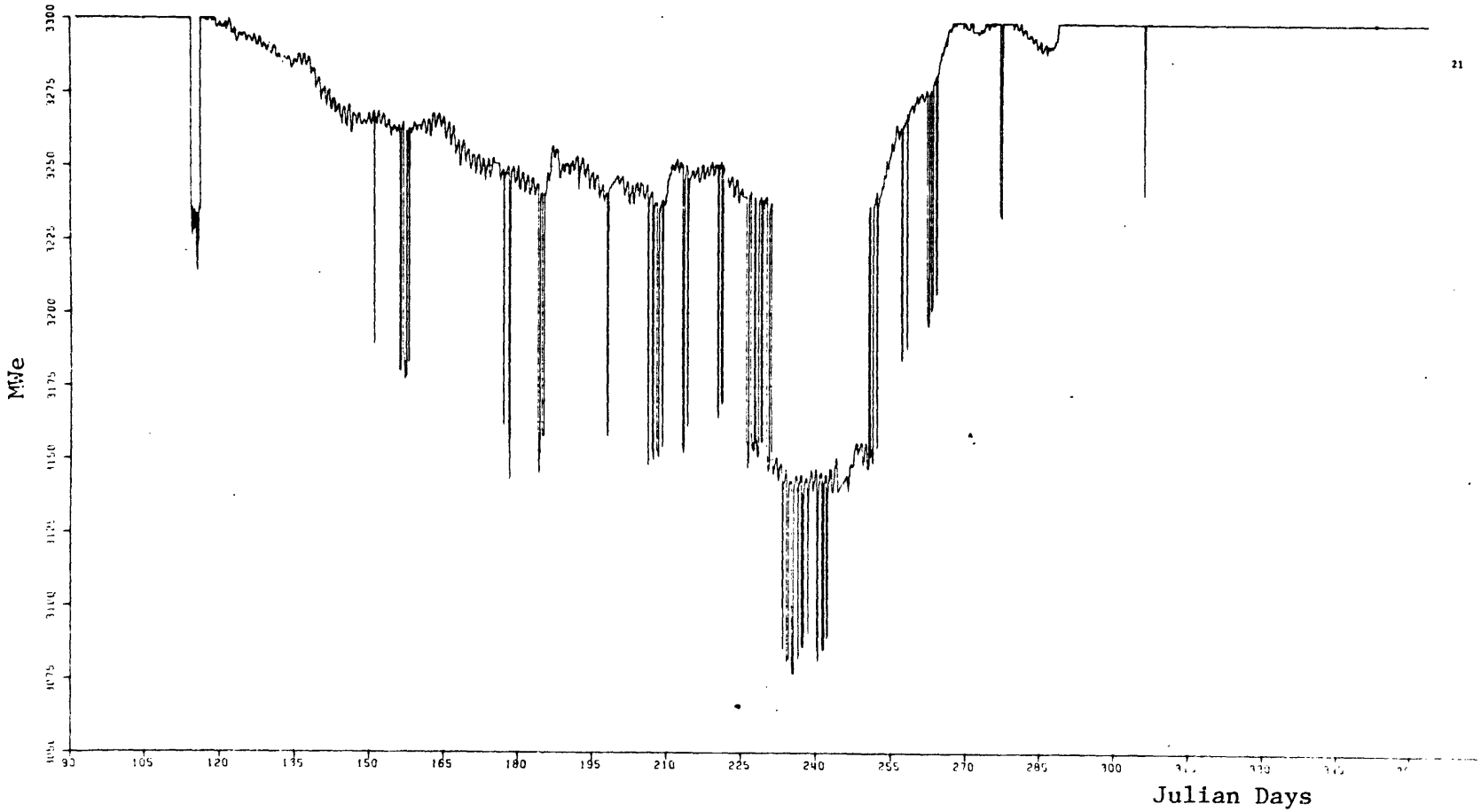

Figure 5.7 Base Case B Power Output in Best Mode (Natural Upstream Temperature = Natural Downstream Temperature)

The change in temperature estimating 1D model described in Section 3.0 was used on the Base Case A analysis. The use of the model by itself cuts down on power losses significantly. The sorted power losses curve, Figure 5.6, actually comes about one half the way between the two Base Cases. A comparison of the power output in best mode graphs Figure 5.8 to Figure 5.6 shows effects mostly in the spring and the fall. More use of helper mode occurs in the fall, however, in the spring reduced power losses are shown where less helper and closed modes are used.

5.3 Effects of Spatial and Time Averaging

The first set of sensitivity analyses considered the location of the downstream monitor, the effect of averaging a set of monitors, and time averaging a specific monitor. The estimated ΔT 1D model was then used on each case to see if any monitors or averaging techniques were specifically affected.

5.3.1 Monitor Location and Spatial Average

Data for downstream monitors offerred possible analysis of Stations 9,10 & 11. The Base Case chosen was Station 9 which resulted in the worst power losses. Figures 5.9 and 5.10 show the power output in best mode plots for individual stations 10 & 11 respectively. The results show progressively less use of both helper and closed modes as you go from Station 9 to Station 10 to mid-channel Station 11.

Downstream stations 9,10 & 11 data were averaged and analyzed to determine the effect of spatial averaging. Figure 5.11 shows the power output in best mode plot for the results. The spatial averaging offers

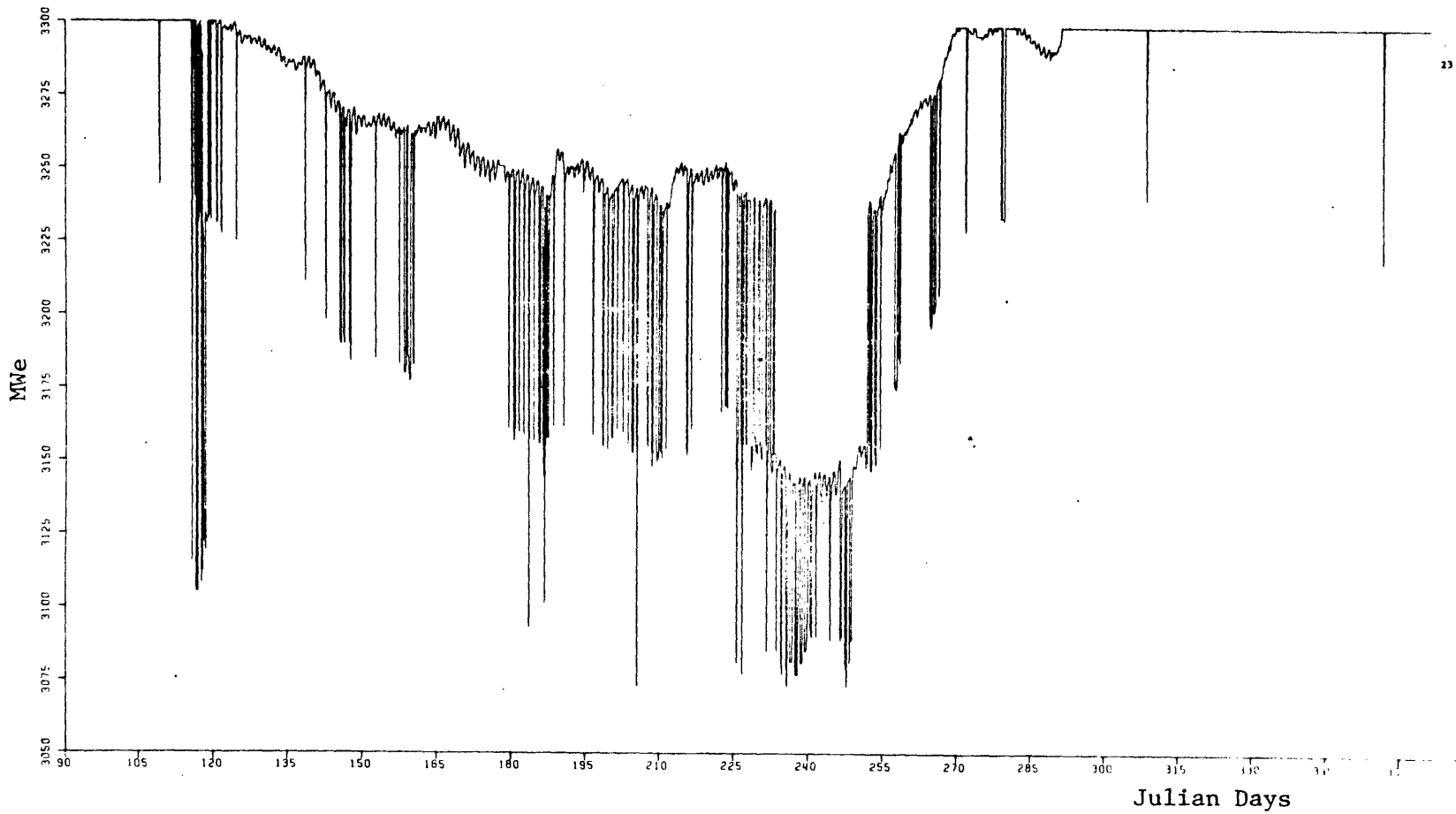

Figure 5.8 Power Output in Best Mode for Addition of Estimated ΔT Model to Base Case A

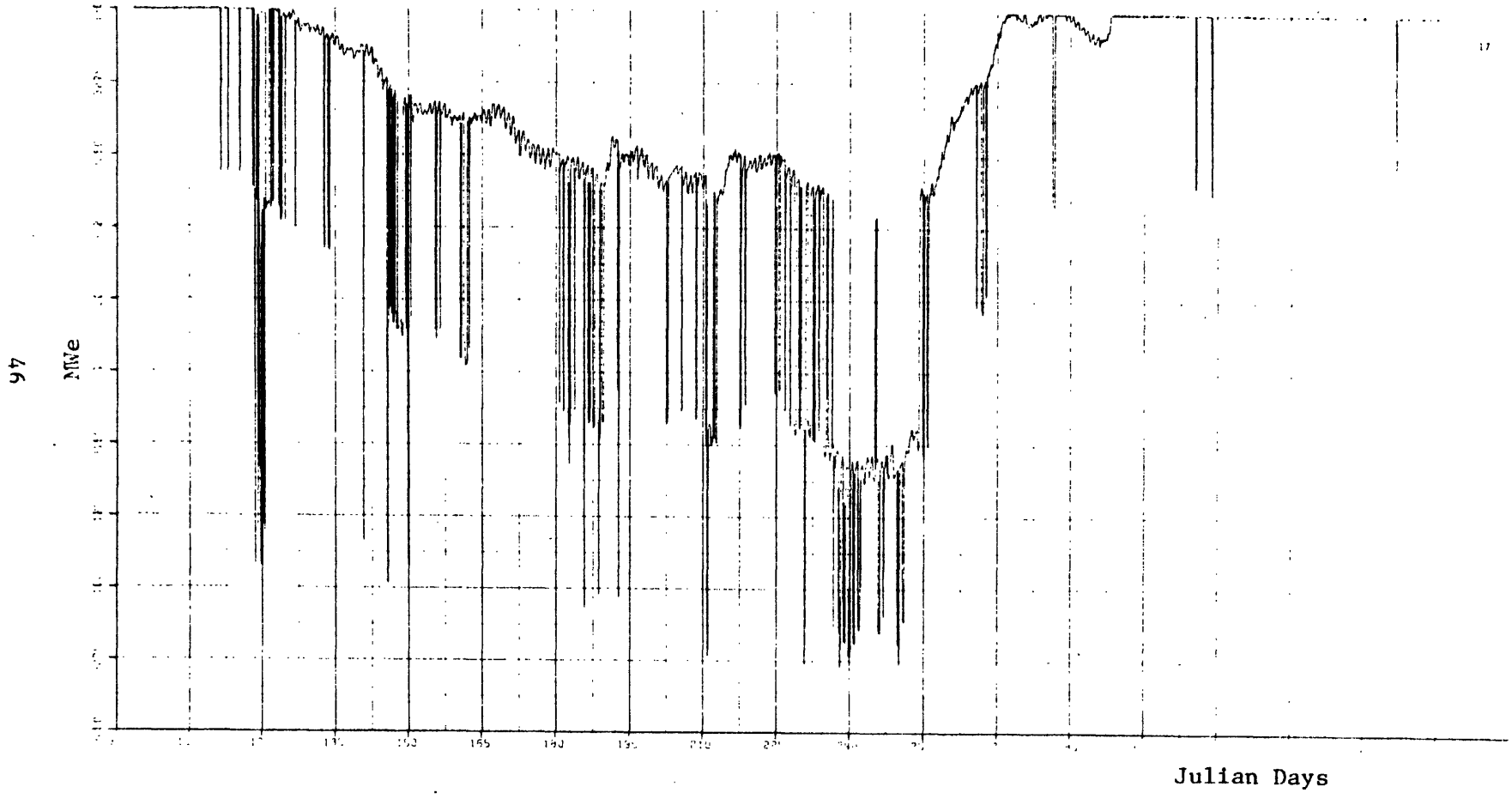

Figure 5.9 Use of Downstream Station 10 on Power Output in Best Mode

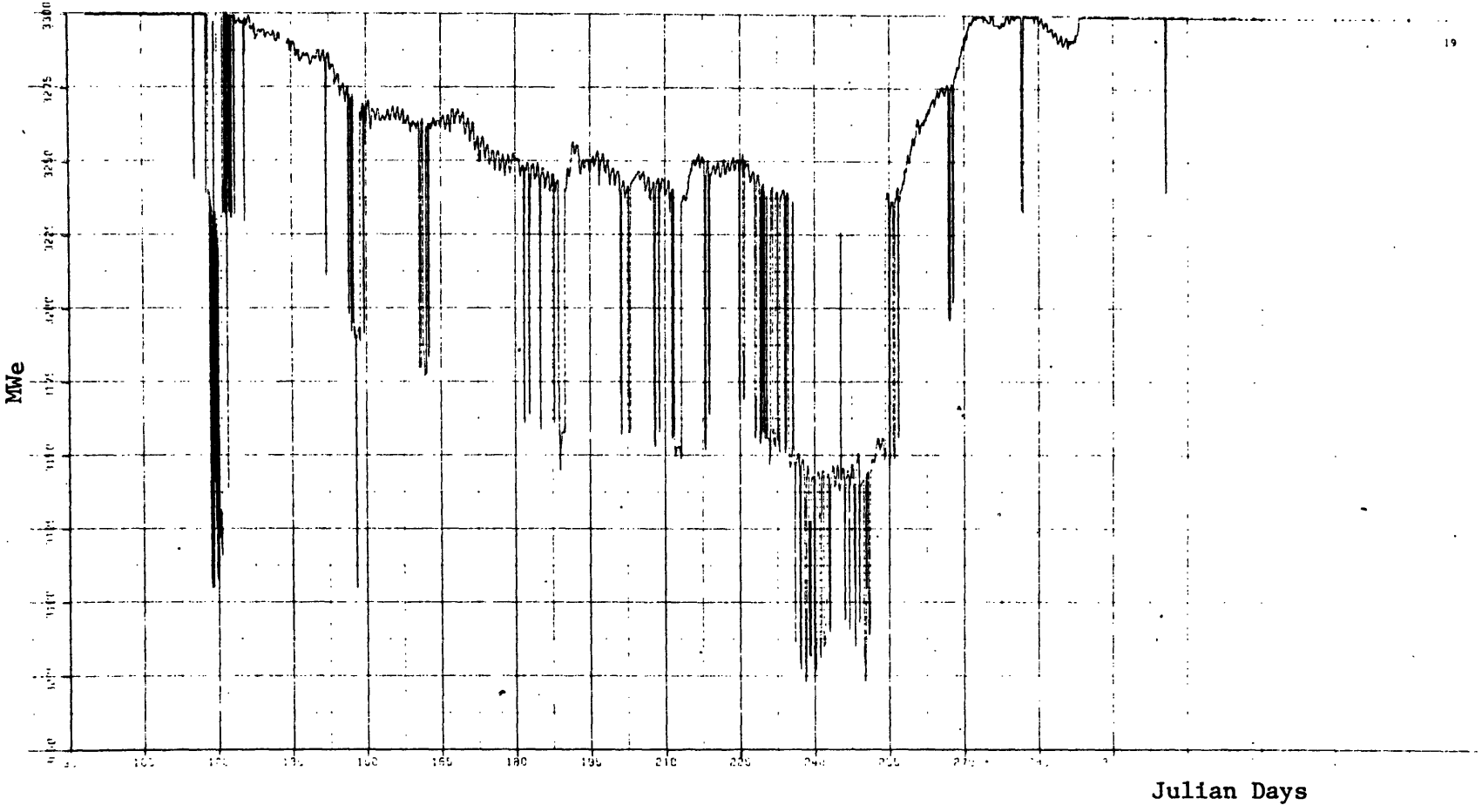

Figure 5.10 Use of Downstream Station 11 on Power Output in Best Mode

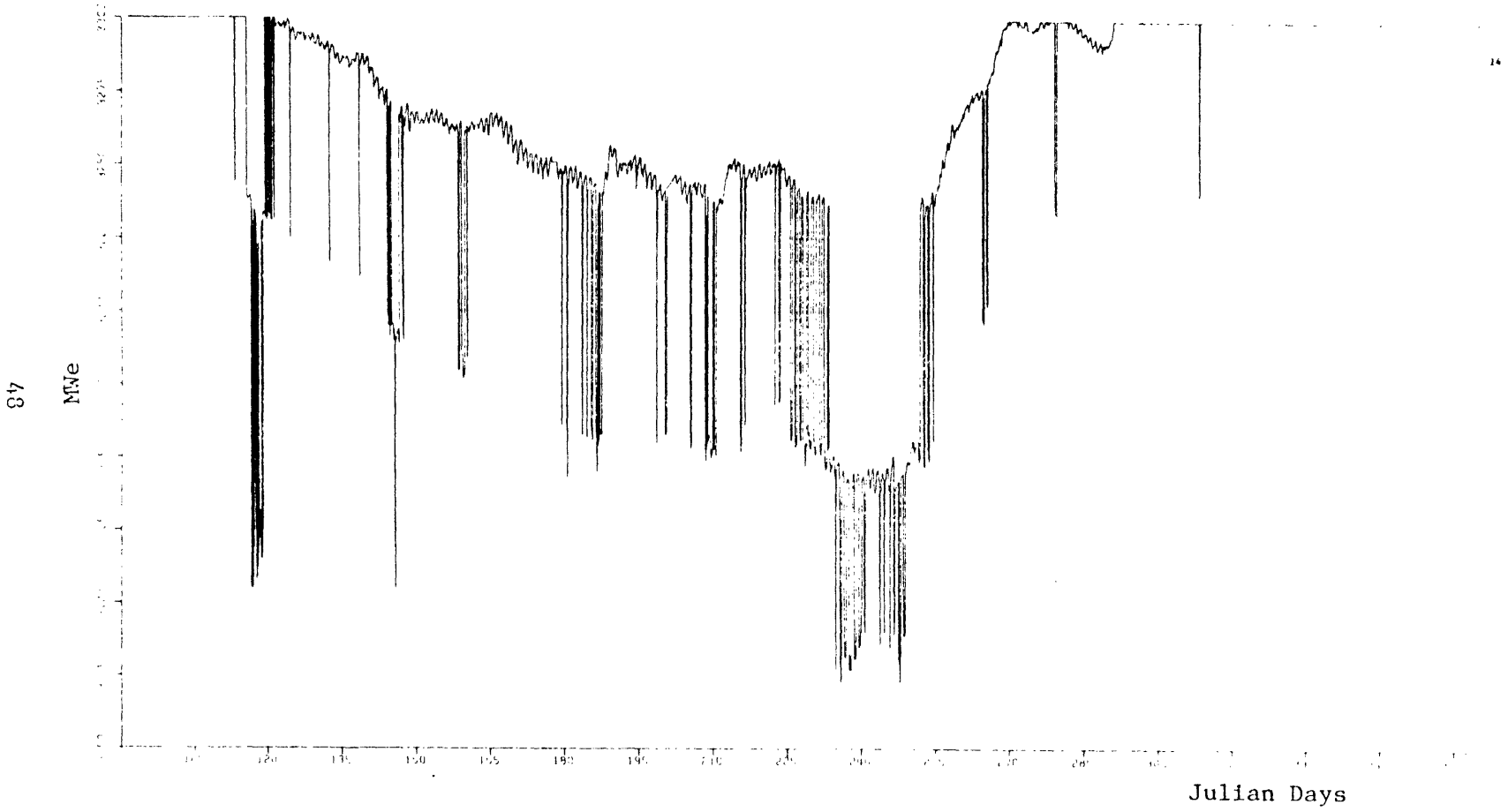

Figure 5.11 The Results of Downstream Stations 9,10 & 11 Averaging on Power Output in Best Mode

less power losses in both the spring and the fall, but, actually uses slightly more closed mode operation during the late summer period.

The estimated ΔT 1D model was applied to the above cases with the resulting power output in best mode plots shown in Figures 5.12, 5.13 and 5.14. In all cases the use of the 1D model lowers the power losses. In Figure 5.12 (Station 10) closed mode operation doesn't occur in the spring. Figure 5.13 (Station 11) shows only one hour of closed mode operation except for the late summer periods. Both stations also show reductions in the use of helper mode operation. The use of the 1D model with the Stations 9,10 & 11 (Figure 5.14) spatial average reduces the use of cooling towers throughout the observation period, except during late summer. Reductions of helper mode are also noticeable, but, not as much as with Station 10 & 11 separately.

Figure 5.15 shows a composite of the sorted power loss curves for the above evaluations. Station 10 shows slightly less losses than the Stations 9,10 & 11 spatial average. This is probably the case due to the influence of Station 9 in the spatial average. Station 11, however, shows a lot less use of helper mode than the Station 10 or Stations 9,10,11 spatial average. This is probably due to its mid-channel location. An interesting result occurs for the addition of the estimated ΔT 1D model. The model does better using the individual stations than the spatial average, much more so than the difference between the single station versus the spatial average without the model.

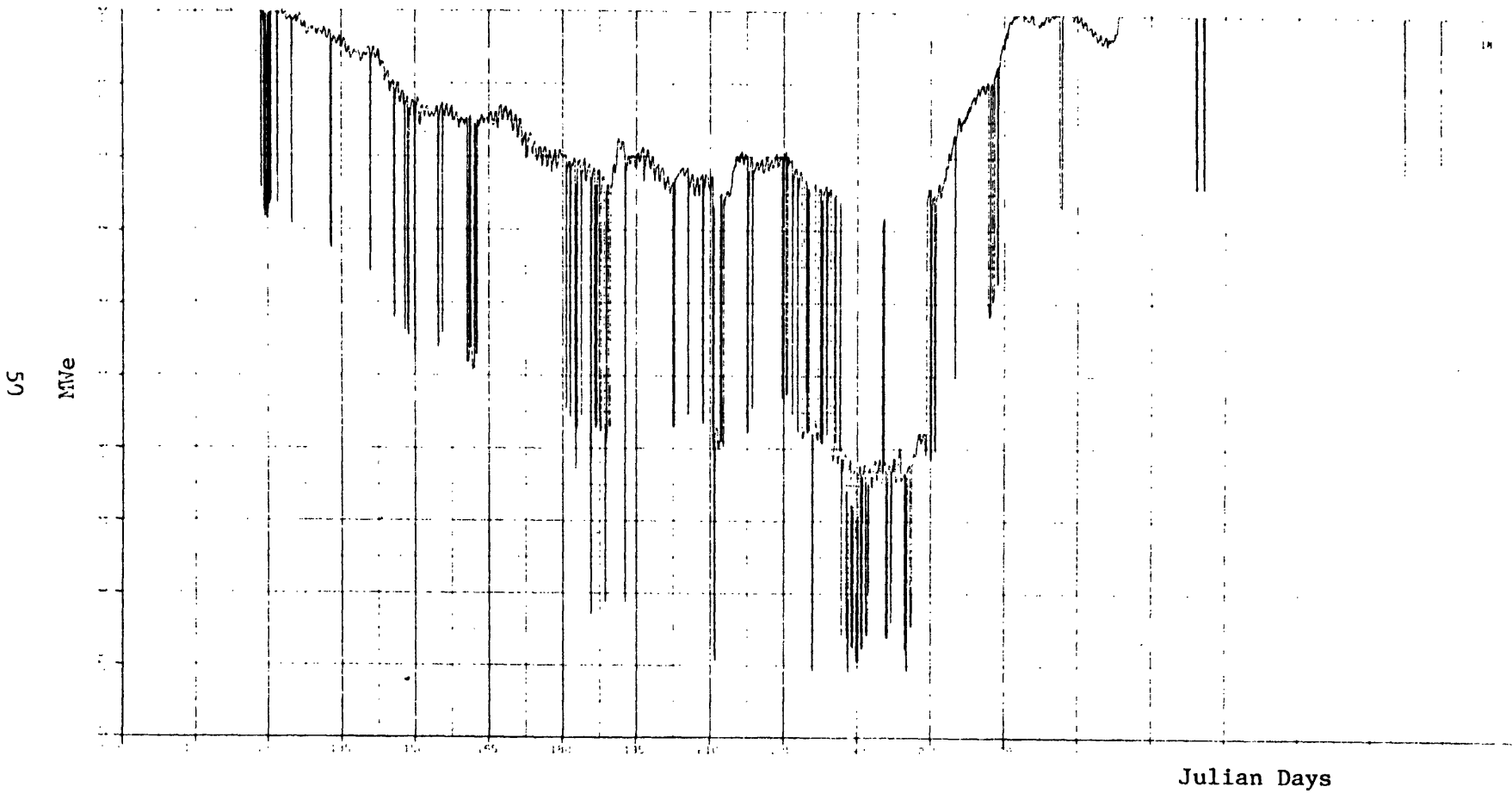

Figure 5.12 Downstream Station 10 Power Output in Best Mode Using Estimated ΔT 1D Model

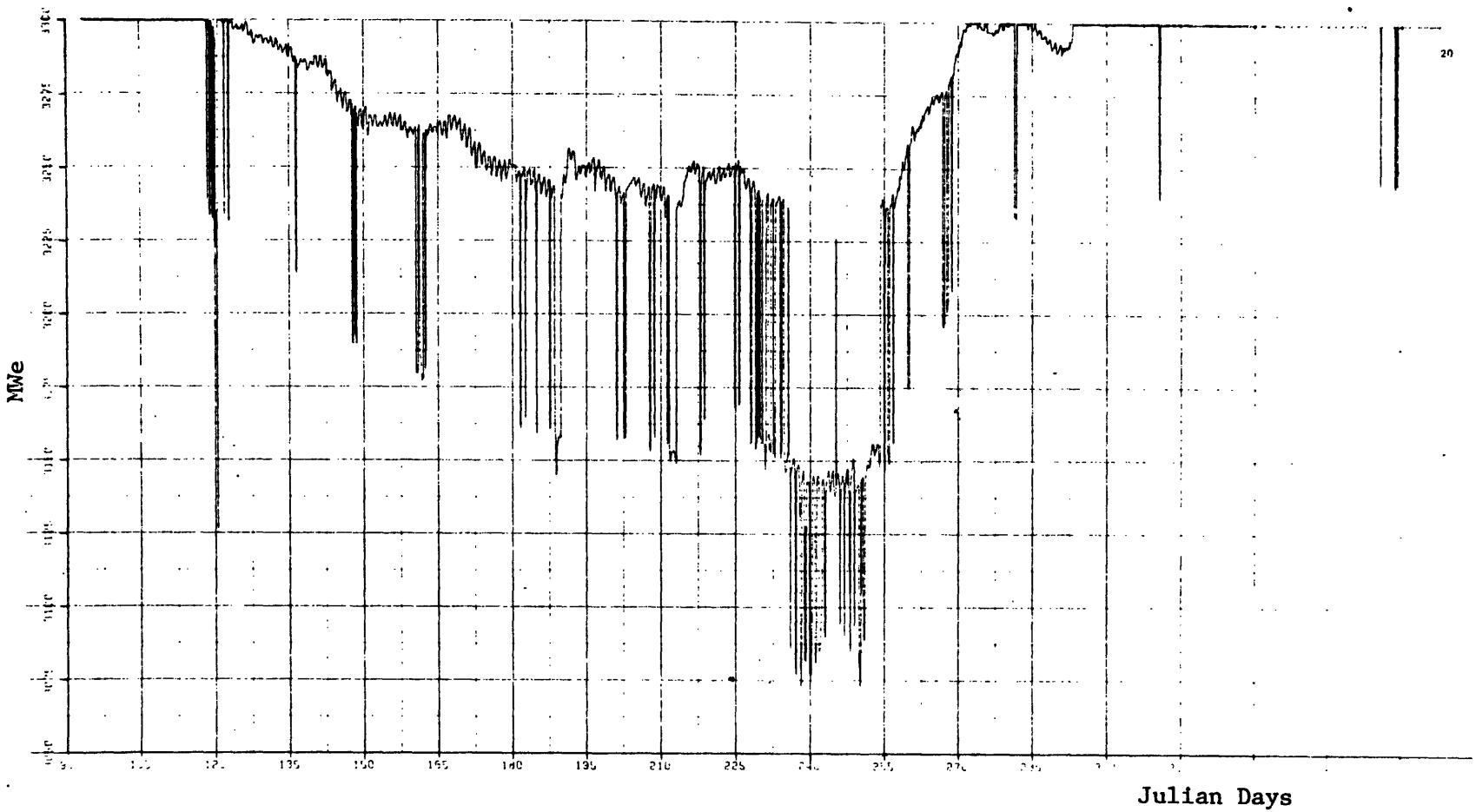

Figure 5.13 Downstream Station 11 Power Output in Best Mode Using Estimated ΔT 1D Model

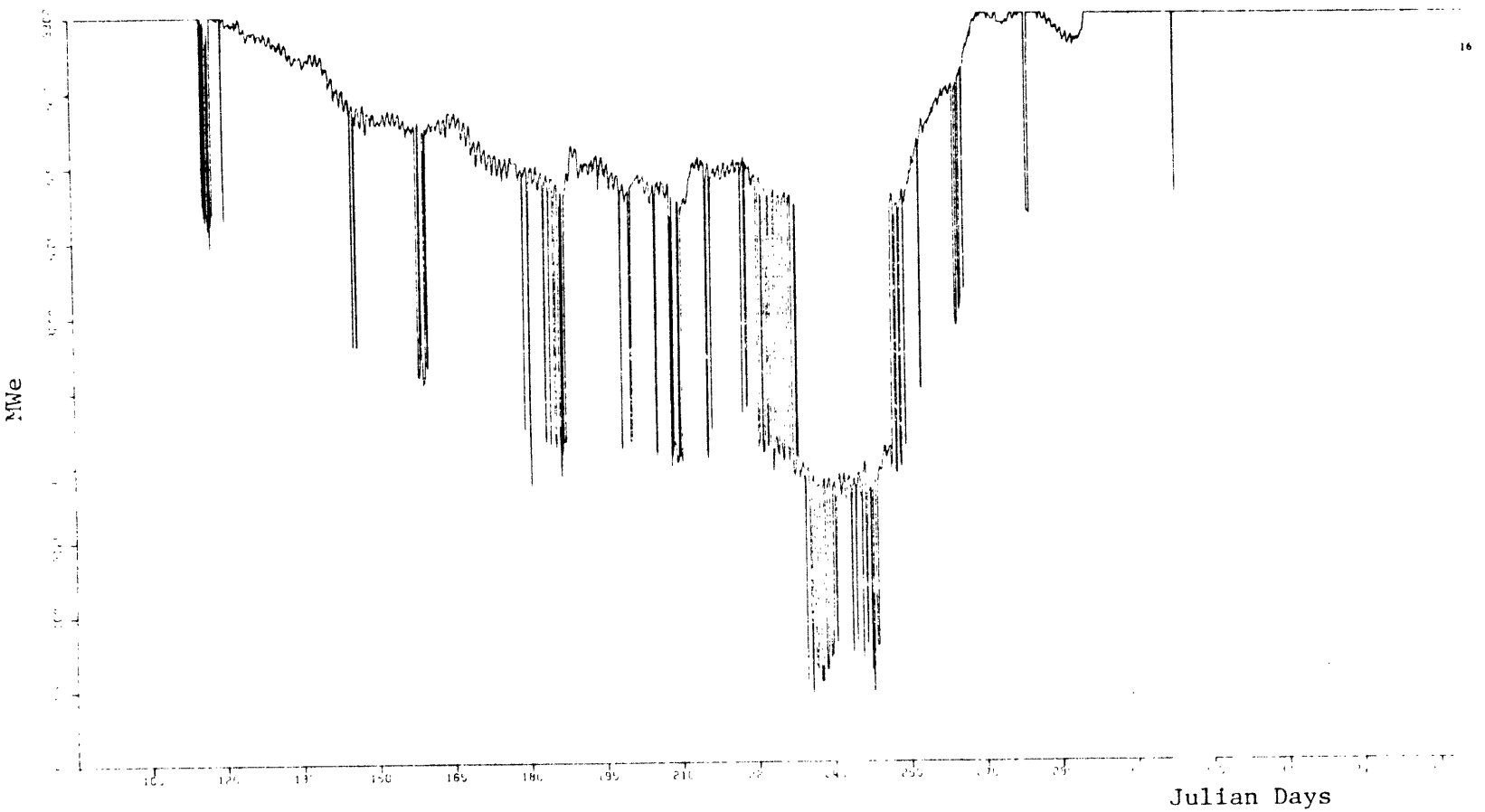

Figure 5.14 Downstream Stations 9,10 & 11 Spatial Average Power Output in Best Mode Using Estimated ΔT 1D Model

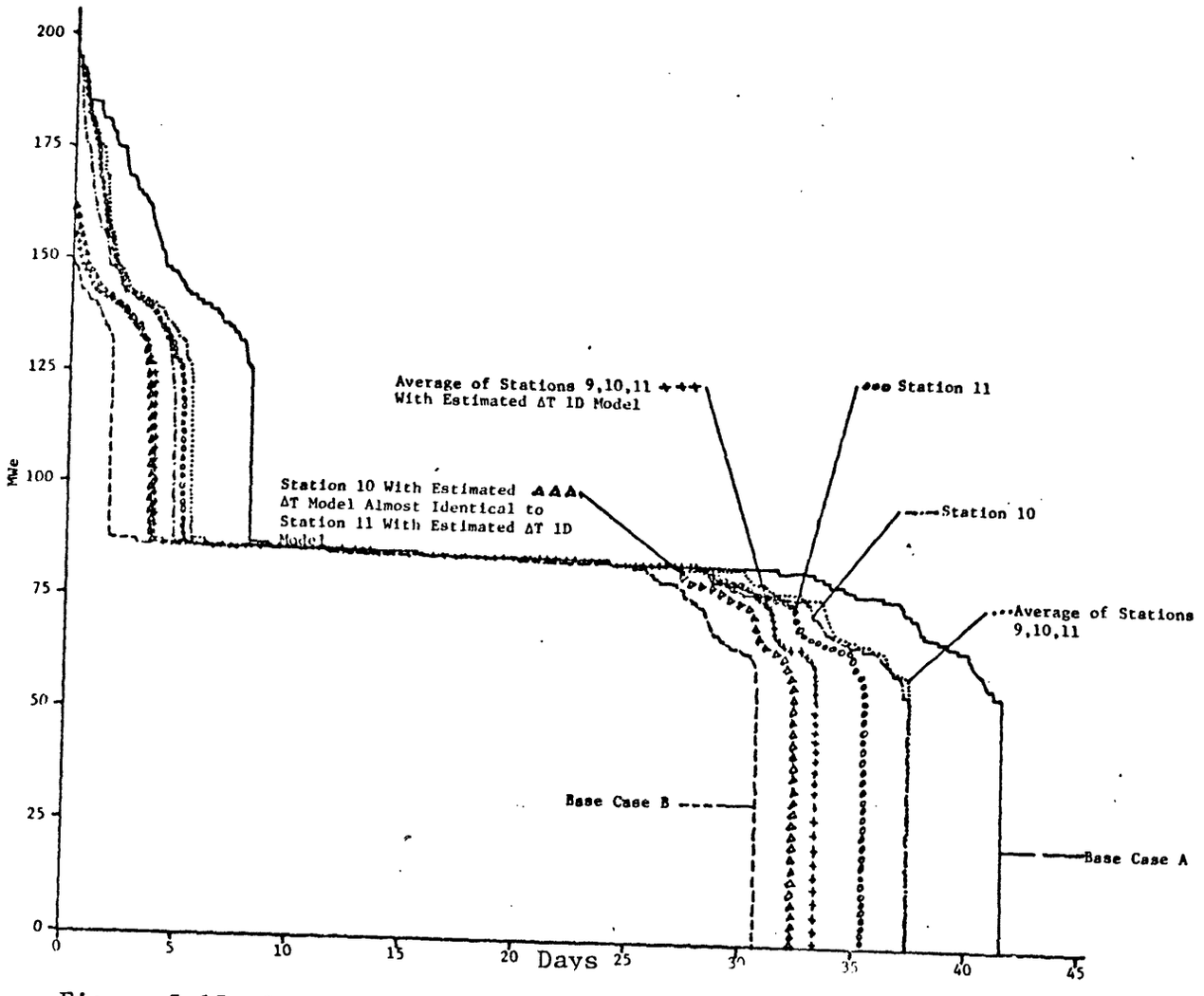

Figure 5.15 Comparison of Sorted Power Loss Curves for Monitor Location and Spatial Average Studies Including the Use of the ΔT 1D Model

5.3.2 Time Averaging

The power output in best mode graphs shown in Figures 5.16 through 5.21 represent the effects of time averaging using Station 9 as the downstream station. Upstream, downstream, and induced river temperatures were all time averaged before selecting the best mode of operation within the standards constraints. Periods of 2,24, and 48 hours were examined both without the estimated ΔT 1D model(Figures 5.16, 5.17, and 5.18)and with it (Figures 5.19, 5.20, and 5.21). The Figures are compared with Base Case A, Figure 5.5, and Base Case A with estimated ΔT 1D Model, Figure 5.8.

In general increased time averaging of river temperatures and induced temperatures decreases power loss by removing or decreasing some of the temperature excursions above the standard's limit. In decreasing this variance, some short term violations causing the plant to switch from open to helper (or helper to closed) have been reduced. This is particularly true during spring heat up periods (see the spring periods of the power output in the best mode graphs). Note, however, that the same mechanism operates in reverse. There are periods where short term temperature dips allowing the plant to switch from helper to open (or closed to helper) are being removed by increased time averaging resulting in increased power loss. This reverse mechanism is most important during fall cool down (see fall portions of power output graphs).

The net effect for the year is decreased power loss with increasing temperature averaging, but a few exceptions in our results demonstrate the importance of the mechanism operating in reverse. Note there is

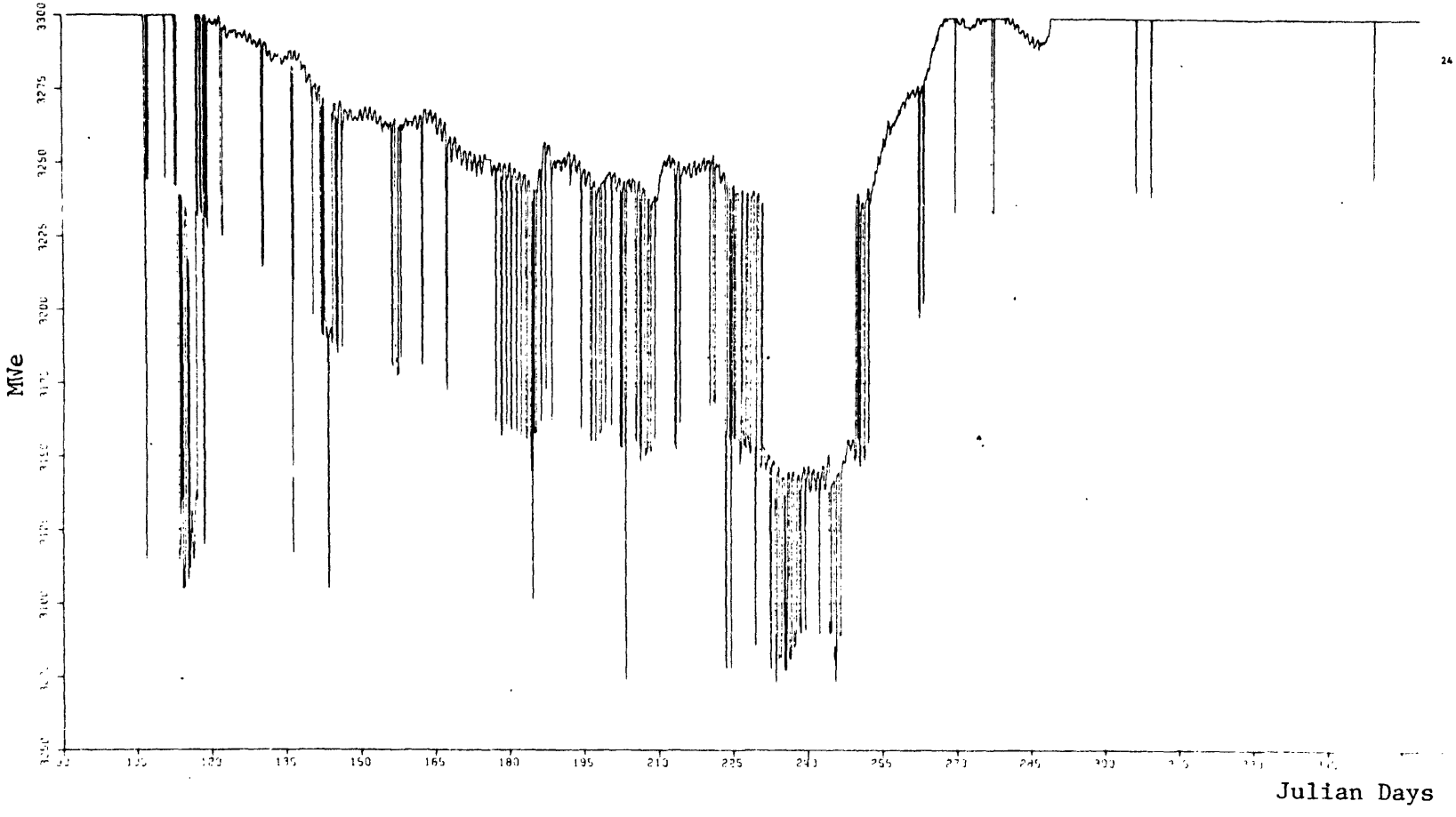

Figure 5.16 Two Hour Running Time Average Power Output in Best Mode (Downstream Station 9)

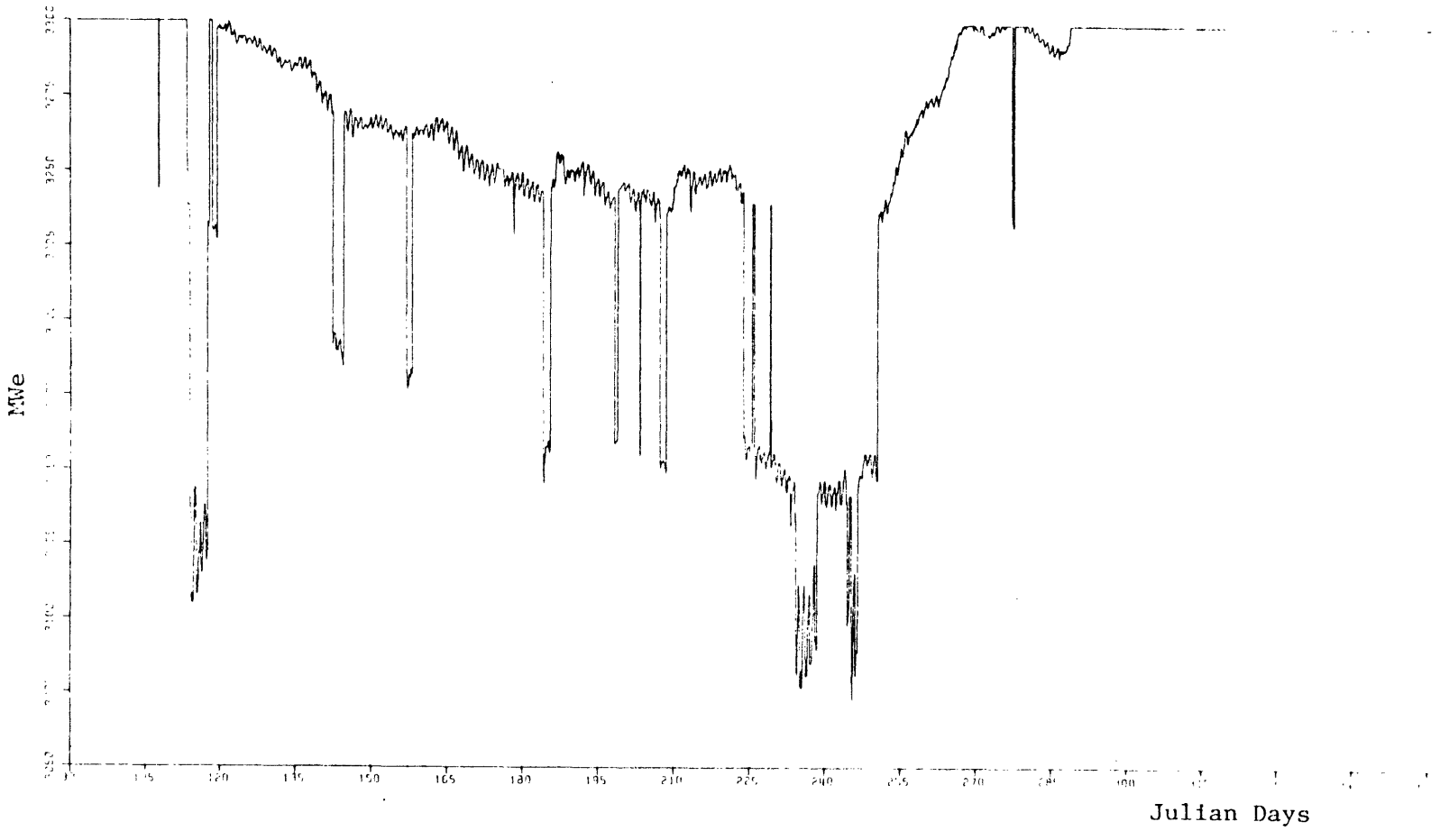

Firue 5.17 Twenty-Four Hour Running Time Average Power Output in Best Mode (Downstream Station 9)

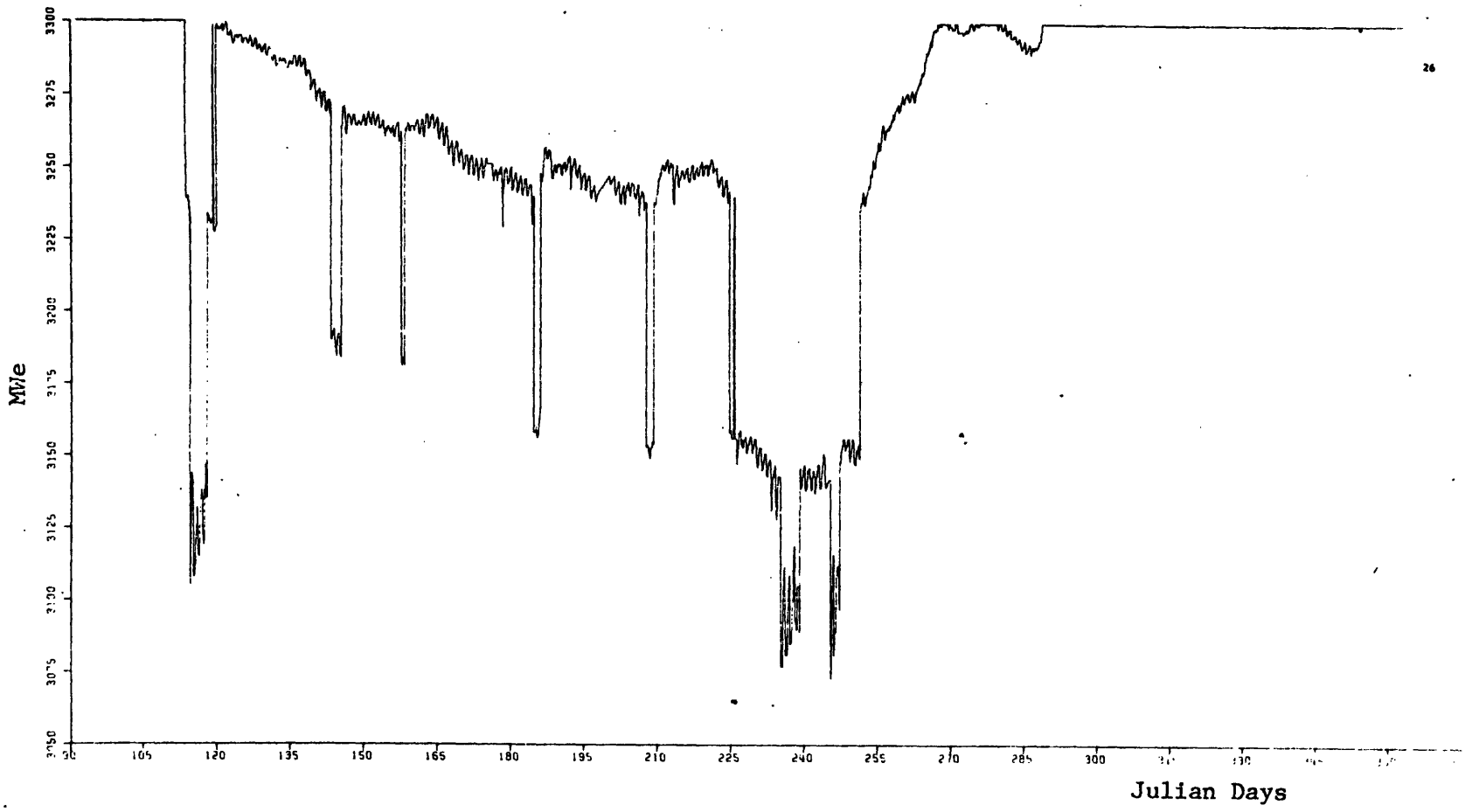

Figure 5.18 Forty-Eight Hour Running Time Average Power Output in Best Mode (Downstream Station 9)

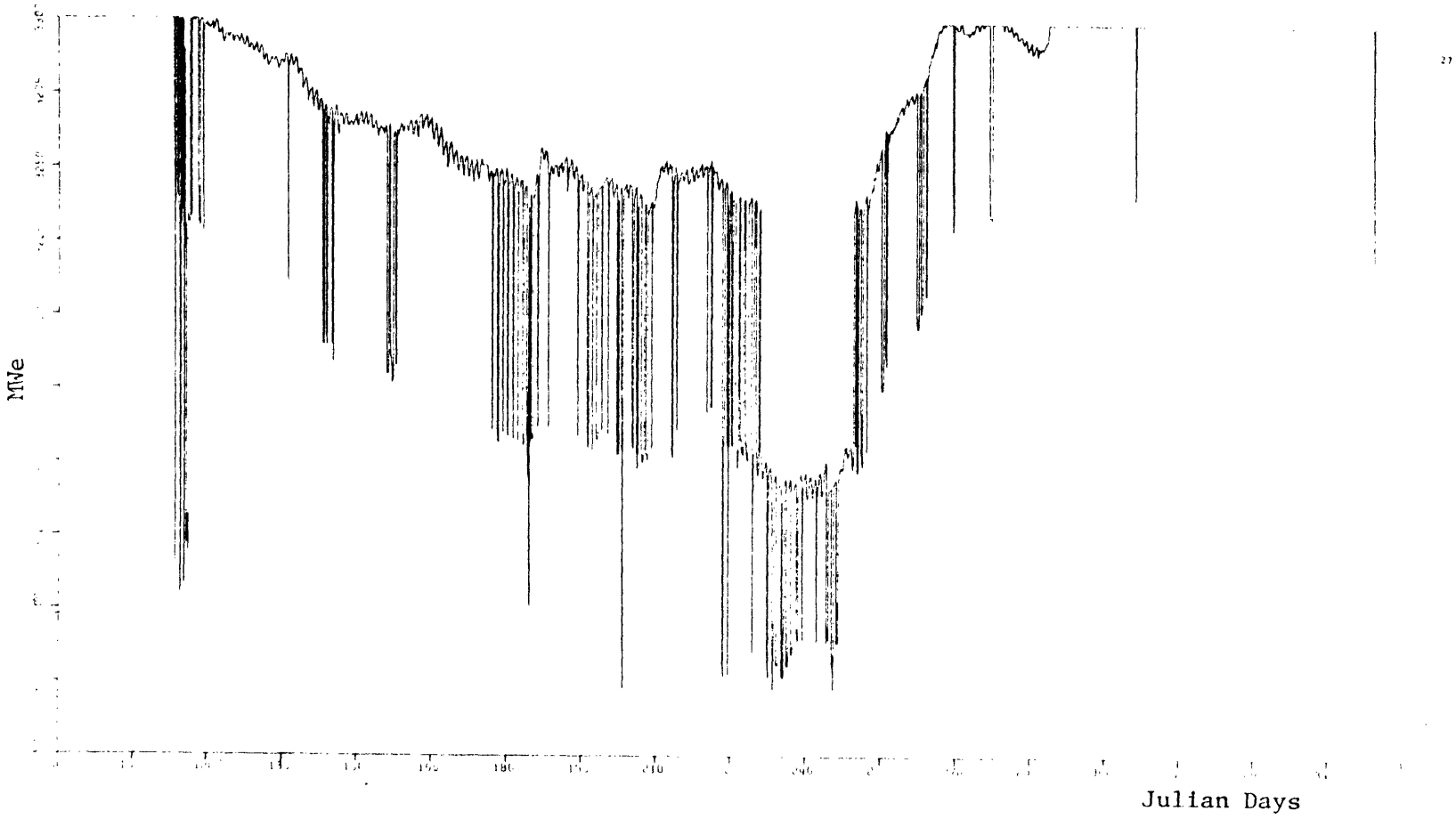

Figure 5.19 Two Hour Running Time Average Power Output in Best Mode Using ΔT 1D Model (Downstream Station 9)

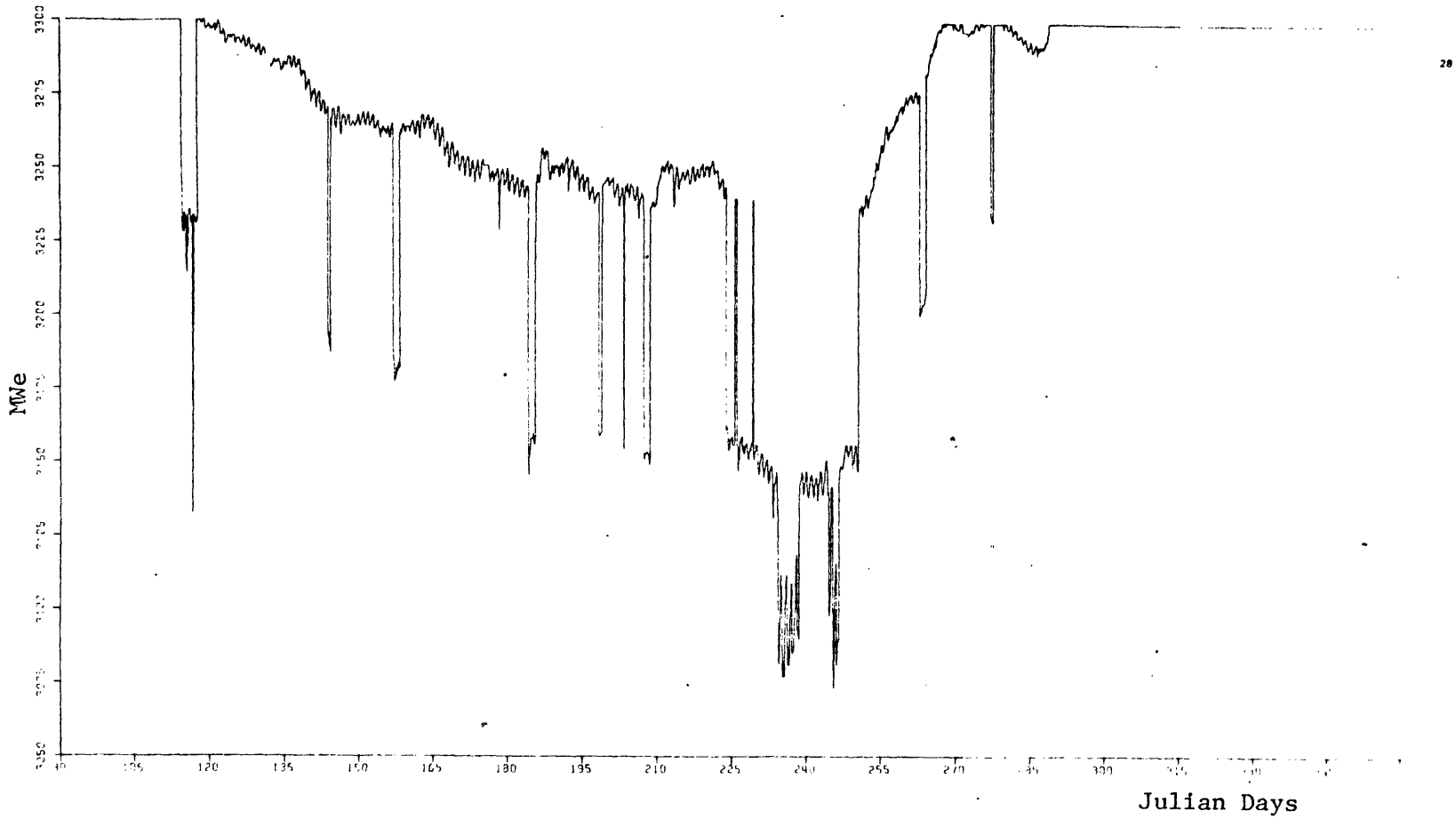

Figure 5.20 Twenty-Four Hour Running Time Average Power Output in Best Mode Using ΔT 1D Model (Downstream Station 9)

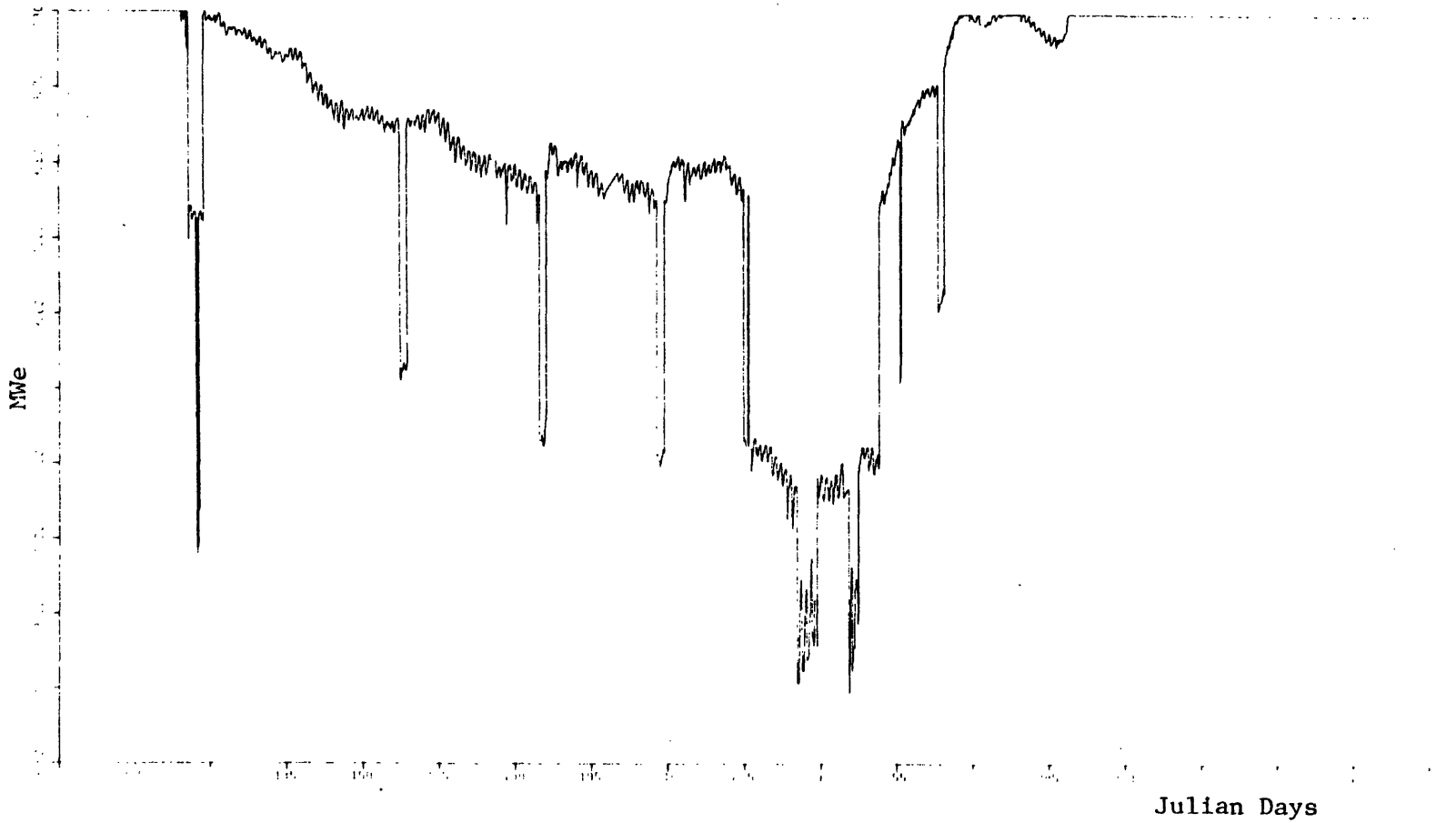

Figure 5.21 Forty-Eight Hour Running Time Average Power Output in Best Mode Using ΔT 1D Model (Downstream Station 9)

one case (Station 9 including the 1D Model's estimated ΔT) where going from no averaging to a two hour running average increased the year's cumulative power loss (see Table of Cumulative Power Loss, Sec. 5.5) in contrast to the general trend. Also observe the reversal in the sorted power loss curves (Figure 5.22). Here generally curves with increasing time averaging are lower than curves with less time averaging and spend less time off of closed mode as illustrated by the intersection point with the time axis. The result is lower cumulative power loss (the area under the sort curves) for cases with more time averaging. There's one area where the curves cross however, between 10-20 days which represents in terms of operating time the shift from closed to helper. The crossing here suggests time averaging is causing the plant to operate more hours in closed mode.

Power loss is decreased for all running averages by including the 1D Model's estimated ΔT. Neglecting that gain, the gain in power production for going to a 48 hour running average from no time averaging is about the same if we include the 1D model's ΔT or not. If running averaging is increased beyond 48 hours, the gain in power production can be expected to approach a limit. The limit will be less than our limiting case where natural downstream temperature was set equal to the natural upstream temperature (see Base Case B curve Figure 5.22) and in some cases the power production of the 48 hour time average of the spatial average of Stations 9,10, & 11 was better than the natural upstream = natural downstream temp. Base Case B (see following section).

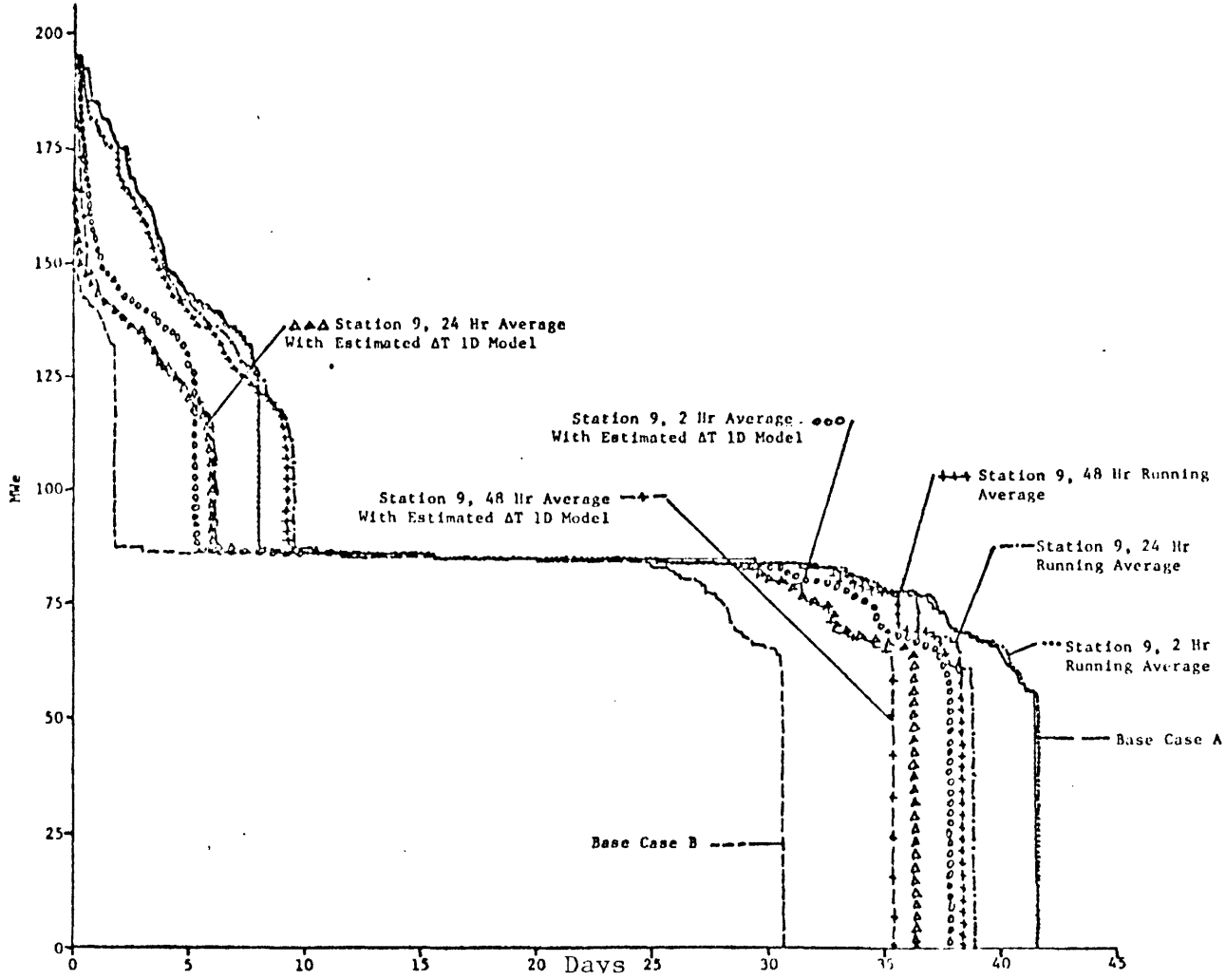

Figure 5.22 Comparison of Sorted Power Loss Curves for Time Averaging Studies Including Use of ΔT 1D Model

5.3.3 Combined Spatial and Time Averaging

In order to assess the limit of various averaging techniques a spatial average of downstream Stations 9, 10, & 11 was combined with a 48 hour running average of the downstream temperatures. Figure 5.23 shows the results as the power output in best mode graph. The general character of the graph follows the effect of the 48 hour running average by smoothing out the operation periods. The addition of the spatial average cuts down on losses primarily in late summer and the early spring.

Adding the estimated ΔT 1D Model to the combined averages cuts out more helper and closed more operation especially in the spring, but, adds some helper operation in the fall. This is shown in Figure 5.24.

Figure 5.25 shows the composite of the sorted power loss curves for the combined averaging, combined averaging with 1D Model, and the Base Cases. An interesting situation occurs when the use of the combined averaging with the estimated ΔT 1D Model gives lower temperatures than the upstream station. This appears during the closed mode-operation at the top of the curve.

5.4 Sensitivity to Changes in Environmental Standards of Plant Design

All the following analyses used upstream Station 6 and downstream Station 9 as a basis and an observation period of April 1 through November 1. Analyses of the effects of using the estimated change in temperature 1D Model or averaging methods were not considered. It was our effort to get an idea of critical areas in the standards

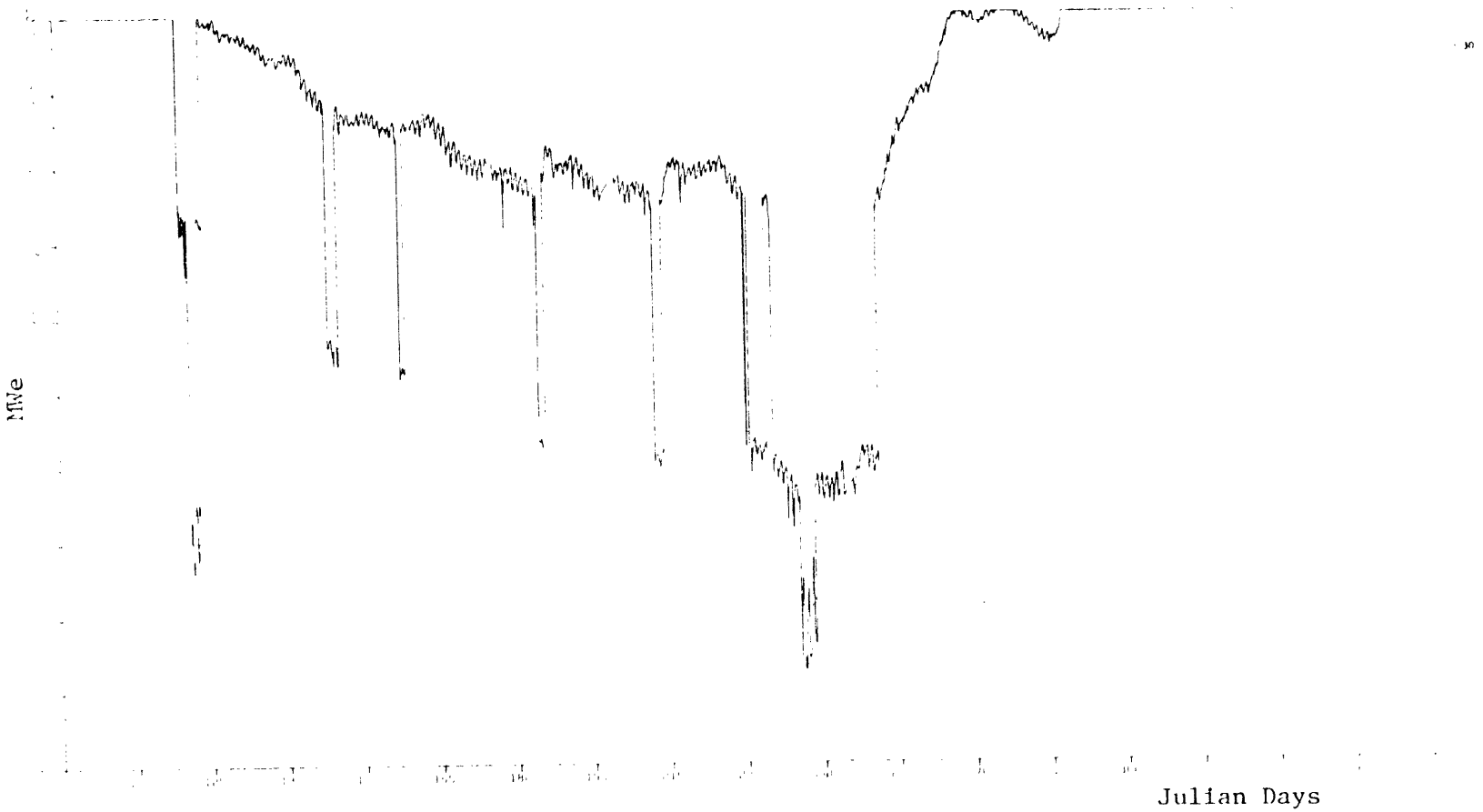

Figure 5.23 Combined Stations 9,10 & 11 Spatial Average and 48 Hour Running Time Average Power Output in Best Mode

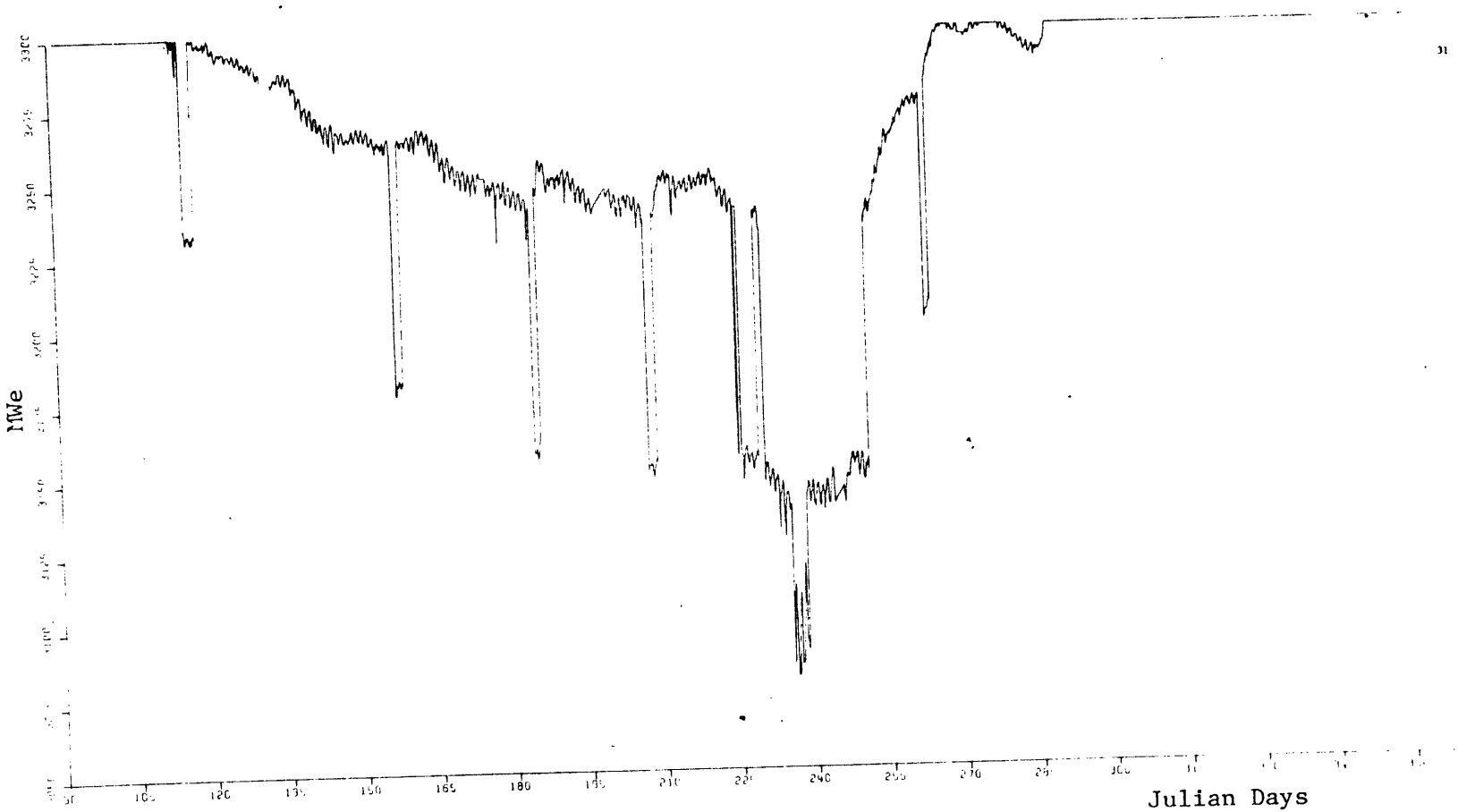

Figure 5.24 Combined Stations 9,10 & 11 Spatial Average and 48 Hour Running Time Average Power Output in Best Mode Using ΔT 1D Model

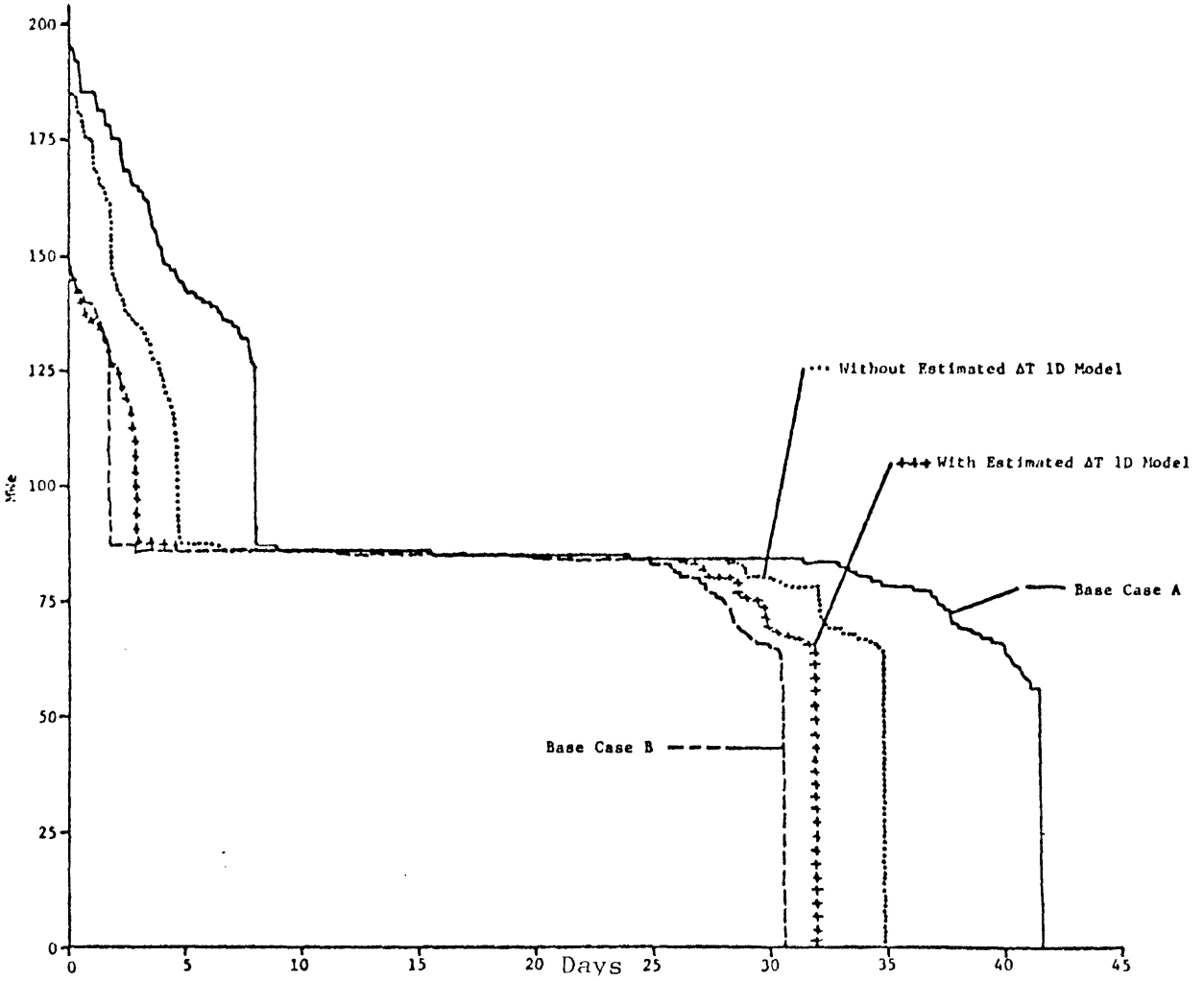

Figure 5.25 Comparison of Sorted Power Loss Curves for Combined Spatial Average (Stations 9,10 & 11) and 48 Hour Running Time Average Including Use of ΔT 1D Model

and plant design that may significantly influence power losses, and to gain an approximate magnitude of their significance.

5.4.1 Changes in Environmental Thermal Standards

Both the maximum allowable change in temperature from upstream to downstream station plus the maximum allowable temperature in the river were considered. At the present these standards are $5^{o}F$ for maximum change in temperature and $86^{o}F$ maximum allowable temperature.

The first case considered changing the maximum allowable change in temperature to $3^{o}F$. The results are shown in Figure 5.26 as the power output in best mode graph. Considerable use of both helper and closed modes of operation is needed except for the late summer period.

The second case used an allowable change in temperature of $10^{o}F$, Figure 5.27. The late summer period is unaffected since maximum temperature is the overriding factor in this period. However, during the fall and the spring a substantial savings of power loss can be found.

The third case considered a $90^{o}F$ maximum allowable temperature. Figure 5.28 shows that less power losses occur during the summer period as expected since the maximum allowable temperature is the overriding factor in cooling tower usage during this period.

Last of all, both a maximum allowable change in temperature of $3^{o}F$ and a maximum allowable temperature of $90^{o}F$ were used for an analysis. Figure 5.29 shows use of the helper mode only during the late summer period and in late April. Cooling towers were only used once during

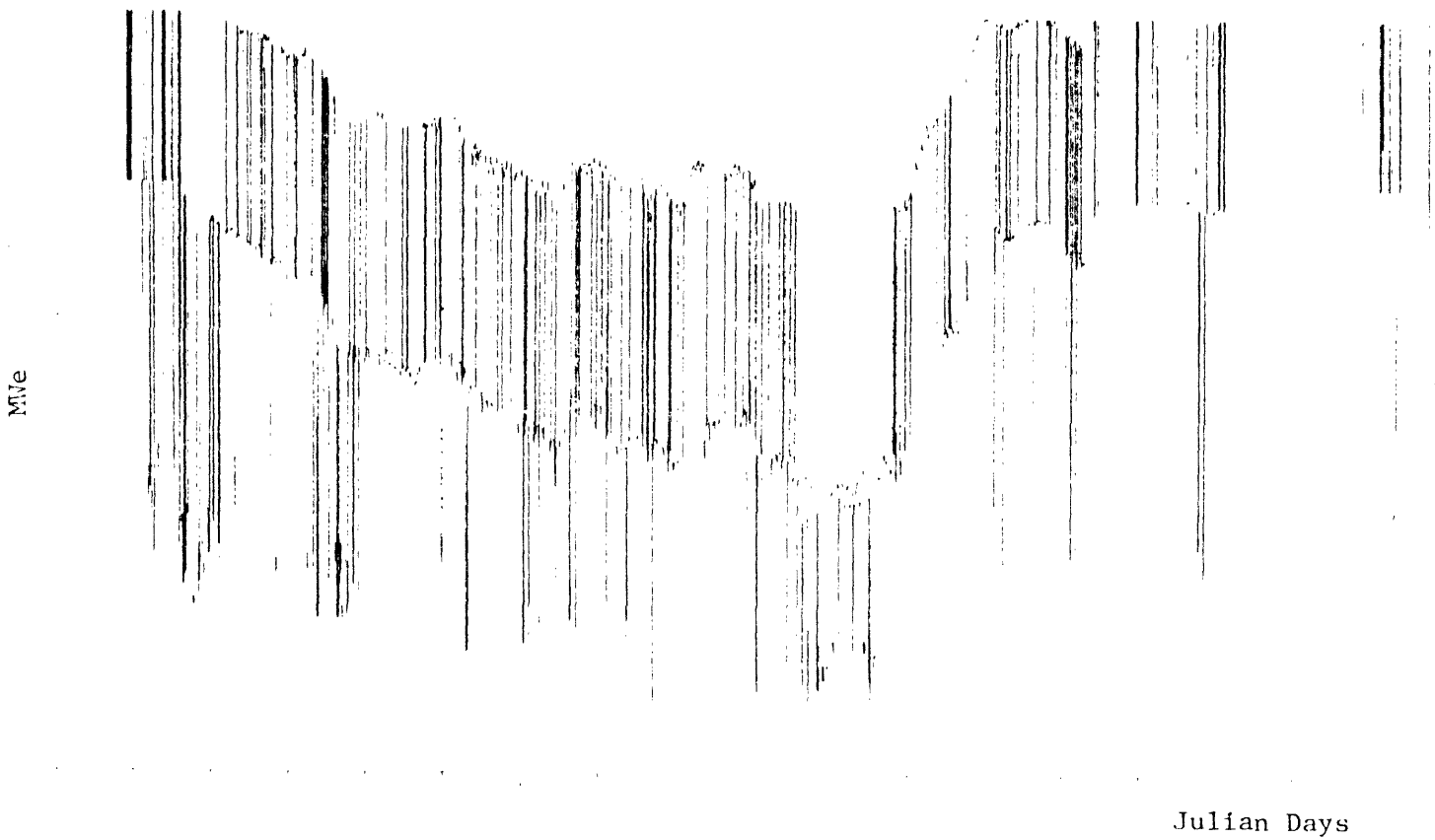

Figure 5.26 $3^{o}F$ Maximum Allowable ΔT Power Output in Best Mode

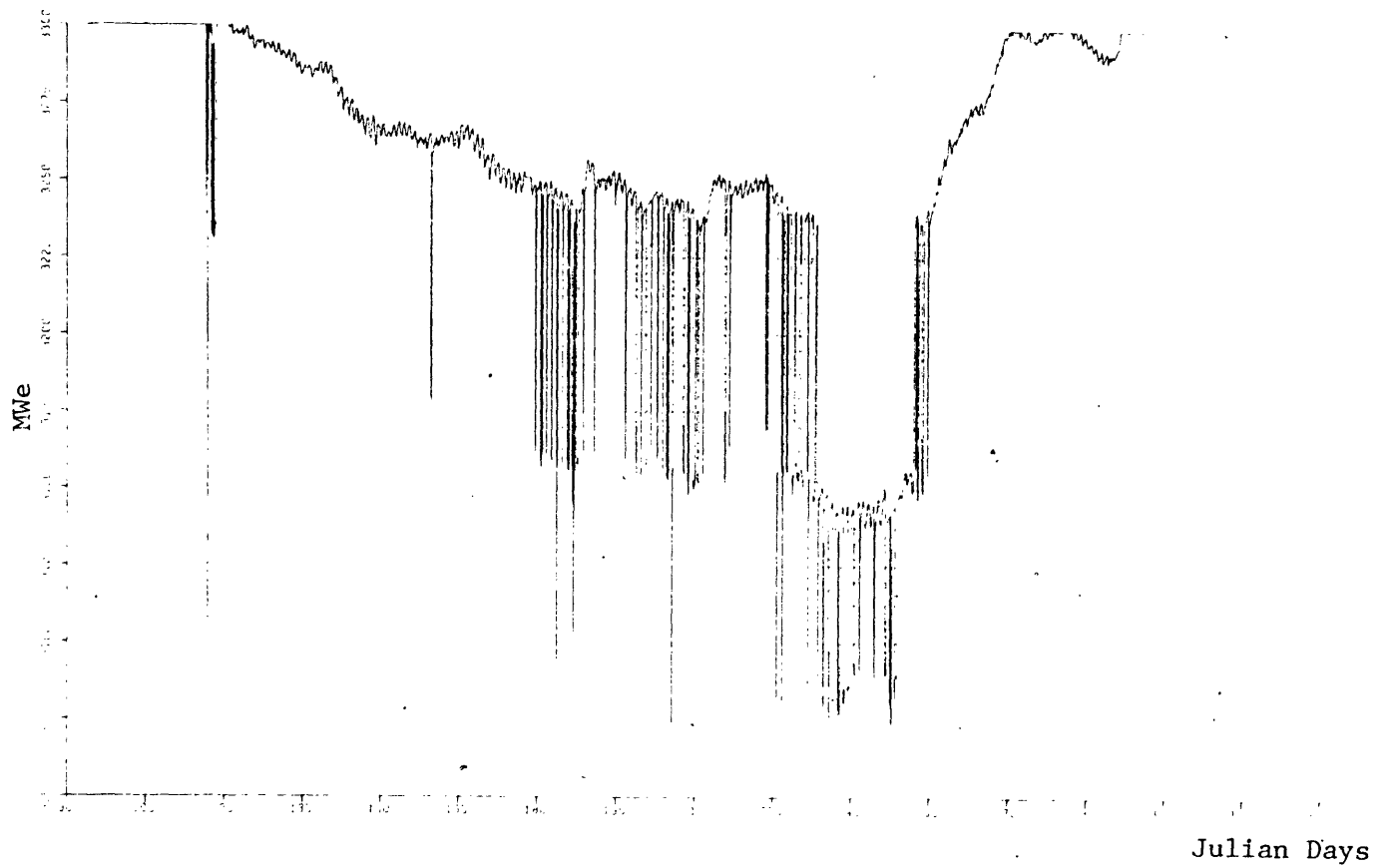

Figure 5.27 $10^{o}F$ Maximum Allowable ΔT Power Output in Best Mode

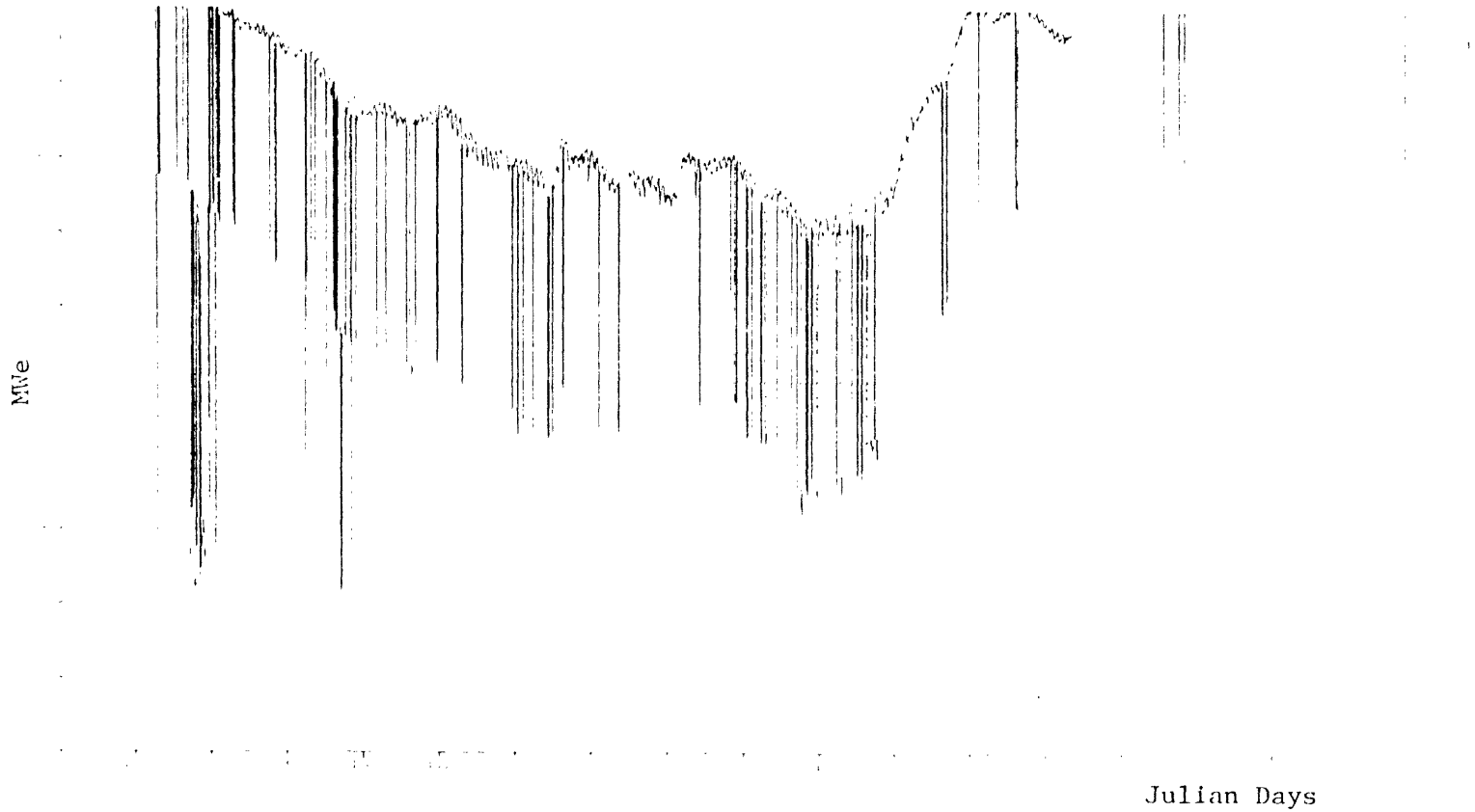

Figure 5.28 $90^{o}F$ Maximum Allowable Temperature Power Output in Best Mode

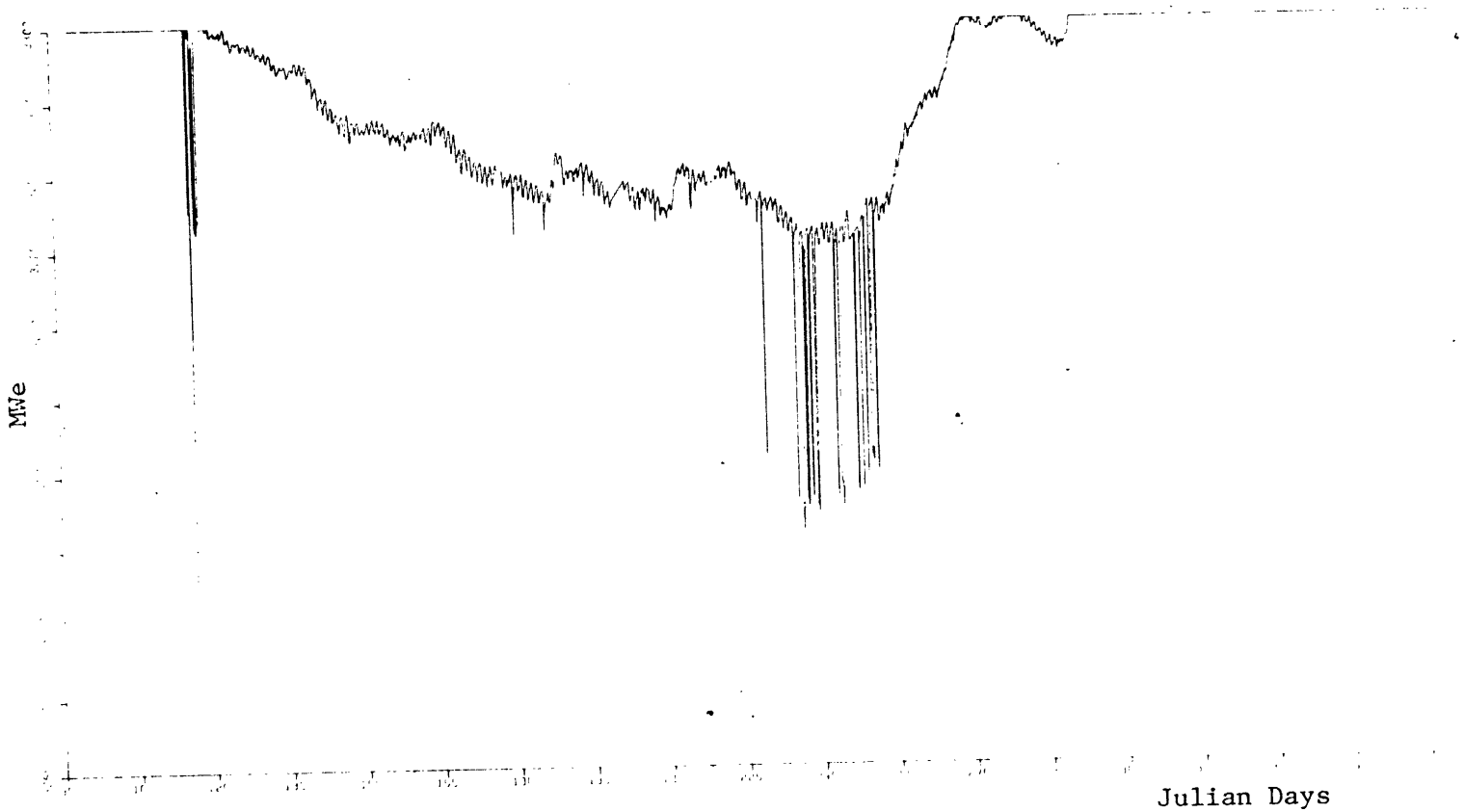

Figure 5.29 $3^{o}F$ Maximum Allowable ΔT and $90^{o}F$ Maximum Allowable Temperature Power Output in Best Mode

the entire period.

Figure 5.30 shows a comparison of the sorted power loss curves for the sensitivity of the thermal standards. Station 9 is plotted as the Base Case A. All sorted power loss curves show reduced power losses except $\Delta T = 3^{o}F$, which has a large amount of losses in this analysis. The tradeoff between the maximum allowable temperature of $90^{o}F$ and the maximum ΔT of $10^{o}F$ can be seen quite explicitly. The $\Delta T = 10^{o}F$ analysis does not save as much on the helper mode, but, does save on high power losses occuring in the spring, and the fall. The maximum temperature of $90^{o}F$ shows a reduction in a lot of the helper mode operation, but, the high spring time losses are not influenced at all. The combination of $\Delta T = 10^{o}F$ and the maximum temperature of $90^{o}F$ shows the expected drastic reduction in losses for the observation period.

5.4.2 Existence of Various Modes of Operation

The possibilities for analyzing various possible modes of operation included all open mode, no open mode, no helper mode (open/closed) and no open or helper mode (only closed).

All open mode operation and all closed mode of operation is shown in Figure 5.1. Open mode losses occur when there is a reduced plant thermal efficiency due to high natural river temperatures. All closed mode always has power losses attributed to it due to cooling tower operation.

The other possibilities are no open (Figure 5.31) and no helper mode (Figure 5.32). The no open analysis just shifts all open mode use to helper mode. In the no helper mode,all helper mode use is shifted

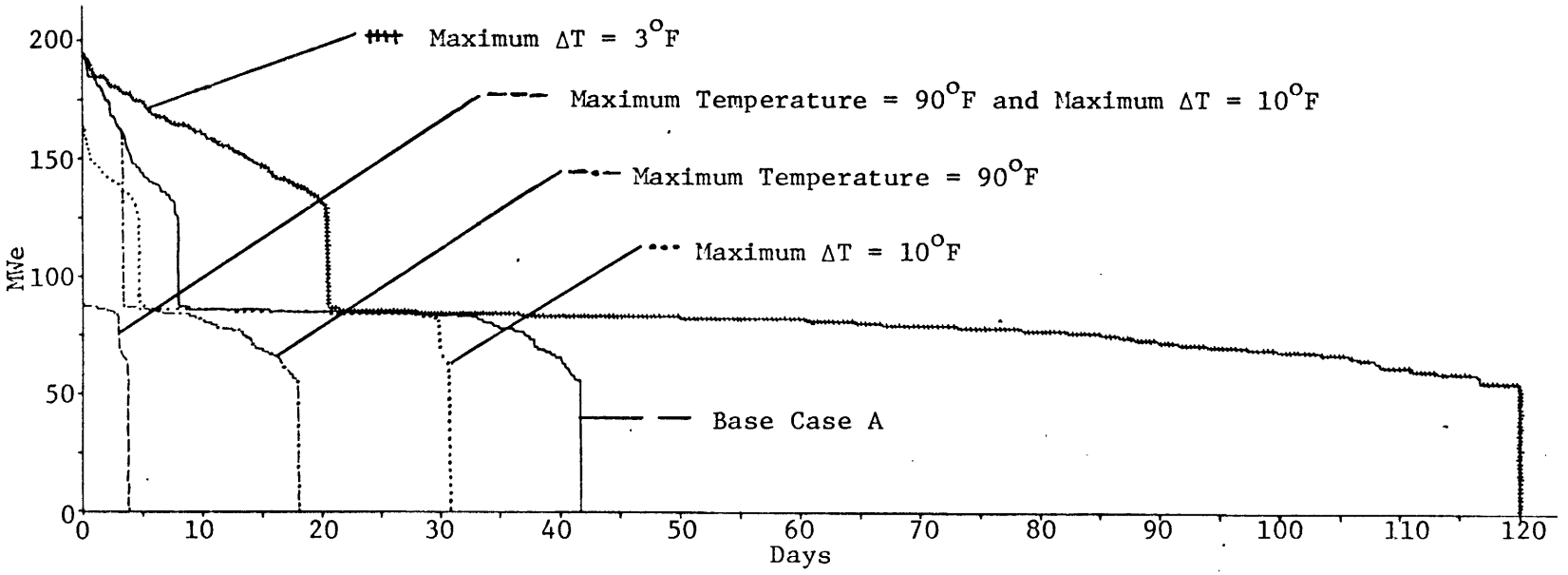

Firue 5.30 Comparison of Sorted Power Loss Curves for the Sensitivity of Thermal Standards Study

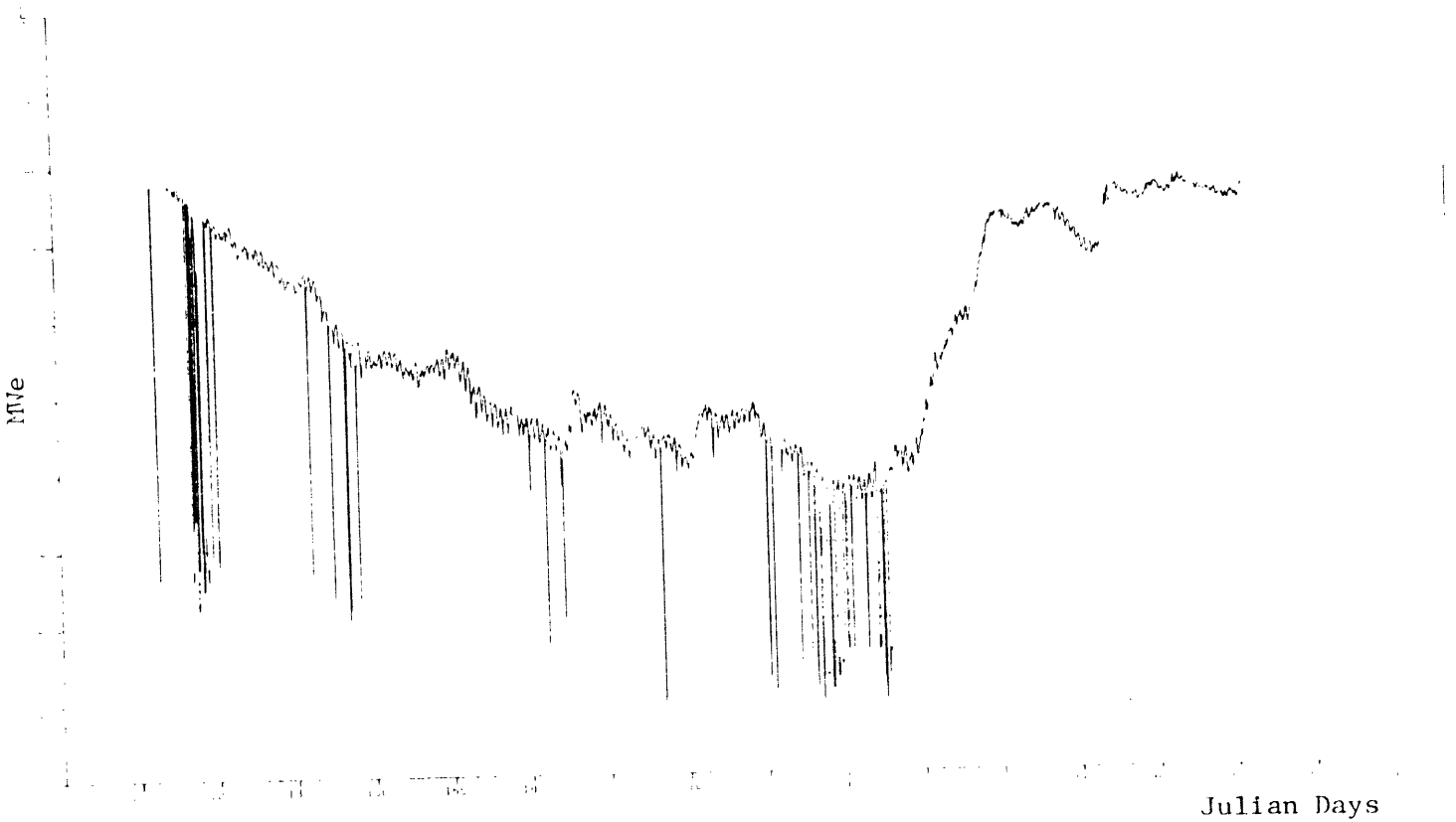

Figure 5.31 No Open Mode Power Output in Best Mode

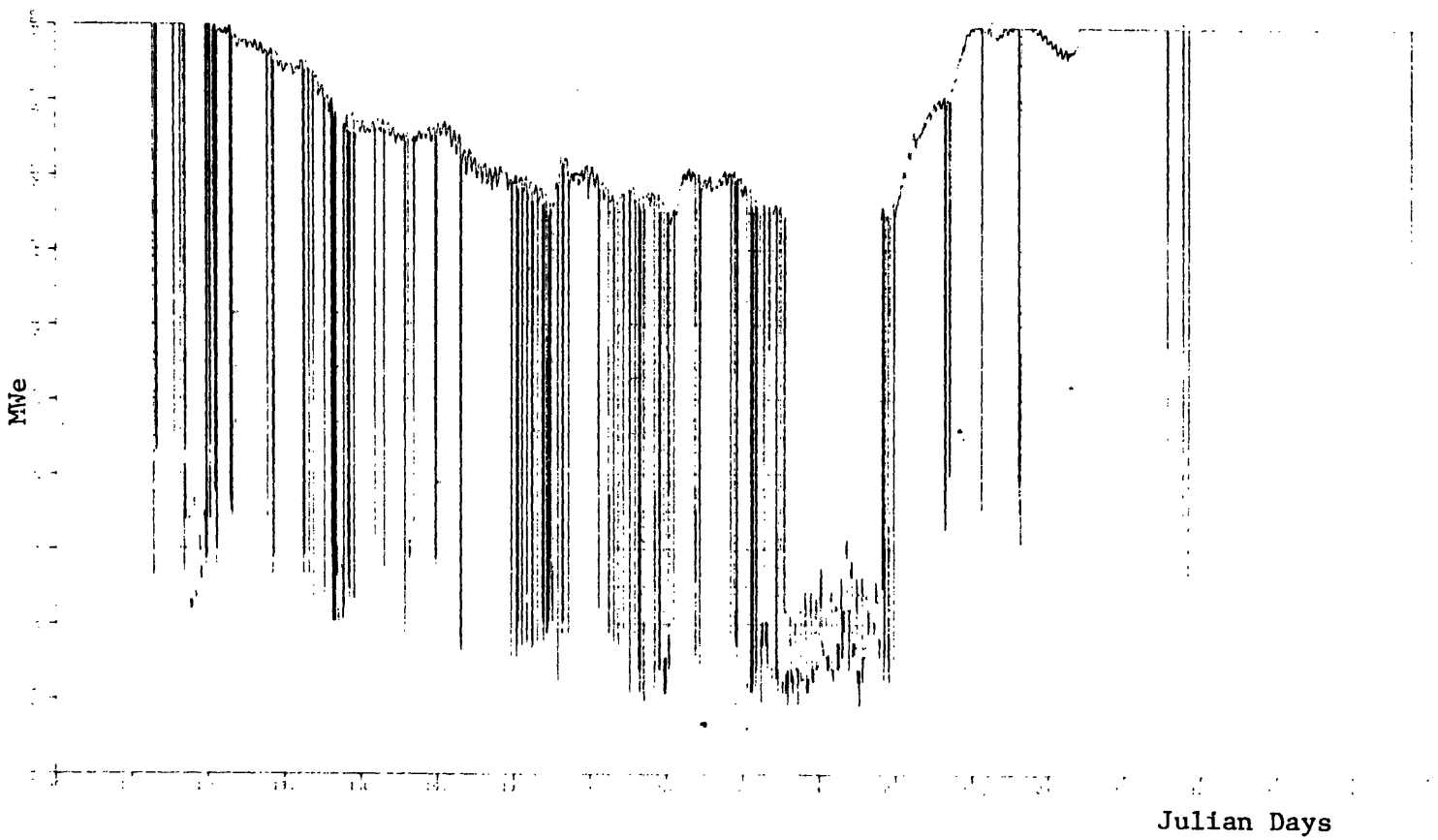

Figure 5.32 No Helper Mode Power Output in Best Mode

to closed mode. The results of these analyses are shown in the composite sorted power loss Figure 5.33. The significance of each is better described by the use of the cumulative hourly power losses. In this case all open mode is considered as having no losses. The other results are shown in Table 5.1.

Table 5.1

Mode	Cumulative Hourly Power Loss, MW hr
All Open	0
No Open	481,040
No Helper	145,664
No Open or Helper (All Closed)	911,858
Base Case A (Station 9)	96,044

5.4.3 Changes in Plant Design

Diffuser mixing and cooling tower performance were the two areas in plant design that were evaluated. Increased or decreased performance was considered for each design.

For diffuser mixing the area of the jet ports was varied to either increase or decrease mixing. In the first case (Figures 5.34) the total area was decreased by 50%. This has the effect of increasing exit velocity out the diffuser and increasing mixing. The second case (Figure 5.35) increased the total area of the jet ports by 400%. This has the effect of modeling decreased mixing. Figure 5.36 shows the sorted power losses for both cases as compared to the Base Case A (Station 9). As expected the decreased mixing case shows significantly

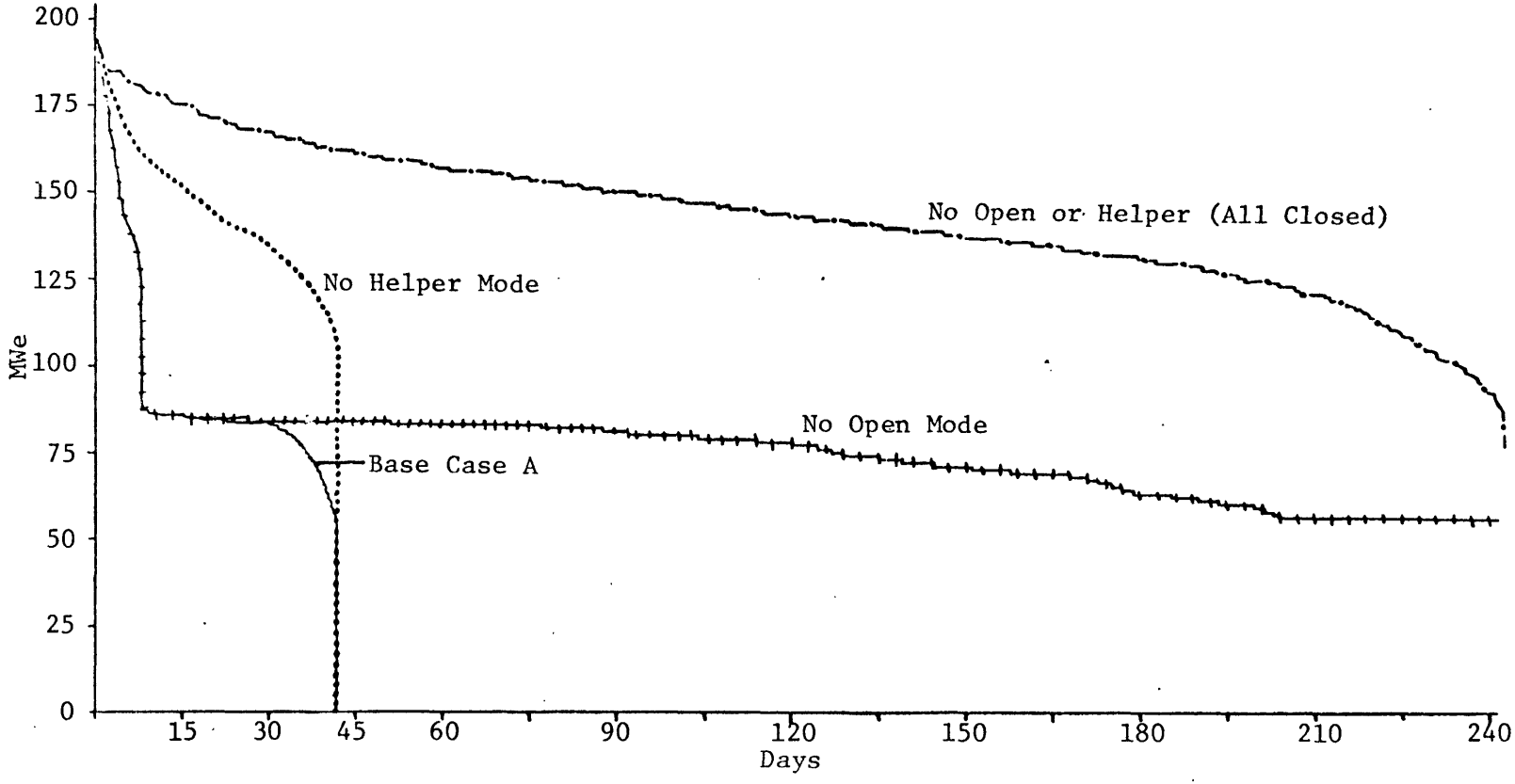

Figure 5.33 Comparison of Sorted Power Losses for Various Mode of Operation Study

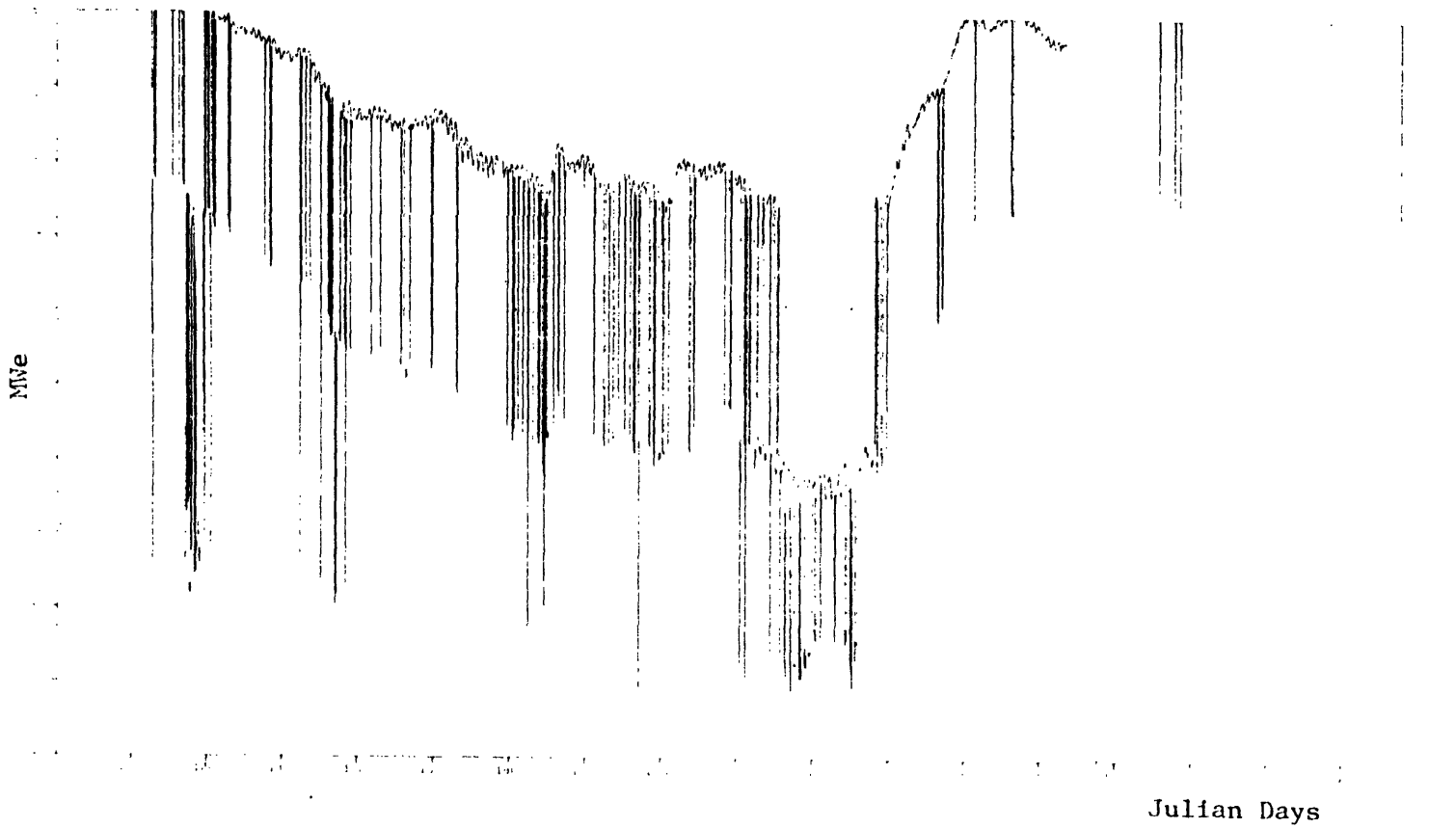

Figure 5.34 50% Decreased Diffuser Mixing Power Output in Best Mode

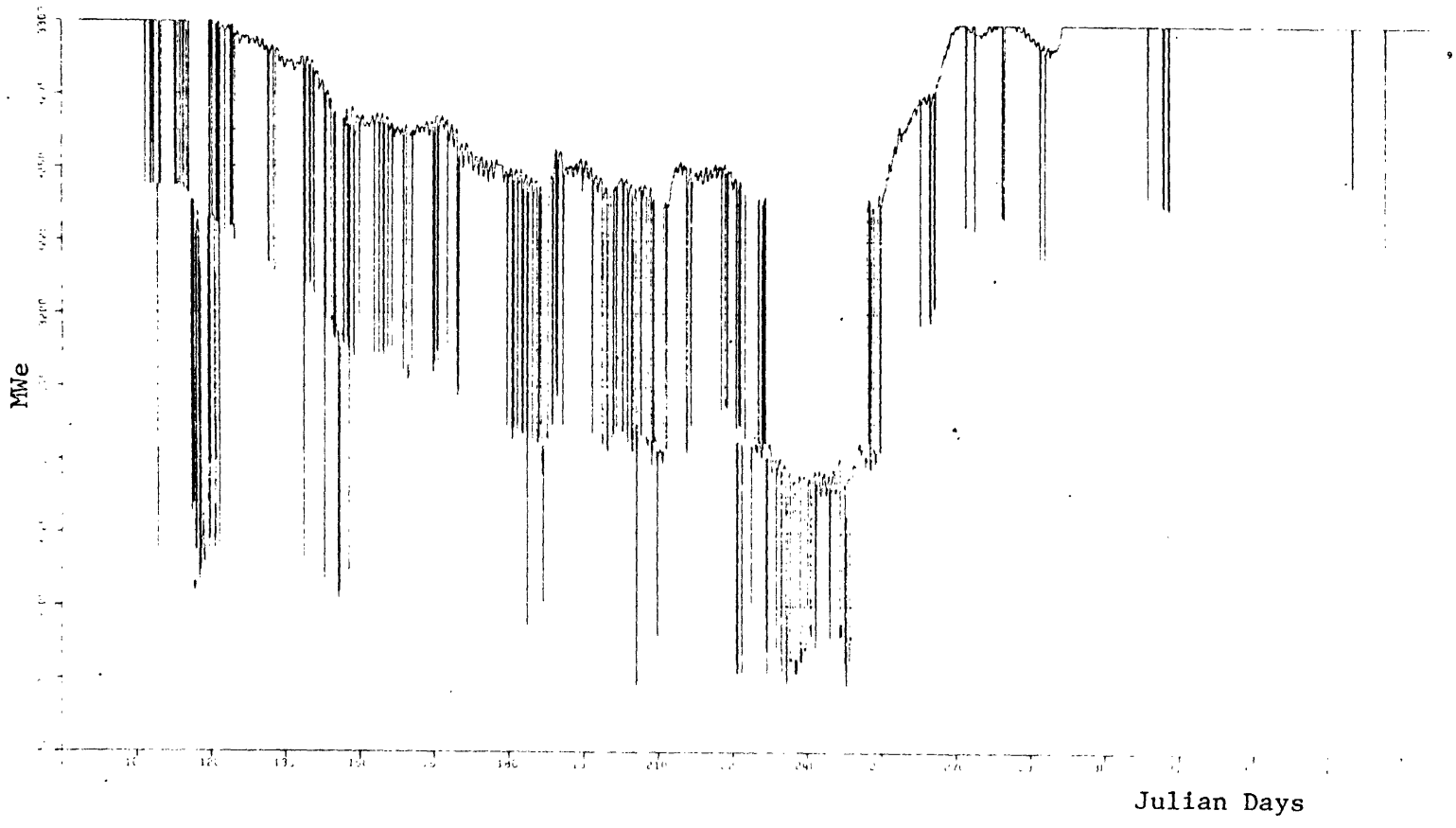

Figure 5.35 50% Increase in Diffuser Mixing Power Output in Best Mode

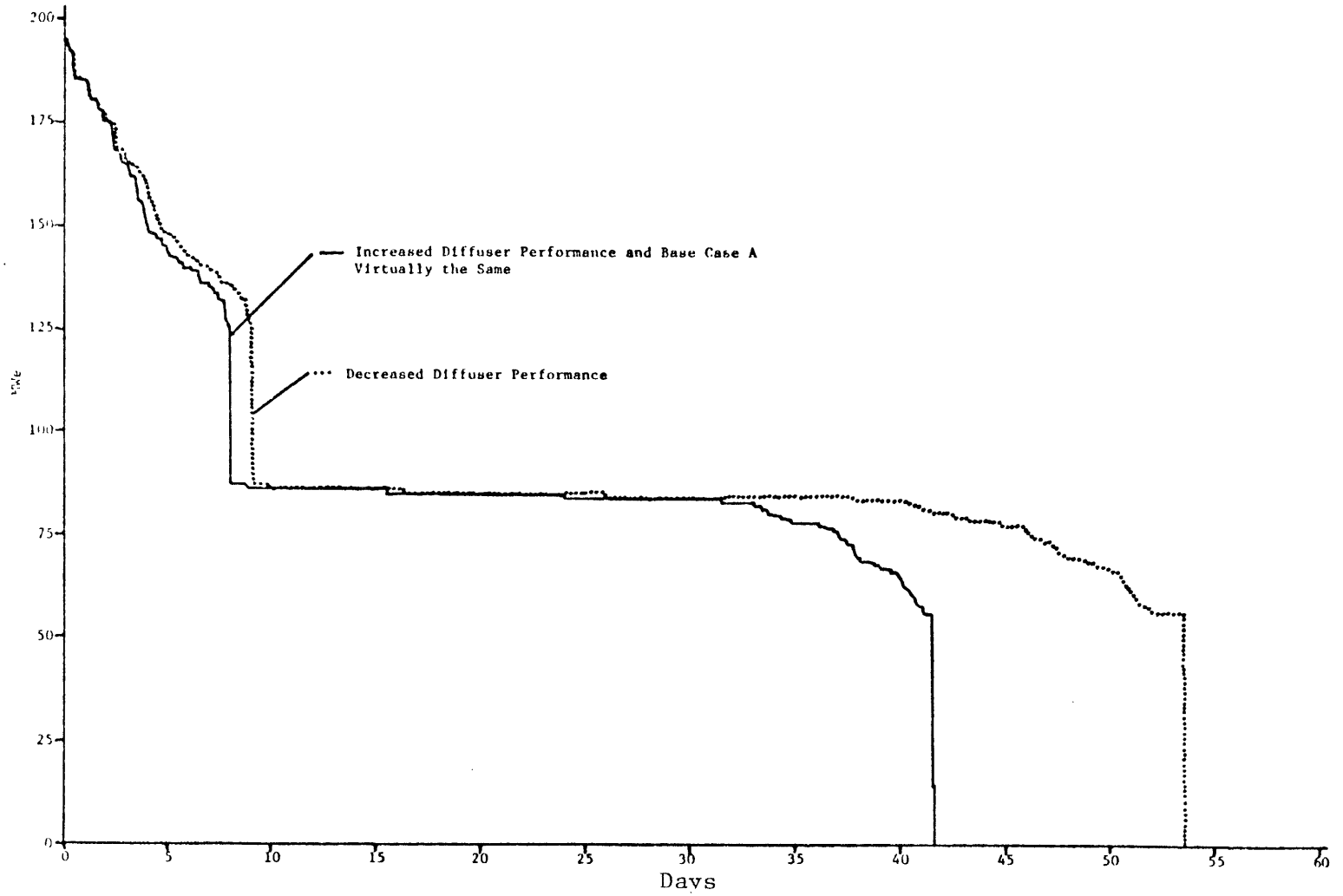

Figure 5.36 Composite of Sorted Power Loss Curves for Diffuser Mixing Performance Study

more losses for the helper mode of operation, but, not much for the closed mode. An interesting result is found for the increased mixing case which is almost exactly the same as the Base Case. Hence, the design of the diffusers at the present time does about as best as can be done.

Cooling tower performance was varied by subtracting $5^{o}F$ from the wet bulb temperature to model increased cooling performance and adding $5^{o}F$ to the wet bulb temperature to model decreased cooling performance. Figures 5.37 and 5.38 show the power output in best mode graphs for the increased cooling and decreased cooling respectively. Figure 5.39 shows the combined sorted power loss curves as compared to the Base Case A. As expected differences only appear in the closed mode of operation range.

5.5 Summary and Display of Cumulative Hourly Power Losses

This section summarizes the results of the sensitivity analyses by displaying the cumulative hourly power losses for each of the evaluations, Table 5.2. The evaluations are grouped as appears in text. These numbers represent losses greater than the plant thermal inefficiencies that would be experienced if the plant ran in open mode.

It is apparant for spatial and time averaging that selection of the downstream monitor is important. Adding various time running averages will decrease power losses somewhat. Using the estimated ΔT 1D model reduces power losses significantly in all cases. Combining spatial and time averaging plus the ΔT 1D model gave the lowest power

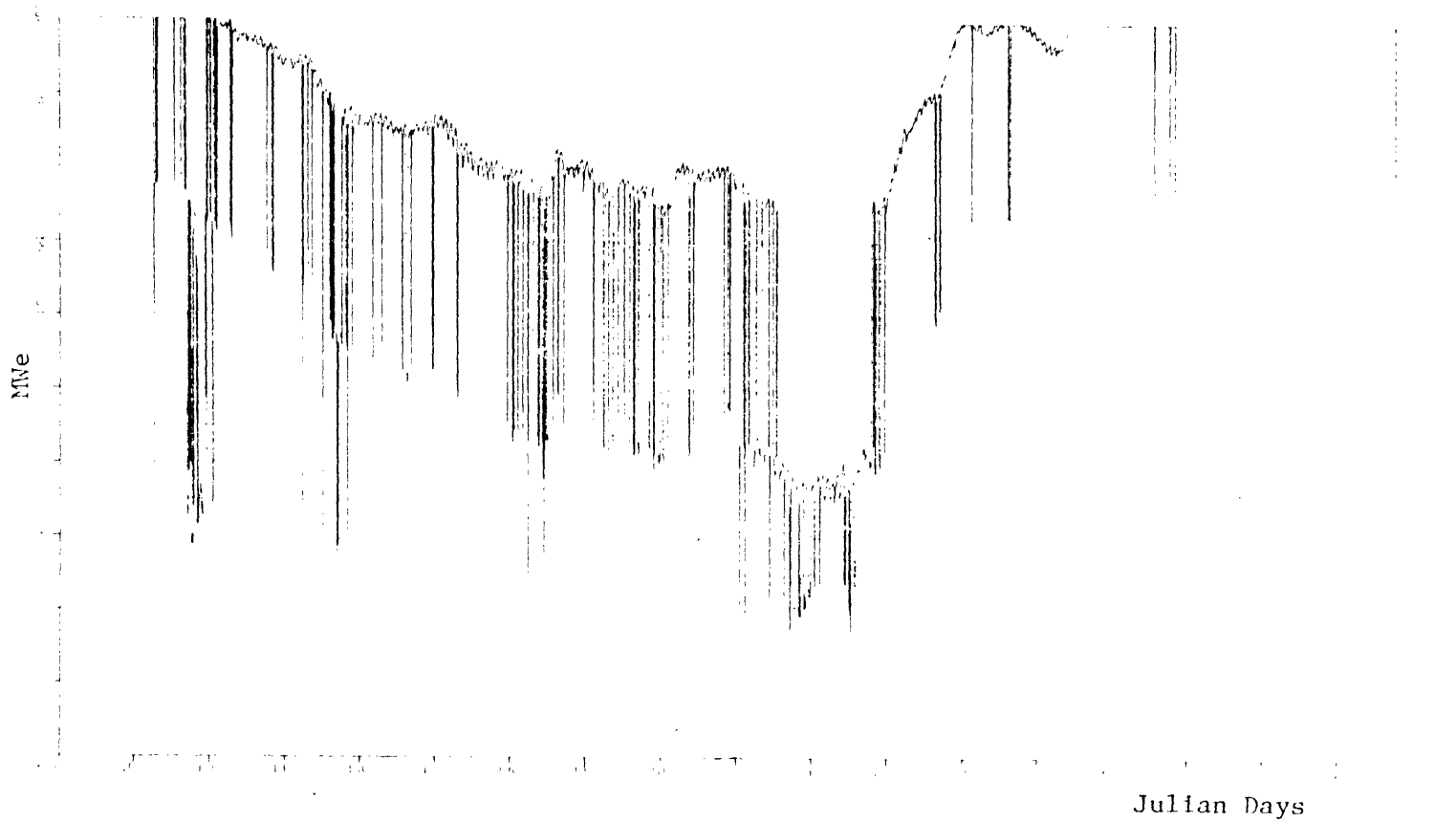

Figure 5.37 Increased Cooling Tower Performance Power Output in Best Mode

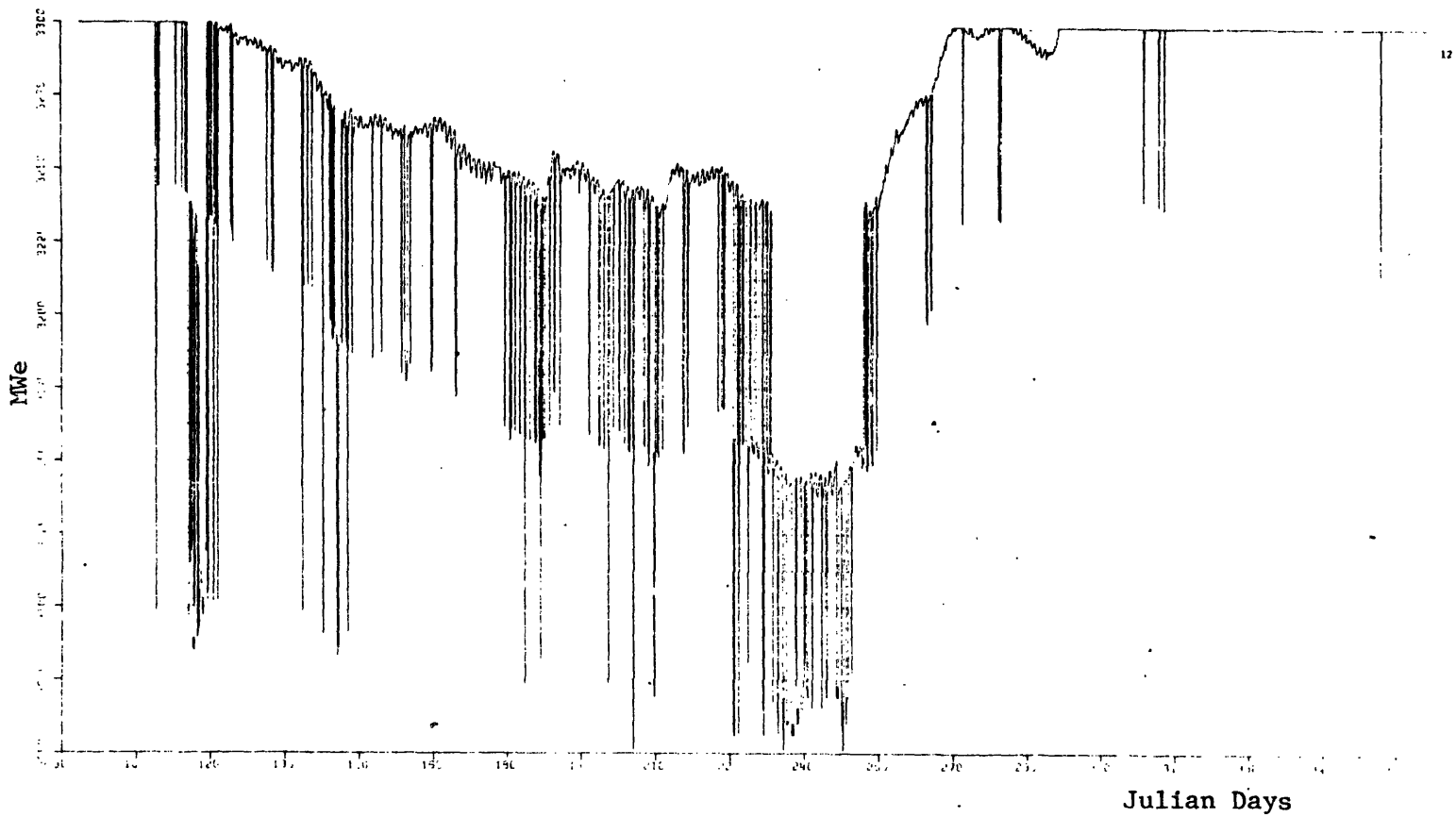

Figure 5.38 Decreased Cooling Tower Performance Power Output in Best Mode

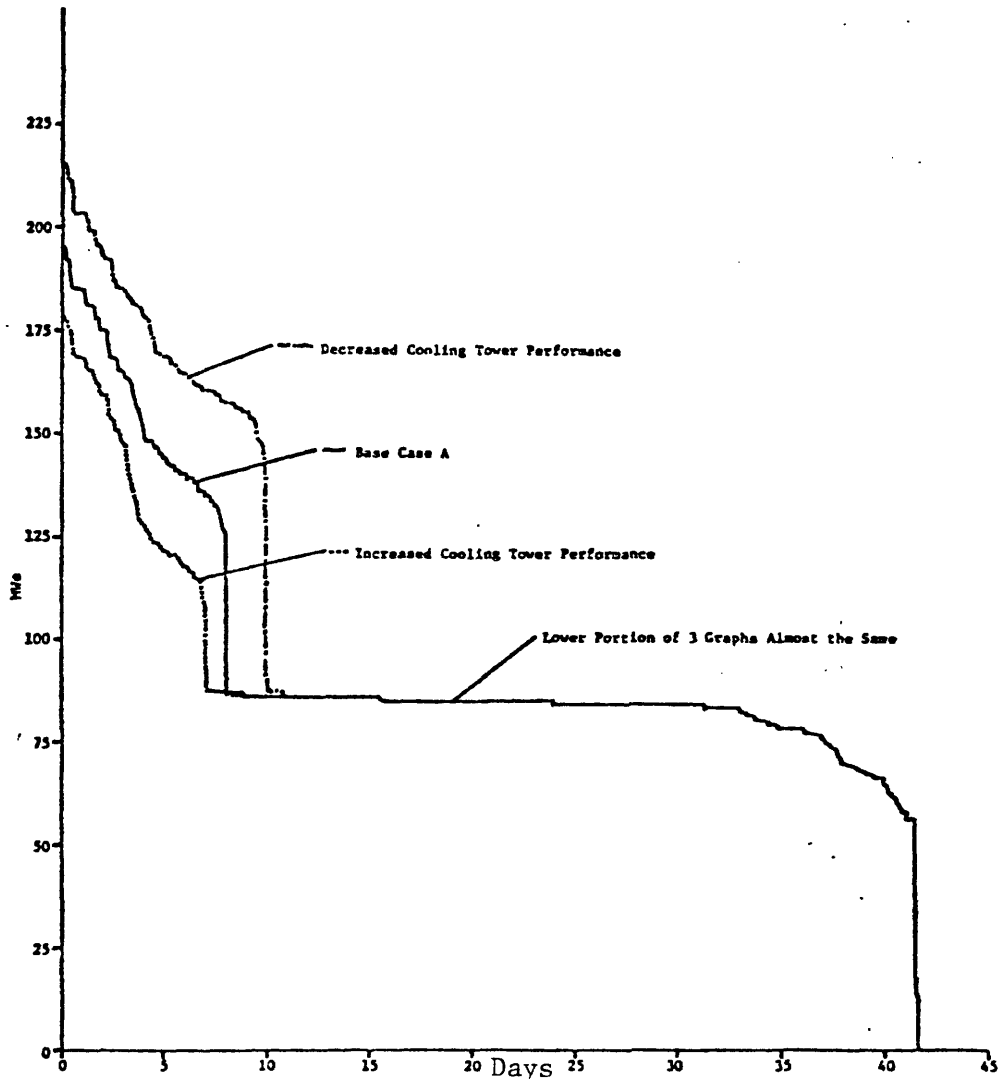

Figure 5.39 Comparison of Sorted Power Loss Curves for Cooling Tower Performance Study

Table 5.2 Display of Cumulative Hourly Power Losses

Analysis	Cumulative Hourly Power Loss (MW hr.)
5.2 Base Cases	
Base Case A, Downstream Station 9	96,044
Base Case B, Upstream Equals Downstream	63,542
Base Case A With Estimated ΔT 1D Model	83,018
5.3 Spatial and Time Averaging	
5.3.1 Monitor Location and Spatial Averaging	
Downstream Station 10	80,865
Downstream Station 11	78,327
Spatial Average of Downstream Stations 9,10, & 11	82,485
Downstream Station 10 With Estimated ΔT 1D Model	69,504
Downstream Station 11 With Estimated ΔT 1D Model	69,557
Stations 9,10, & 11 Spatial Average With Estimated ΔT 1D Model	71,599
5.3.2 Time Averaging	
2 Hour Running Average of Station 9	95,963
24 Hour Running Average of Station 9	92,280
48 Hour Running Average of Station 9	90,490
2 Hour Running Average of Station 9 With Estimated ΔT 1D Model	83,280
24 Hour Running Average of Station 9 With Estimated ΔT 1D Model	78,890
48 Hour Running Average of Station 9 With Estimated ΔT 1D Model	77,726

Table 5.2 (cont.)

Analysis	Cumulative Hourly Power Loss (MW hr.)
5.3.3 Combined Spatial and Time Averaging	
Stations 9,10,& 11 Spatial Average and 48 Hour Running Average	76,650
Stations 9,10,& 11 Spatial Average and 48 Hour Running Average with Estimated ΔT 1D Model	67,188
5.4.0 Sensitivity to Changes in Environmental Standards or Plant Design	
5.4.1 Changes in Environmental Thermal Standards	
Maximum Allowable ΔT of $3^{o}F$	268,732
Maximum Allowable ΔT of $10^{o}F$	68,667
Maximum Allowable River Temperature of $90^{o}F$	41,734
Maximum Allowable ΔT of $10^{o}F$ and Maximum Allowable River Temperature of $90^{o}F$	7,543
5.4.2 Existence of Various Modes of Operation	
All Open Mode Operation	0
No Open Mode Operation	481,040
No Helper Mode Operation	145,664
All Closed Mode Operation (No Open or Helper)	911,858
5.4.3 Changes In Plant Design	
Increased Diffuser Mixing	95,960
Decreased Diffuser Mixing	120,807
Increased Cooling Tower Performance	91,438
Decreased Cooling Tower Performance	103,718

losses and approached the Base Case B value.

In the environmental standards and plant design analyses the values speak for themselves. Interestingly, the maximum allowable river temperature of $90^{o}F$ has significantly less losses than the maximum allowable change in temperature of $10^{o}F$. Also, as seen from analyses of the power output in best mode graphs, the savings occur during the late summer period when maximum power output is more important.

VI. Comparison with Operating Data

The Browns Ferry Nuclear Plant went back into full operation late in the year 1976. From available data, the period January through October 1977 was used to compare the natural and plant induced temperature models with a period of actual plant operation. This work consisted of: recalibrating the natural temperature difference model (Section III) to take into account a new set of instream monitors; utilizing meteorological data, river flows, and instream monitor data to produce a natural temperature difference prediction for the year 1977; revising the plant simulation model (Section IV); and finally, comparing the two model results with 1977 data from the instream monitors used for compliance purposes.

6.1 Recalibration of Natural Temperature Difference Model

On several occasions during the years 1975 and 1976, the thermal instream monitors showed the plant in violation of its maximum allowable temperature rise of 5°F. After analyzing the situations, it was discovered the violations were caused by natural temperature variations and not the plant. TVA decided to change the primary upstream monitor to station 4 thereby decreasing the distance between upstream and downstream monitors from 15 miles to about 5 miles. It was also decided to remove station 6, and replace station 9 with station 13 (which is farther from the right bank and less affected by natural heating). Figure 6.1 shows the locations of the new monitors.

In order to represent the actual situation at the site, the natural temperature difference model was re-evaluated for the stretch of the river from station 4 to stations 10, 11 and 13 (the previous analysis presented in Section III was for station 6 to station 1). The model

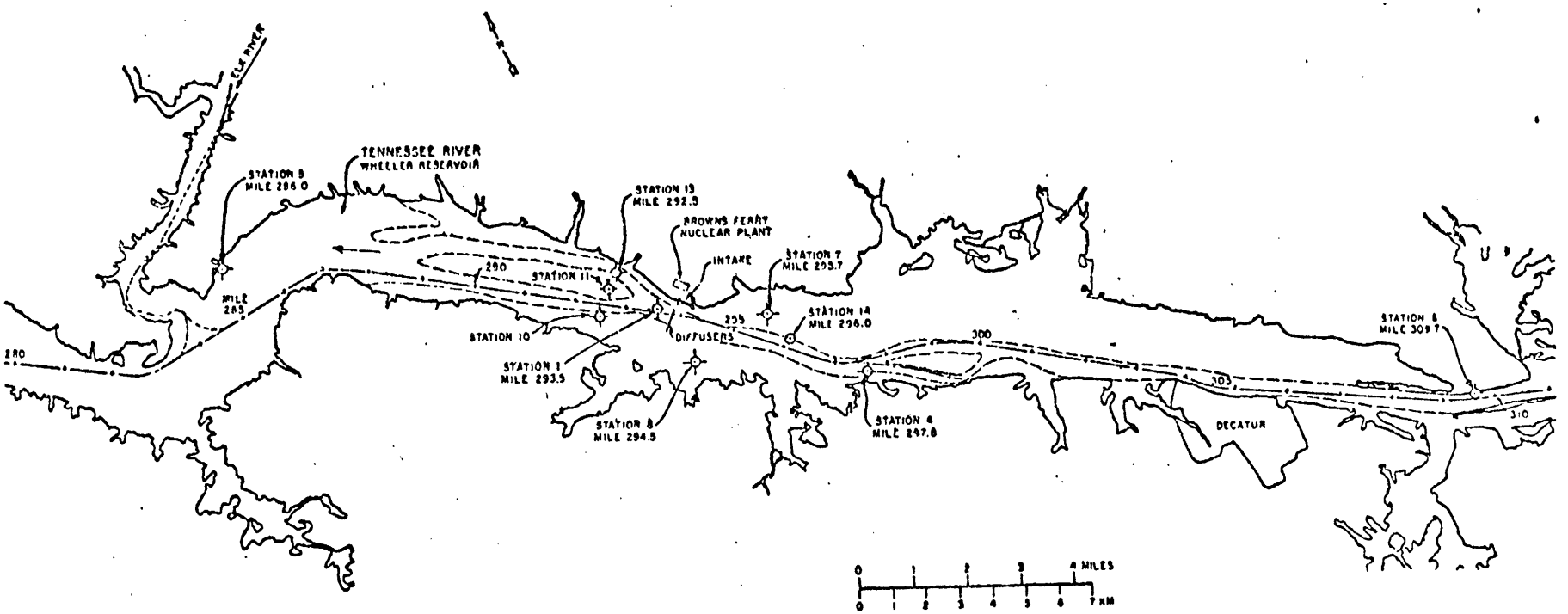

Figure 6.1 Revised Locations of Temperature Monitors for Browns Ferry Nuclear Plant

corrections needed consisted of a change in the river length and the average cross sectional area. Figure 6.2 shows the calibration of the model using average cross sections as compared to measured data for the years 1975 and 1976. An area equal to 100,000 ft^2 was found to best fit the measured data (stations 9, 10, 11 minus station 4) for the period when the plant was not in operation. The increase in cross sectional area is physically reasonable since the previous stretch of river (station 6 to station 1) consisted of narrower channeled flow in the upstream region. Figure 6.3 shows the difference of the measured minus the predicted variation. The model does quite well except for a slight negative offset occurring in the summer months.

6.2 1977 Natural Temperature Difference Prediction

Meteorological data for Huntsville, Alabama were obtained from the National Weather Service for the period January 1, 1977 to the end of October, 1977, which was the latest verified data available at the time of our analysis. It was determined that the temperature effects in November and December were not significant since this is usually a time when the plant complies very well to its thermal standards. Figures 6.4, 6.5, 6.6 show forty-nine hour running averages of the ambient air temperatures, relative humidity, and wind speeds for this period. This meteorological information along with forty-nine hour running averages of air pressure, completed solar flux, and computed atmospheric flux were used to compute net flux as described in Section III. The resulting net flux is shown in Figure 6.7. The magnitudes of the flux during various seasonal periods agree with the previous 1975, 1976 data.

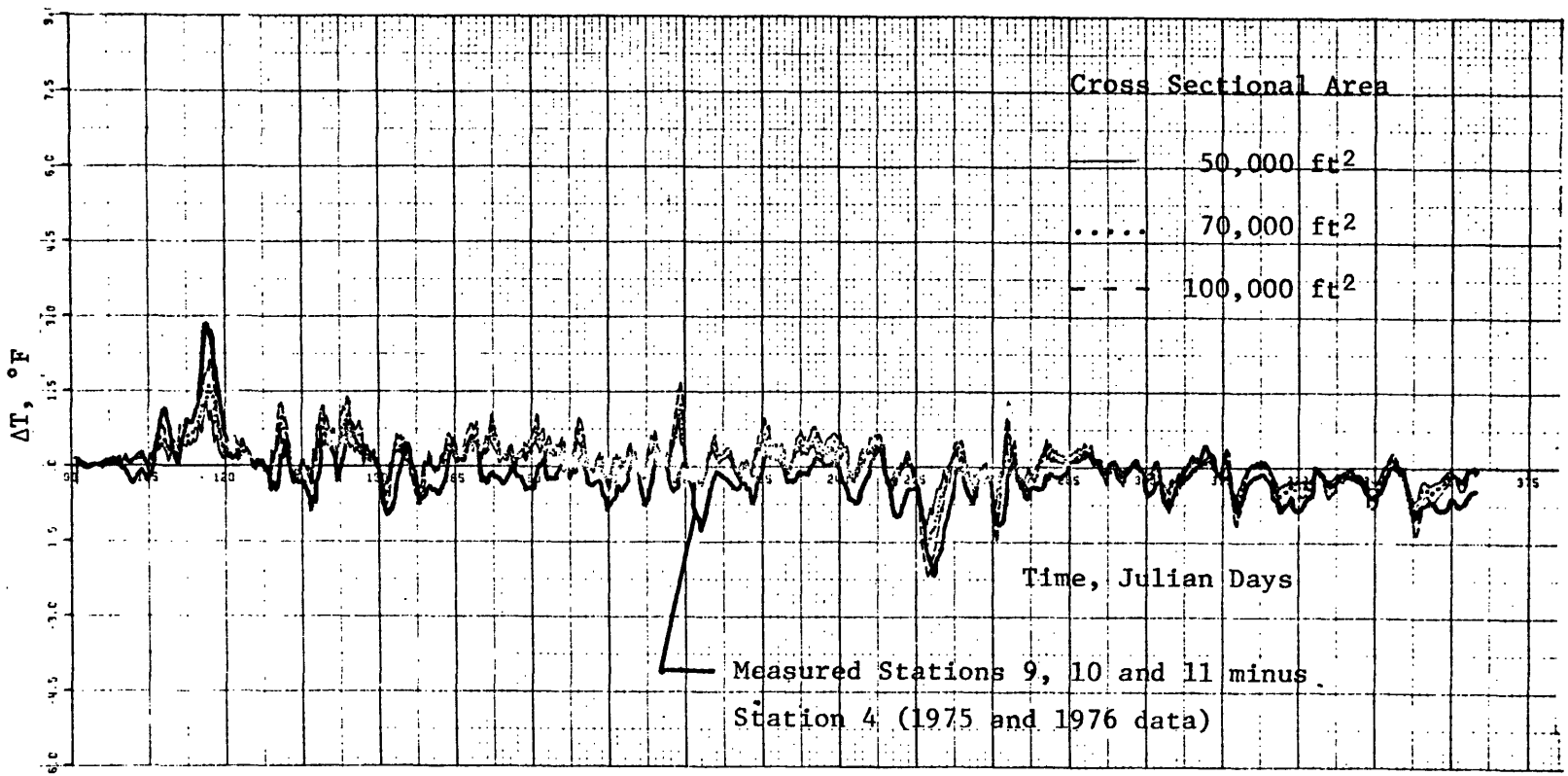

Figure 6.2 Comparison of Varying the Cross Section Area of River in the Natural Temperature Difference Model

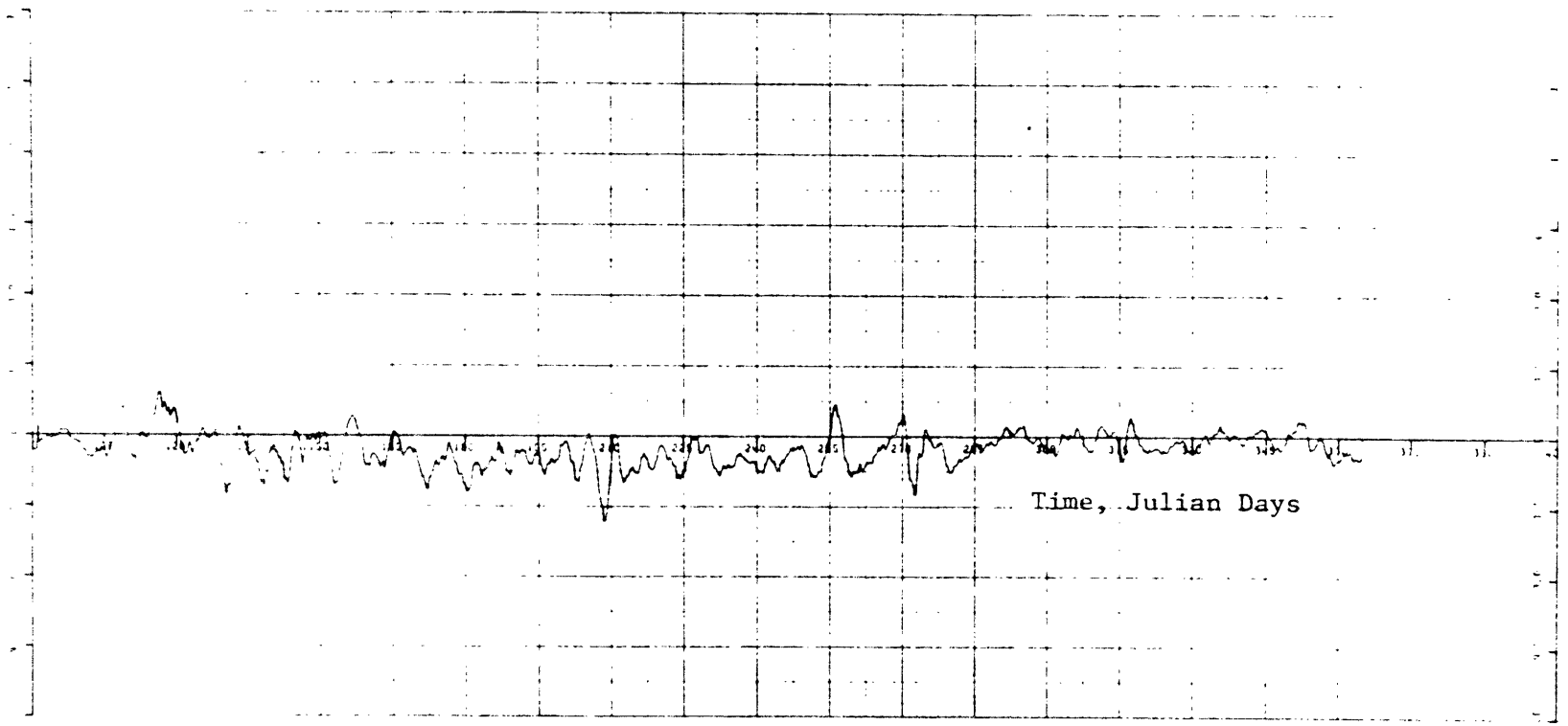

Figure 6.3 Residual Series after Subtration of Recalibrated 1-D Model Prediction from Measured Averaged Natural ΔT.

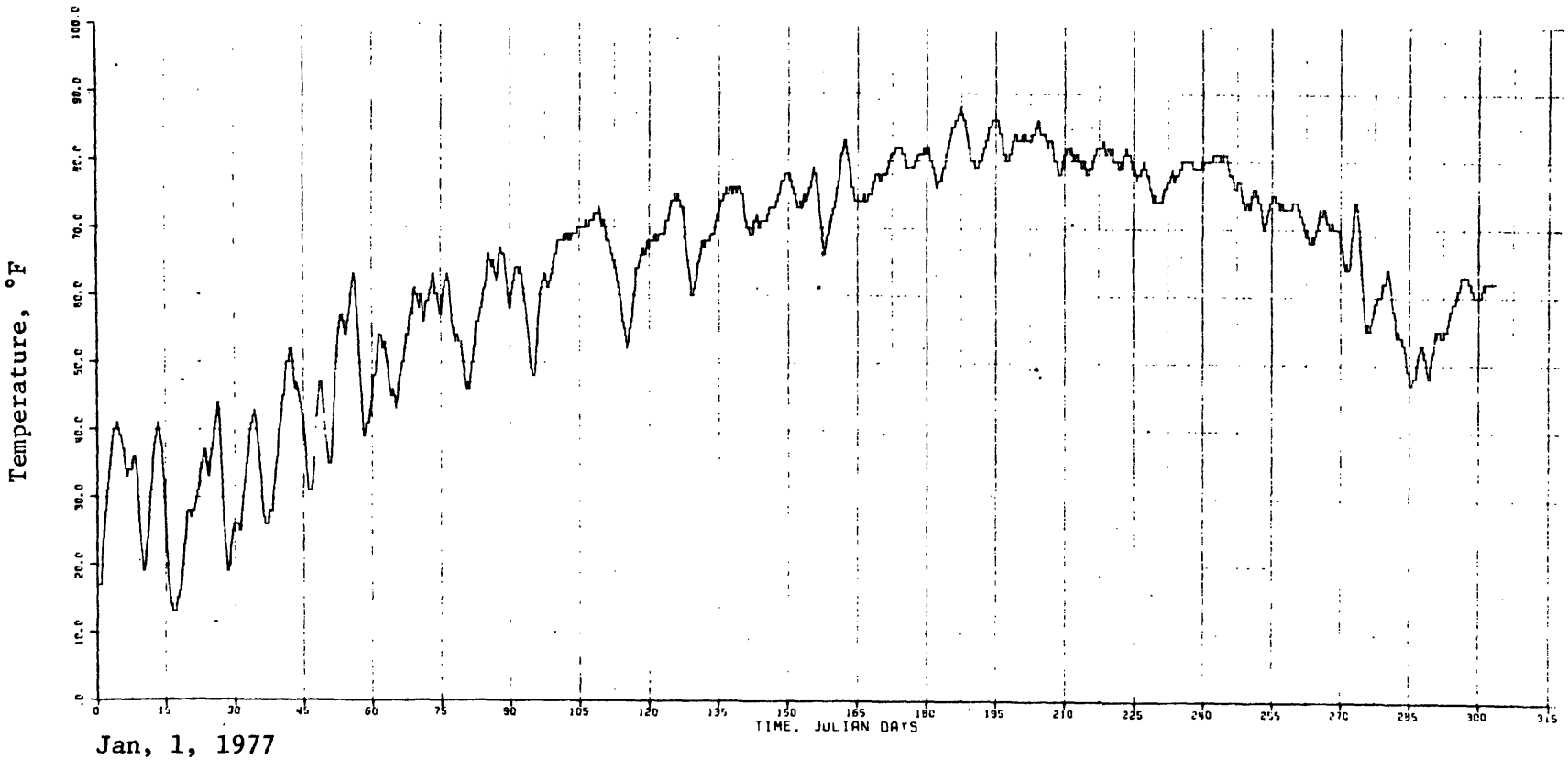

Figure 6.4 49 Hour Running Averages of Ambient Air Temperatures at Huntsville, Alabama for January through October 1977.

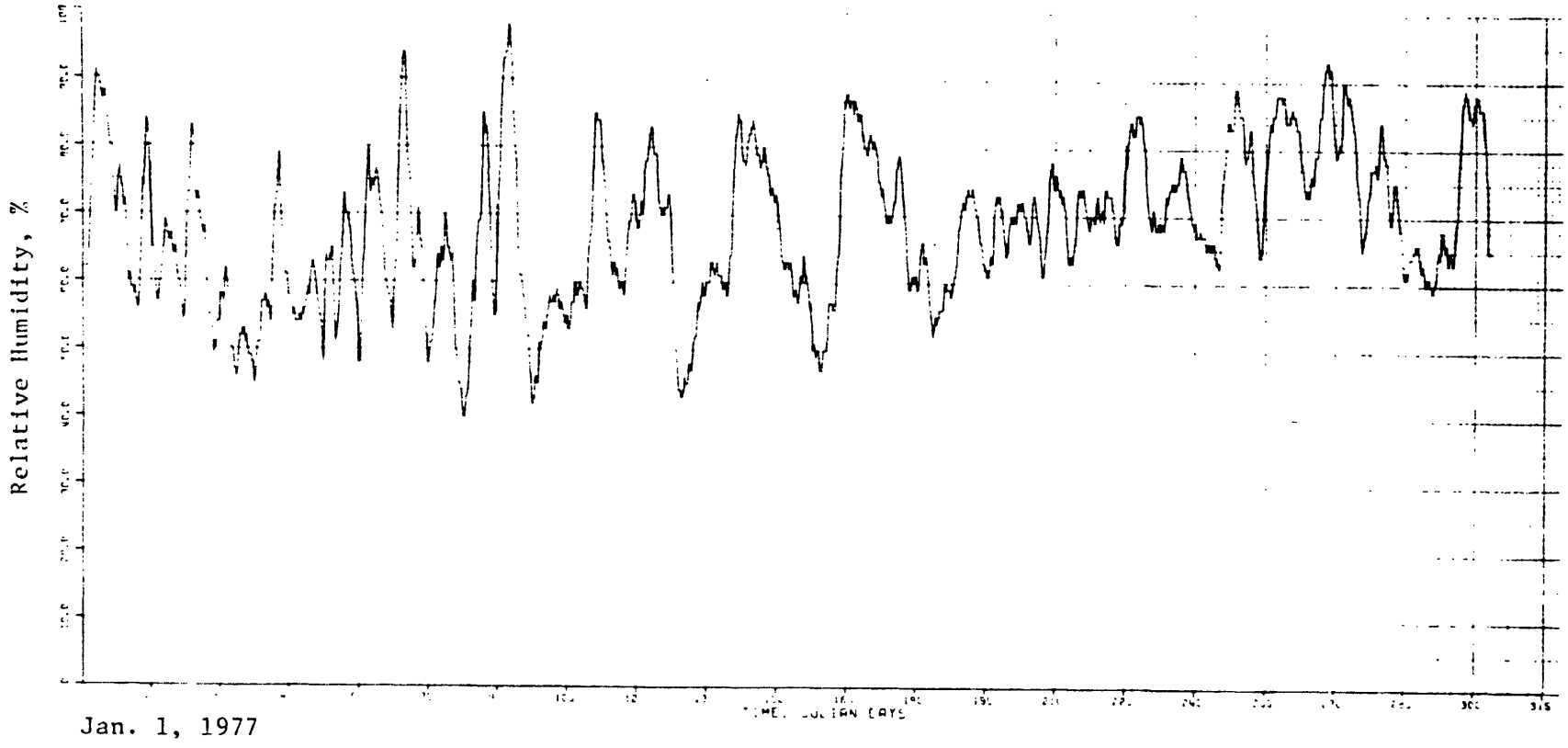

Figure 6.5 49 Hour Running Averages of Relative Humidity at Huntsville, Alabama for January through October 1977

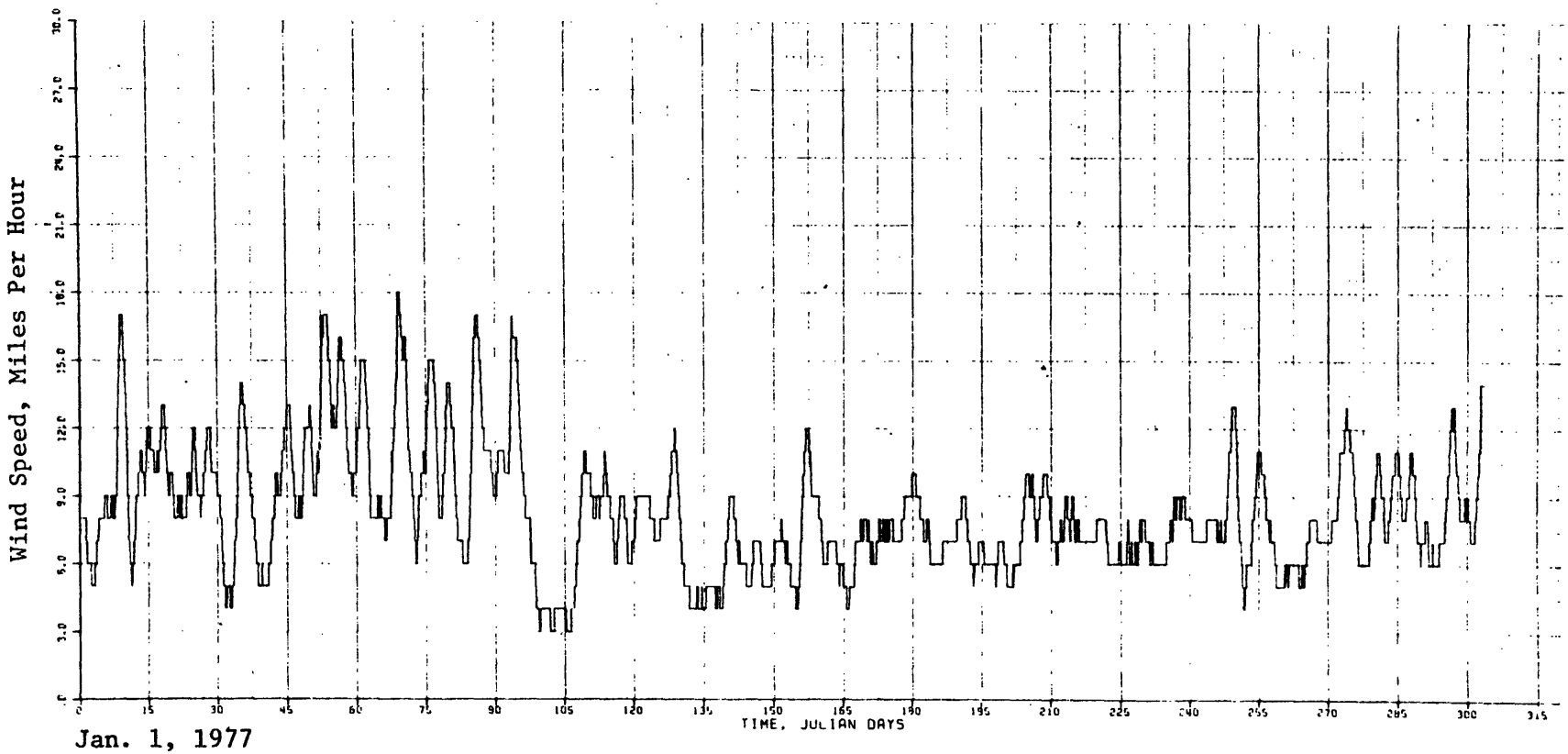

Figure 6.6 49 Hour Running Averages of Wind Speeds at Huntsville, Alabama for January through October 1977

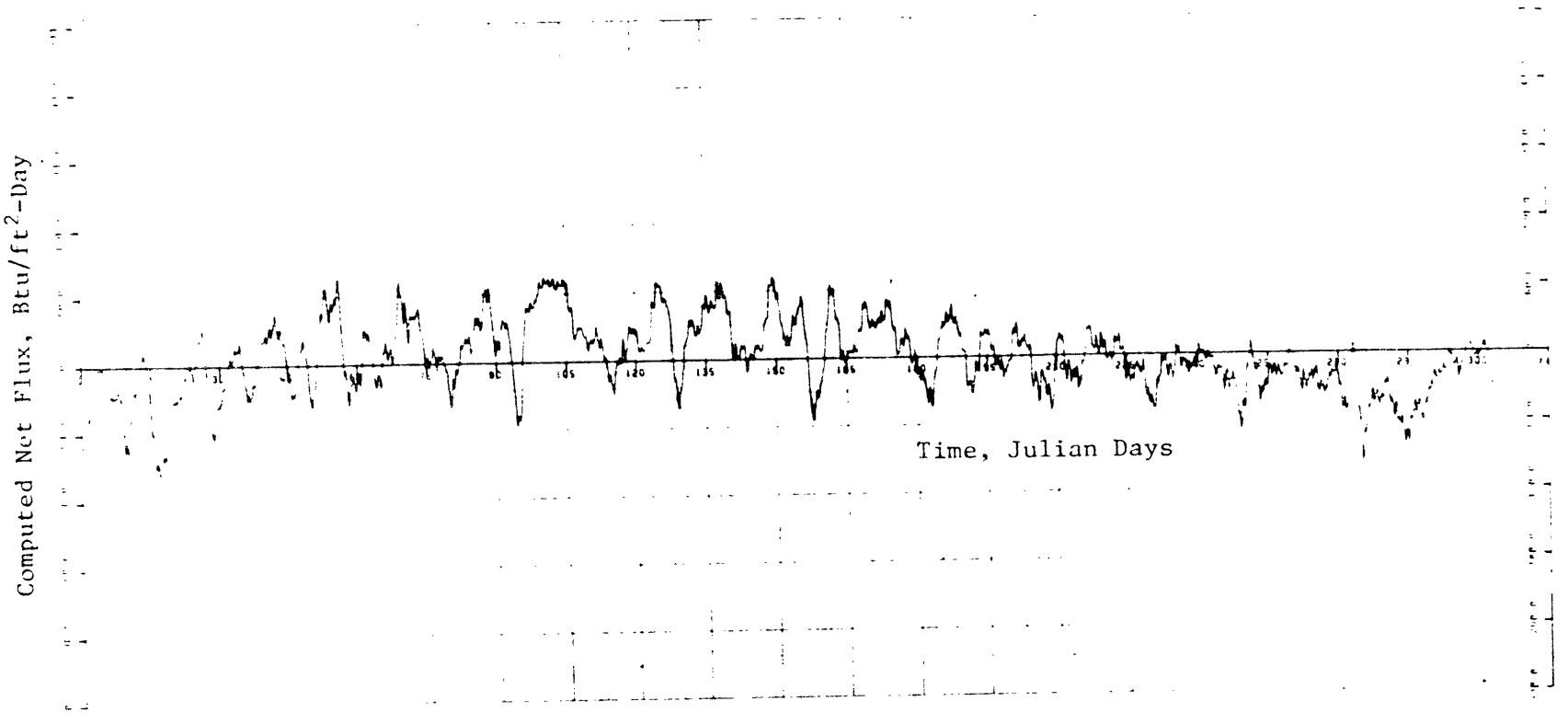

Figure 6.7 Net Flux Computed Using 1977 Forty-Nine Hour Running Averaged Inputs

The recalibrated natural temperature model (Section 6.1) was run using the following 1977 data: forty-nine hour running averaged river flows at the Browns Ferry site and upstream station 4 temperature measurements, and the net flux (calculated using forty-nine hour averaged inputs). The river flow at the Browns Ferry site was determined from a two term equation utilizing flow values from Guntersville and Wheeler Dams. The discharges from Guntersville and Wheeler Dams are shown in Figures 6.8 and 6.9 respectively. The calculated hourly flow at Browns Ferry is shown in Figure 6.10 while the forty-nine hour running averages are shown in Figure 6.11. Figures 6.12 and 6.13 show the temperature measurements at station 4, 5 foot depth, for hourly and forty-nine hour running averaged values. The resulting natural temperature difference prediction for the 1977 period is shown in Figure 6.14. The magnitudes of the natural temperature variation are lower than the previous analysis (Section III) since the travel distance was cut down substantially. However, variations approach .75 to 1.0°F frequently during the year showing there is still a significant natural temperature difference to be accounted for.

6.3 Revised Plant Induced Temperature Simulation Model

The simulation model described in Section IV was modified to better describe real time plant operation. The major revisions to the model centered around accepting individual unit load values (as opposed to one target plant load), using given cooling mode usage, and considering only predicted plant induced temperature rise. The revised model uses hourly wet bulb temperatures, unit loads, cooling modes, and river flows

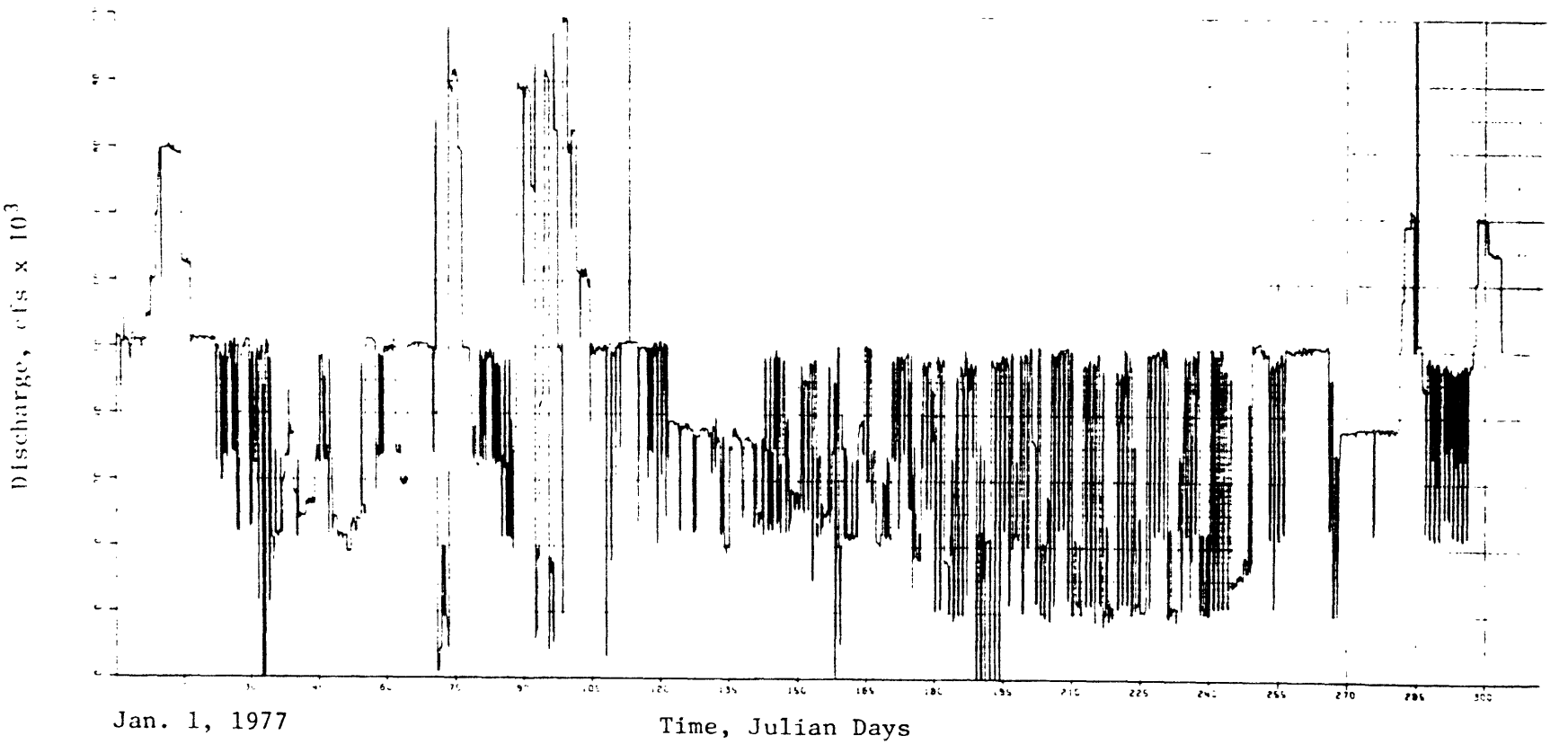

Figure 6.8 Discharge From Guntersville Dam for 1977 Period

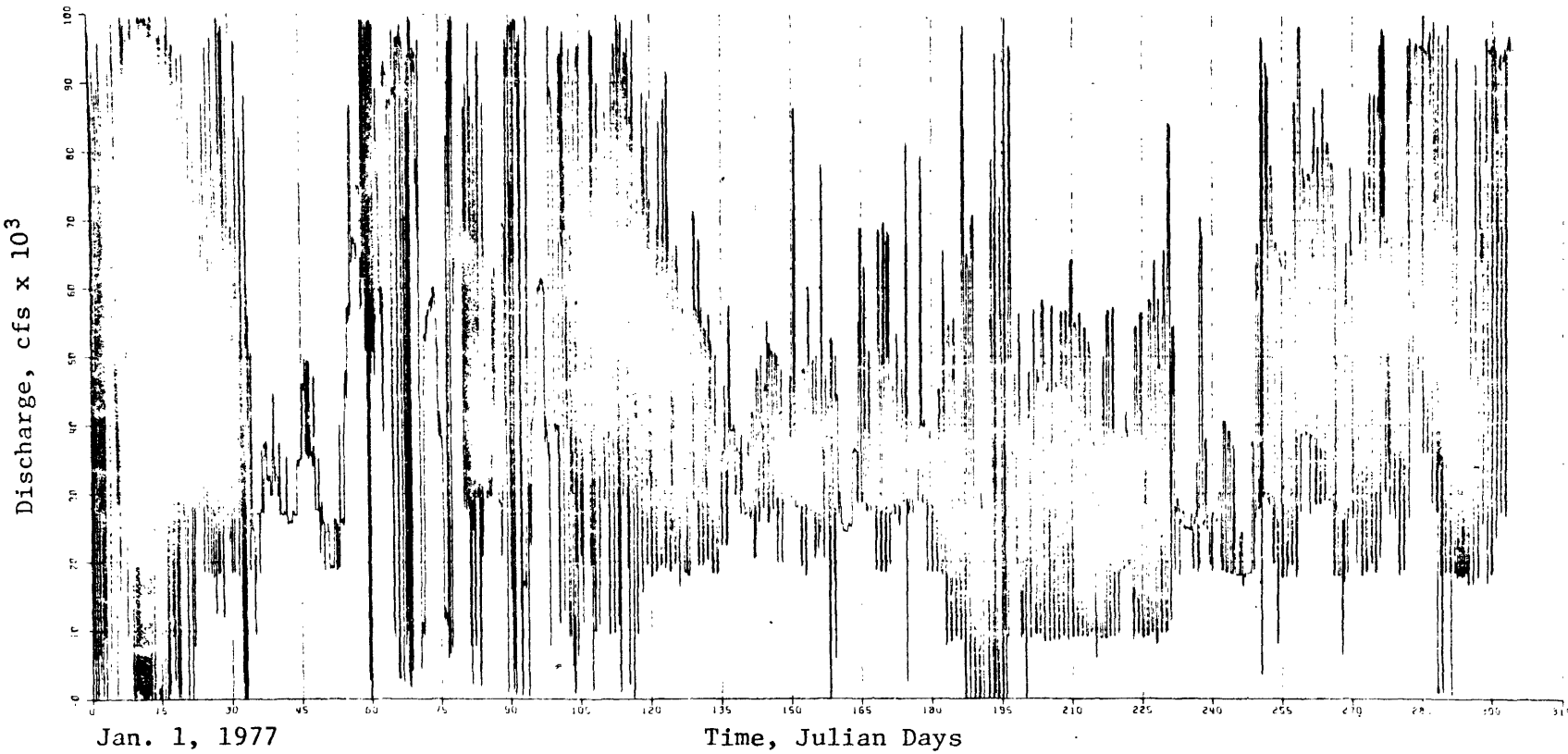

Figure 6.9 Discharge From Wheeler Dam for 1977 Period

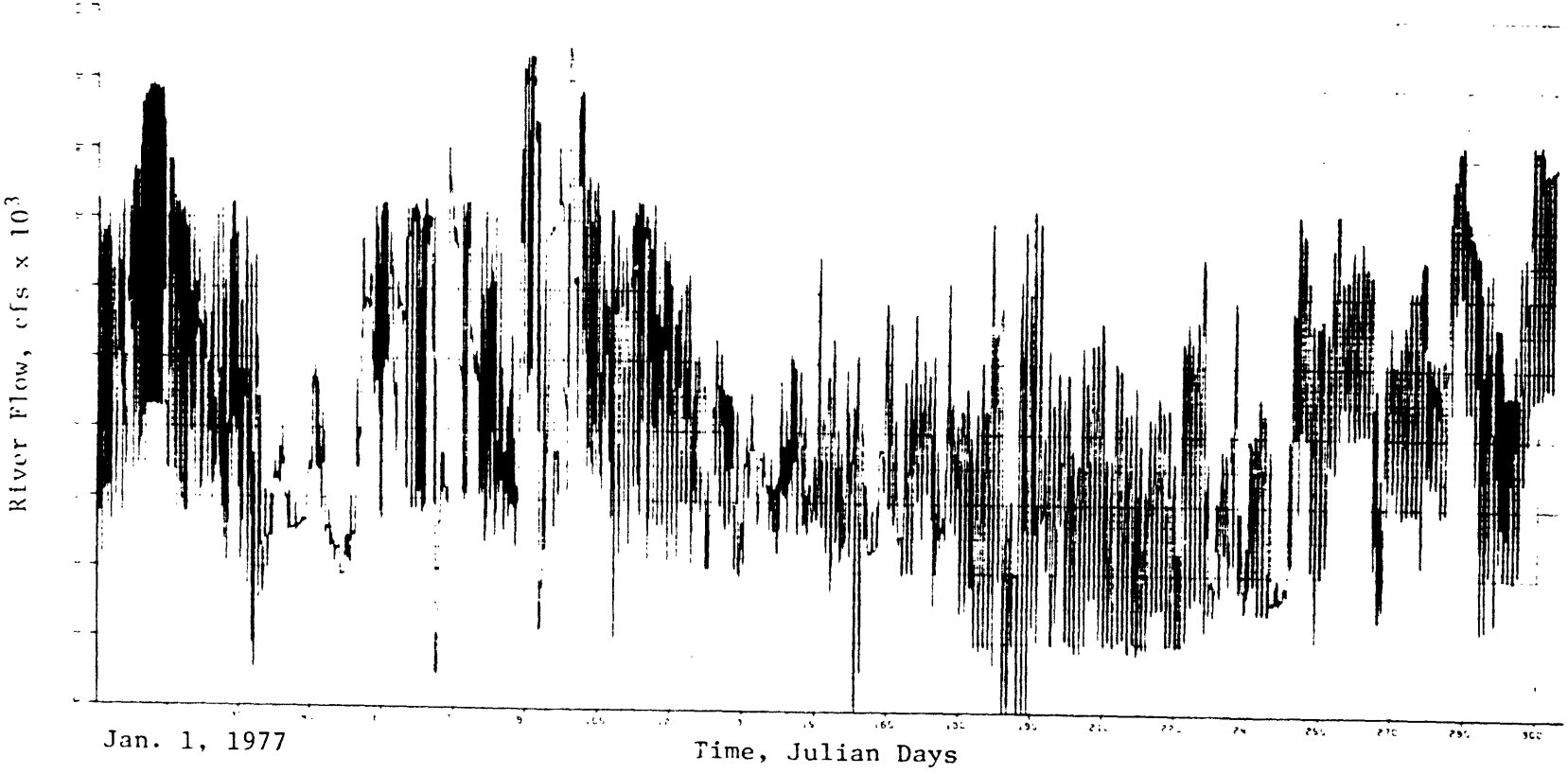

Figure 6.10 Calculated Hourly River Flow at Browns Ferry

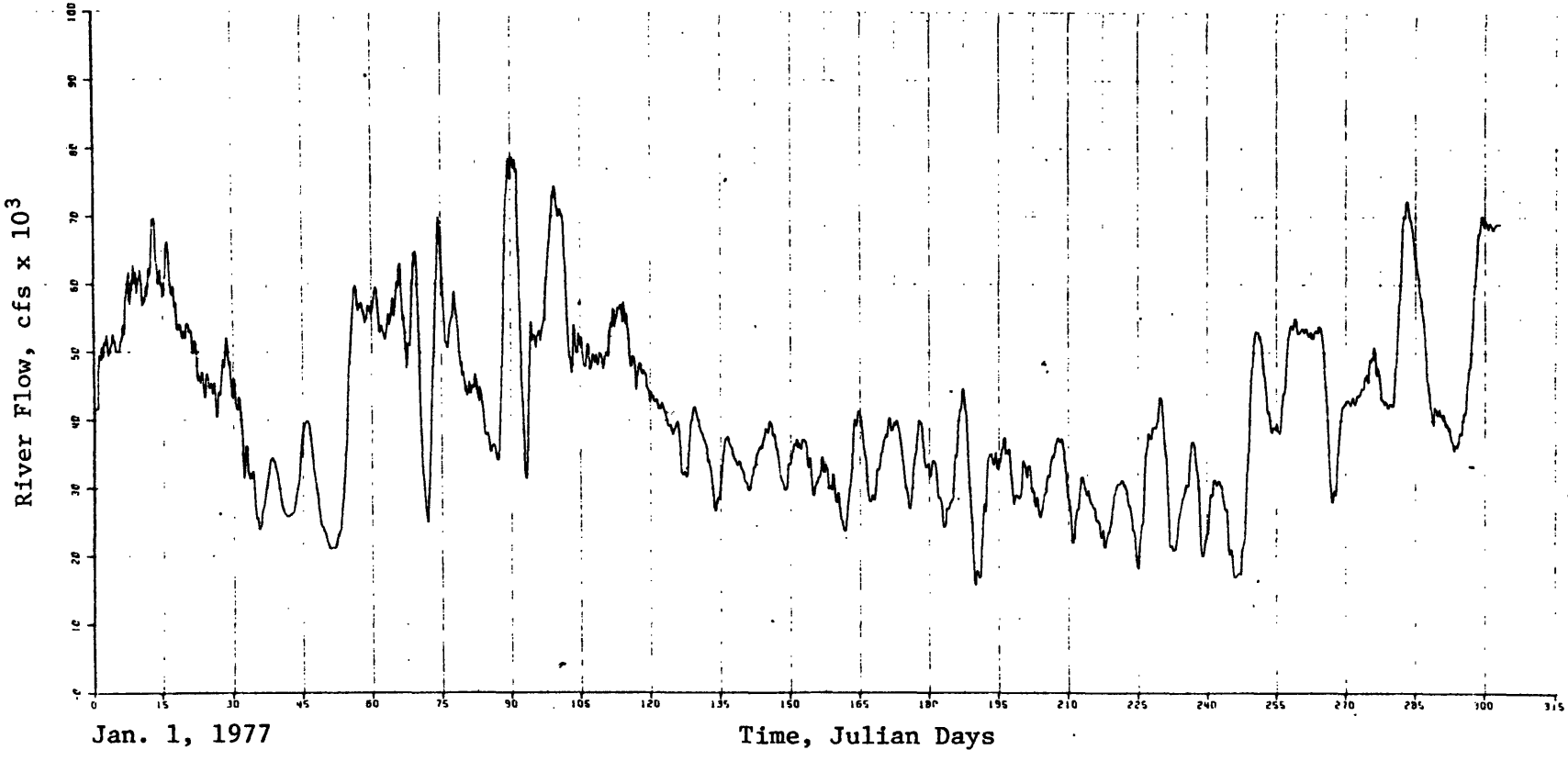

Figure 6.11 Forty-Nine Hour Running Averages of Calculate River Flows at Browns Ferry

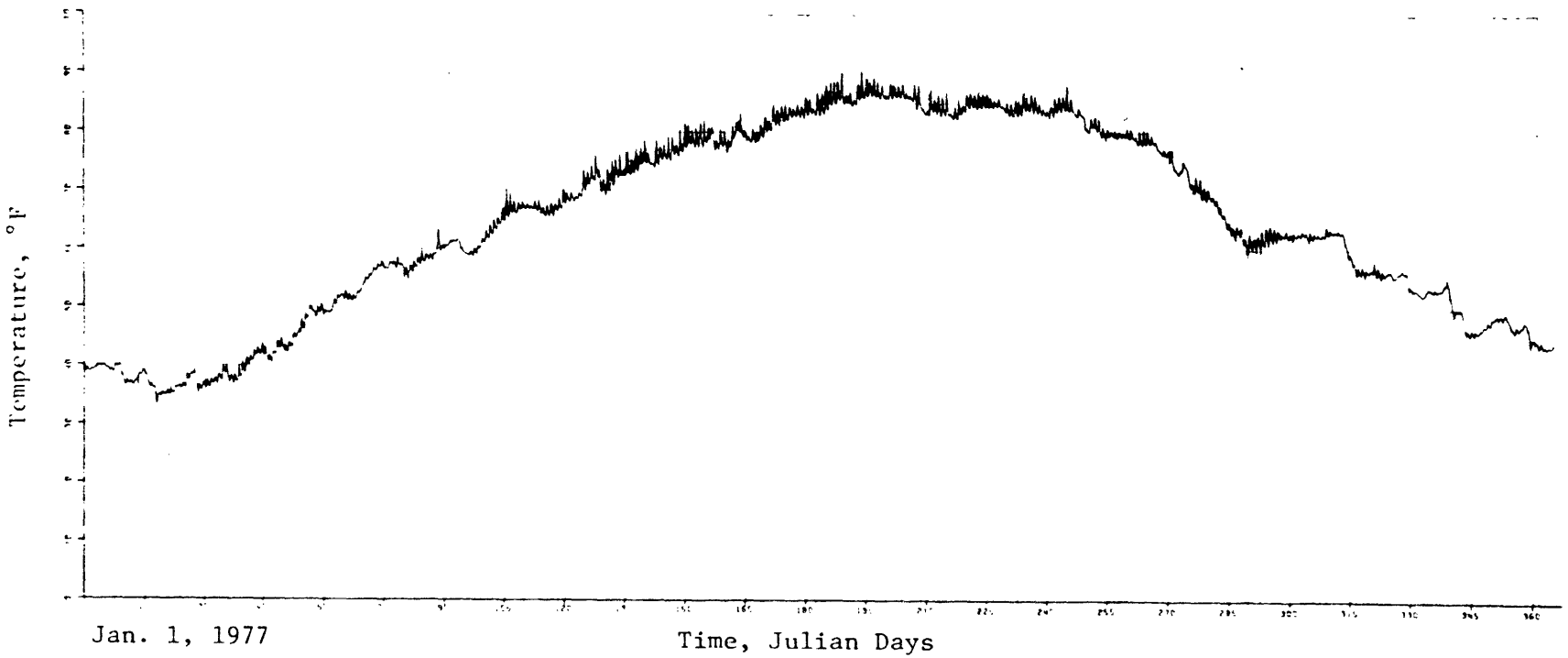

Figure 6.12 Hourly River Temperatures at Upstream Station 4 for 1977

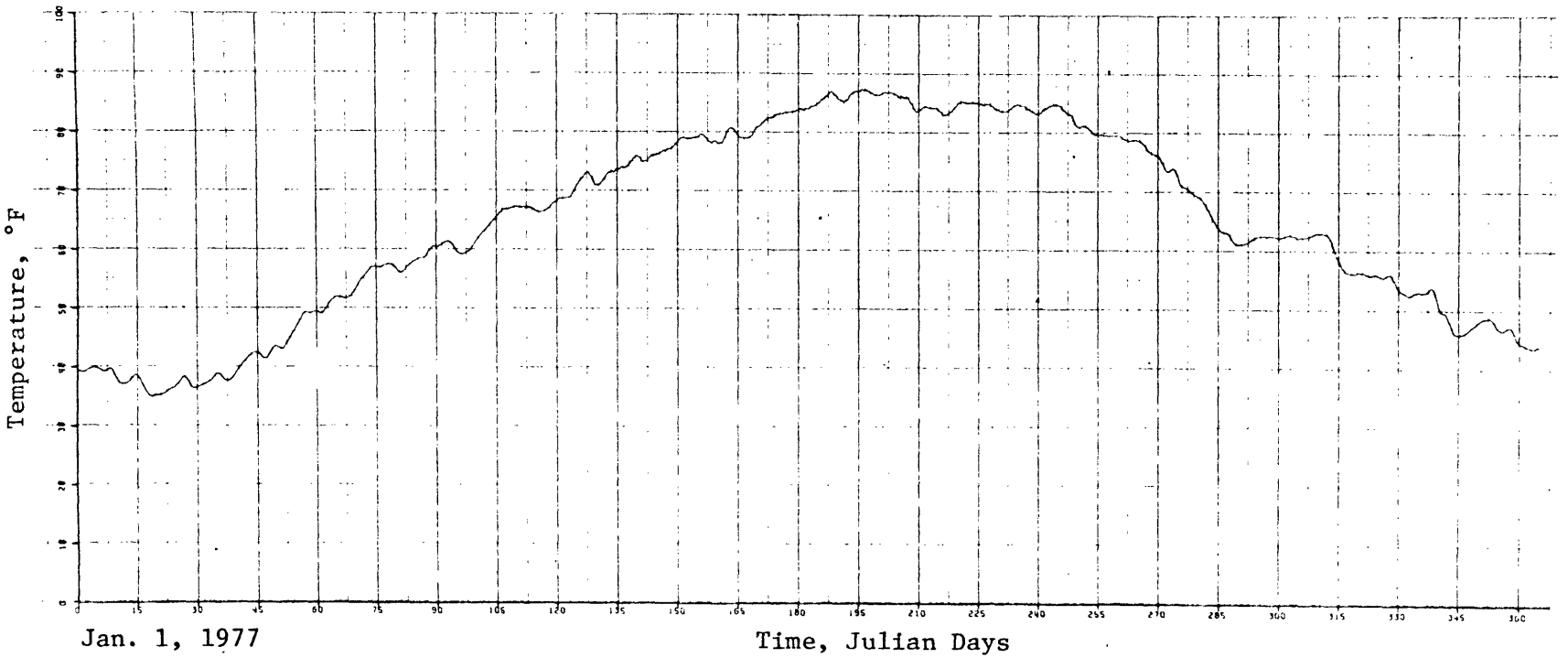

Figure 6.13 Forty-Nine Hour Running Averaged River Temperatures at Upstream Station 4 for 1977

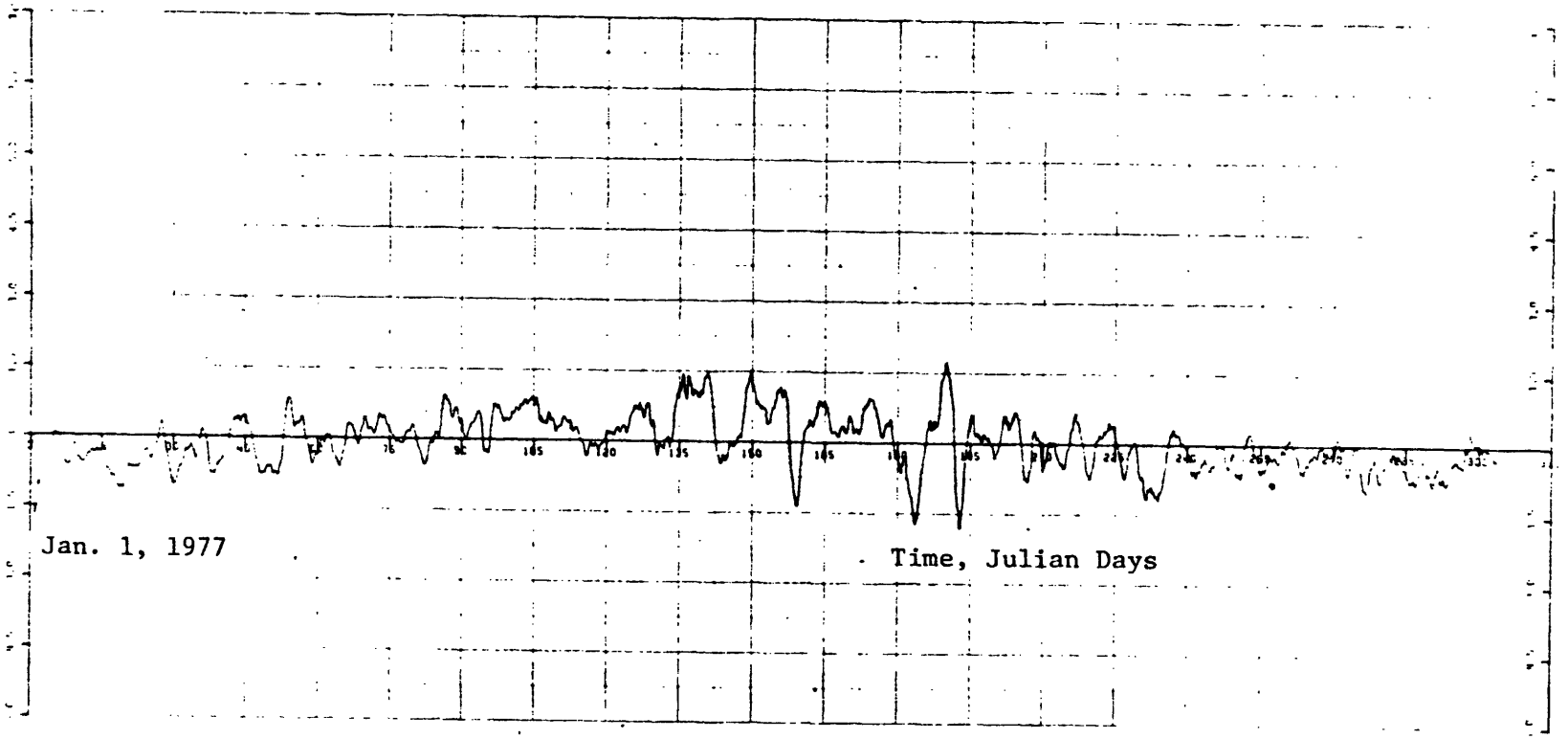

Figure 6.14 1.D Model Natural Temperature Difference Prediction for 1977 Period

at Browns Ferry for input and determines the total plant induced temperature rise predicted for the total three units. The total hourly plant loads (3 units combined) are shown in Figure 6.15.

6.4 Comparison of Model Results with Measured Temperature Differences

The results of the 1-D natural temperature difference model and the plant induced temperature simulation model were compared with the measured temperature difference from the instream monitors. Evaluations of the differences in instream monitor readings show there is quite a variation in values of measured temperature differences (ΔTs). Figure 6.16 shows the individual ΔTs for downstream stations 10, 11 and 13 minus station 4. To alleviate this problem, an average of the three downstream stations is used in the model comparisons. Figure 6.17 shows this averaged value minus station 4 on an hourly basis. Figure 6.18 shows a forty-nine hour running average of measured spatially averaged ΔTs that are used in the actual comparison.

The predicted natural temperature difference was subtracted from the measured averaged temperature difference to obtain a corrected measured ΔT. This corrected measured ΔT was then compared to the plant temperature rise prediction, Figure 6.19. The residual series obtained by subtracting the corrected measured ΔT from the predicted plant induced temperature difference is shown in Figure 6.20. There is better agreement of the predicted plant versus corrected measured values for winter, early spring, and fall periods. Several occurances of high predicted plant temperatures versus low corrected measured temperatures are apparent. These occurances appear to be correllated with minimums in river flows. It is possible that during these low flow situations upstream station 4 may be

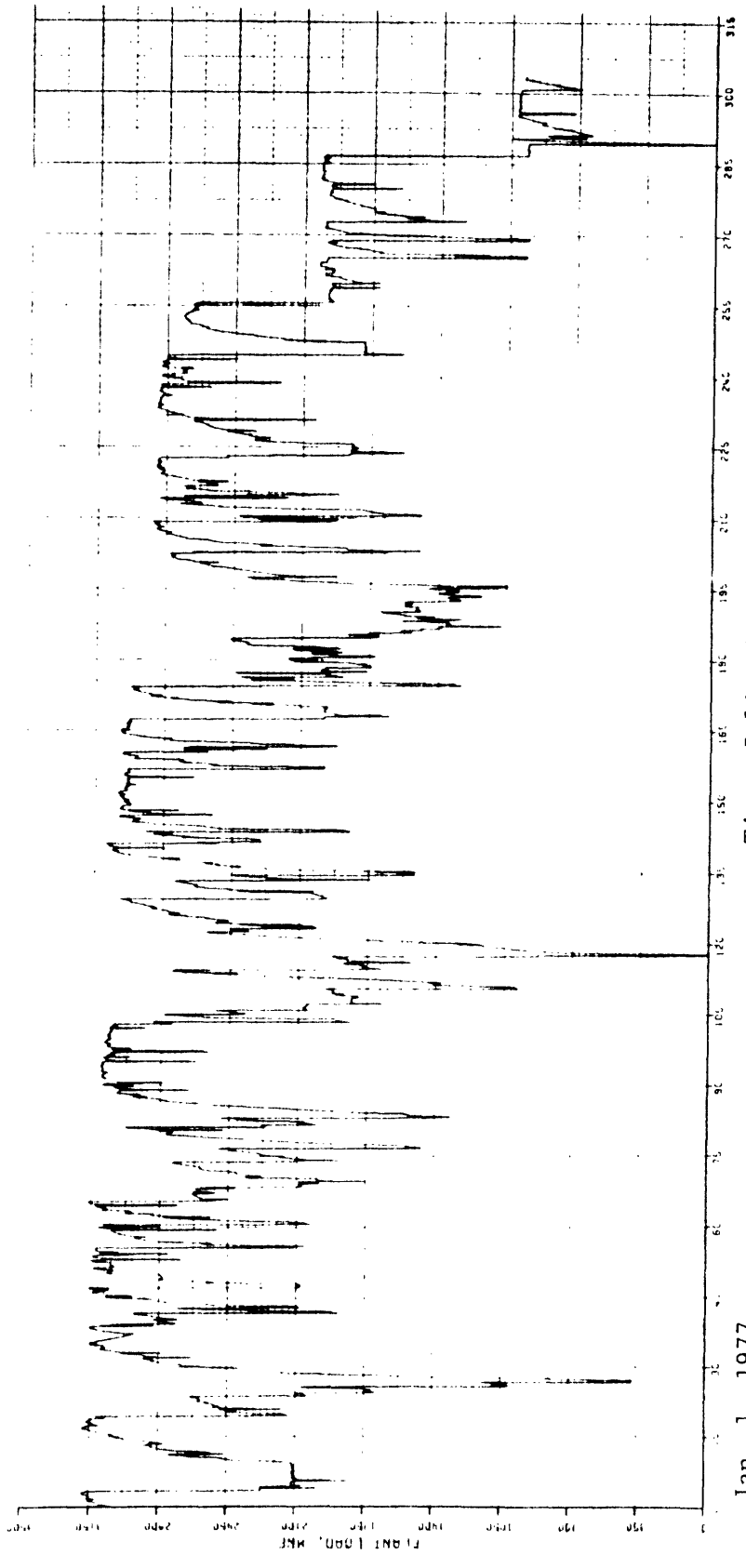

Figure 6.15 Total Three Unit Plant Load

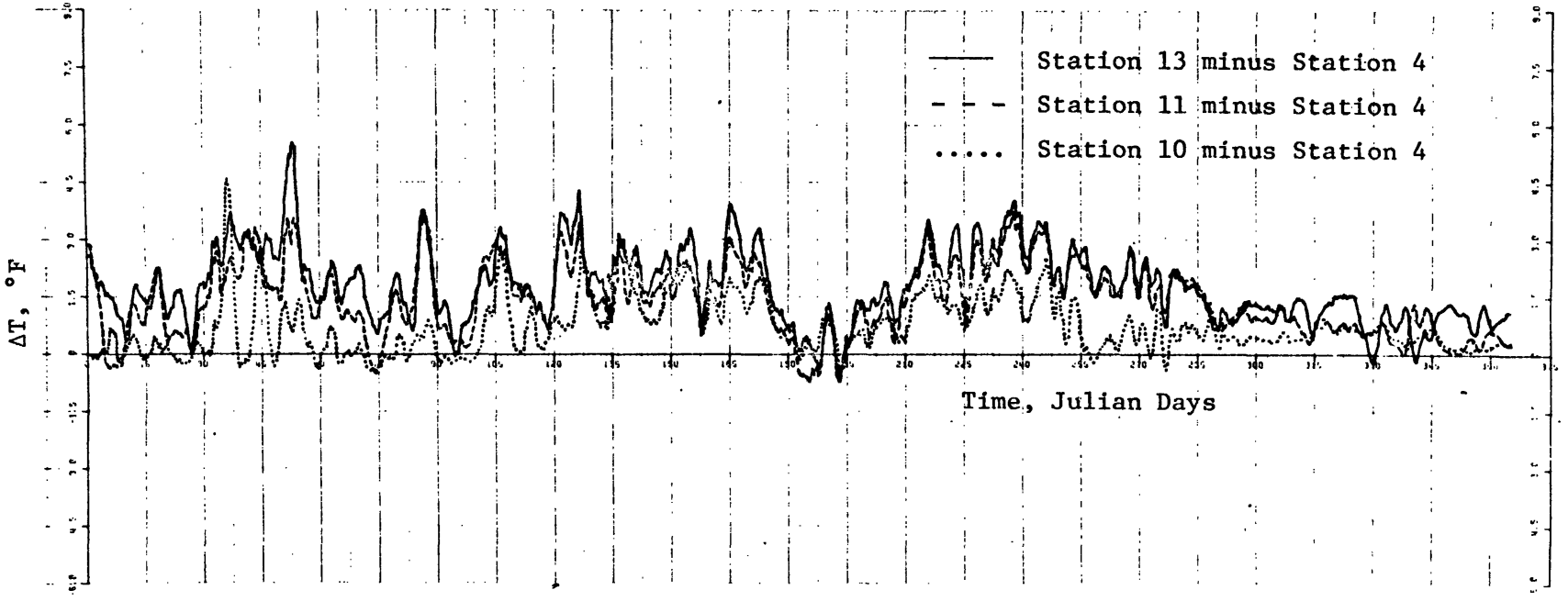

Figure 6.16 Individual Differences in Temperature for Various Downstream Stations and Upstream Station 4

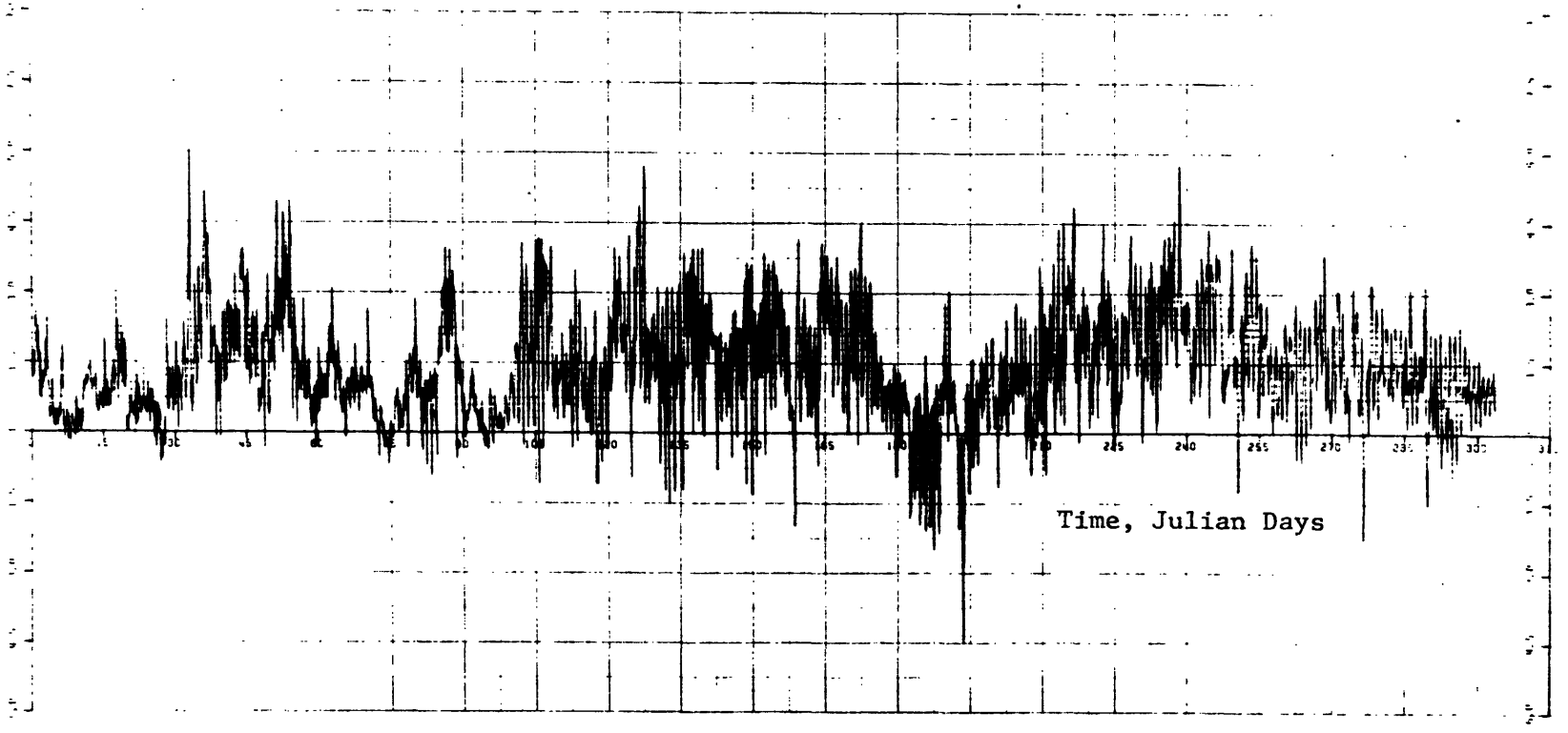

Figure 6.17 Measured Temperature Difference (ΔT), Spatially Averaged, Stations 10, 11 and 13 Minus Station 4

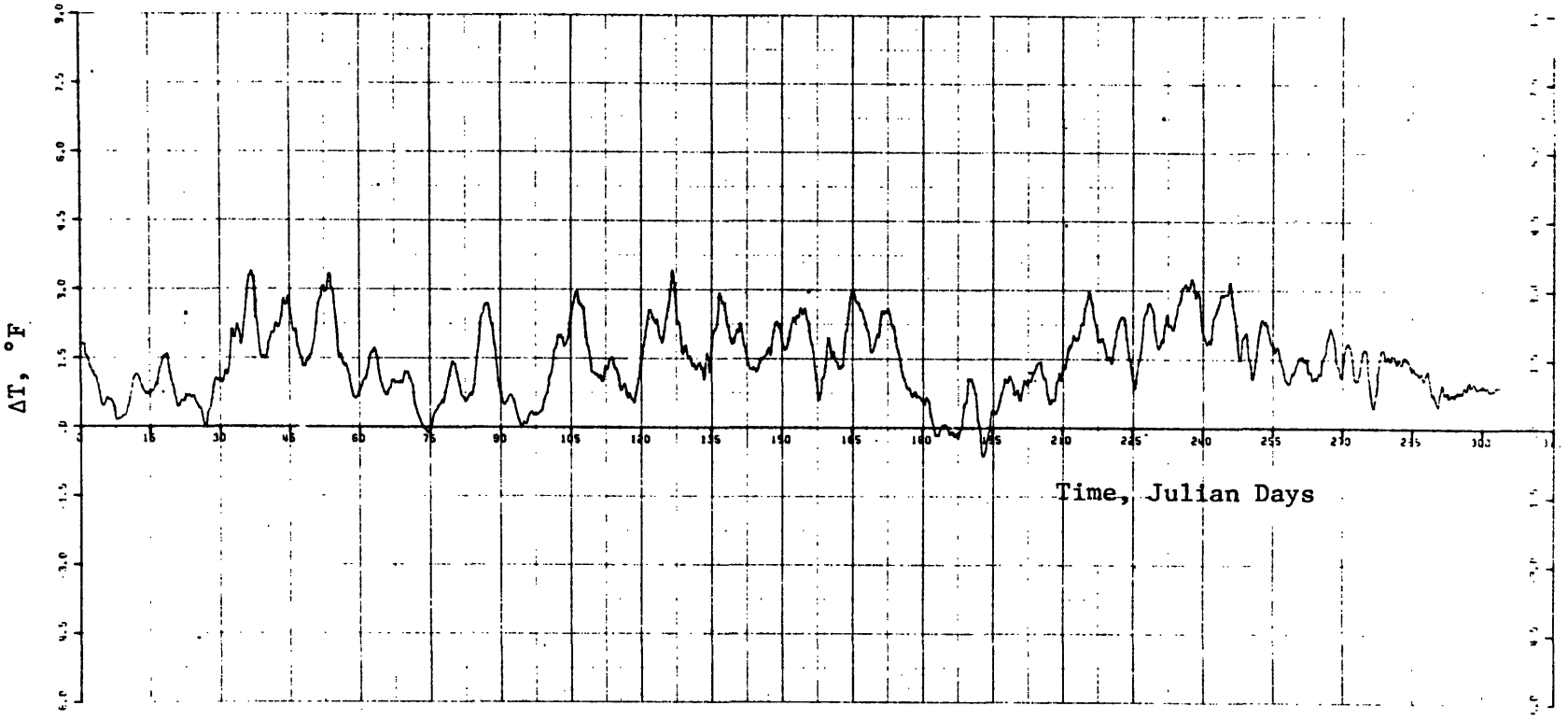

Figure 6.18 Four-Nine Hour Running Average of Measured Temperature Difference

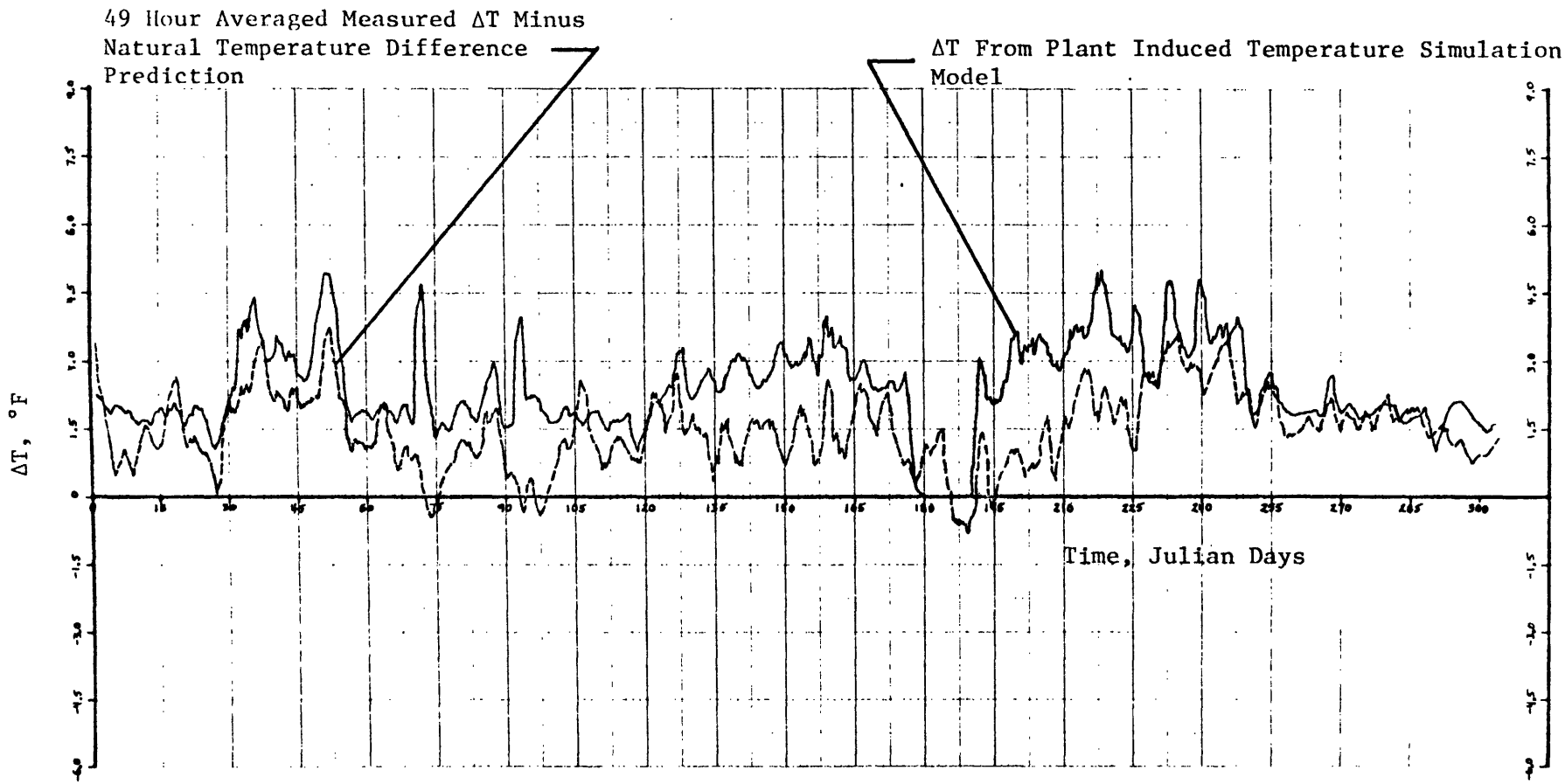

Figure 6.19 Comparison of Plant Induced Temperature Rise Prediction with Averaged Measured ΔT Minus Natural Temperature Difference Prediction

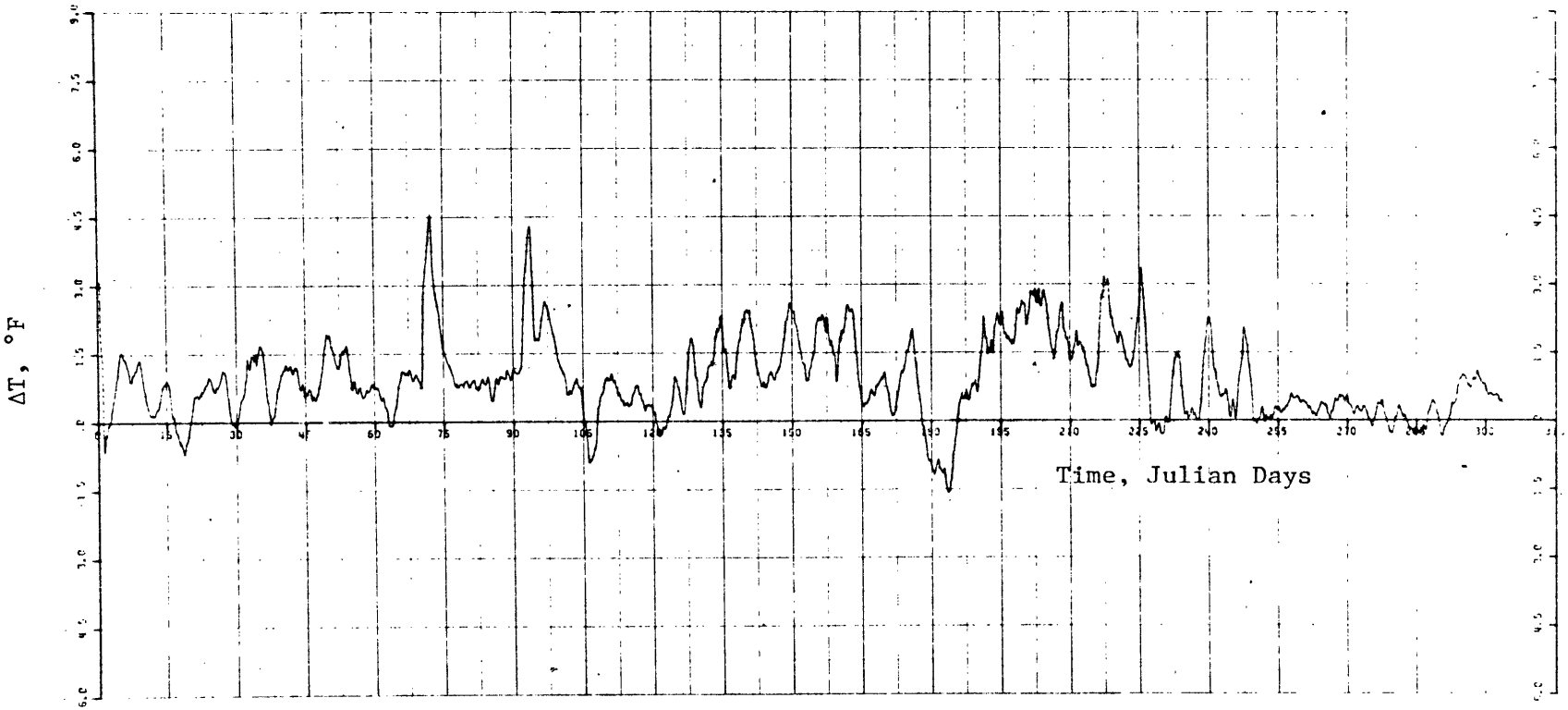

Figure 6.20 Residual Series After Subtraction of Measured ΔT Minus Natural Temperature Difference Prediction From Plant Induced Temperature Rise Prediction

influenced by warmer water resulting from plant operation or natural solar heating causing the measured temperature difference to be small. The influence of natural or artificial heat at station 4 may also be the cause of the overestimation of upstream-downstream temperature differences.

REFERENCES

Almquist, Charles W., "A Simple Model for the Calculation of Traverse Mixing in Rivers with Application to the Watts Bar Nuclear Plant," TVA Division of Water Management, Water Systems Development Branch, Report No. 9-2012, Norris, Tennessee, March, 1977.

Atomic Energy Commission, Browns Ferry Nuclear Plant Units 1,2,3 - Environmental Statement, July, 1971.

Freudberg, S.A., "Modeling of Natural River Temperature Fluctuations," S.M. Thesis, M.I.T., September, 1977.

Harleman, D. R. F., Hall, L., and Curtis, T. G., "Thermal Diffusion of Condenser Water in a River During Steady and Unsteady Flows with Application to the T.V.A. Browns Ferry Nuclear Power Plant," M.I.T. Ralph M. Parsons Laboratory for Water Resources and Hydrodynamics, Technical Report No. 111, Sept., 1968.

Ryan, Patrick J., and Harleman, Donald R. F., "An Analytical and Experimental Study of Transient Cooling Pond Behavior," M.I.T. Parsons Laboratory for Water Resources and Hydrodynamics, Technical Report No. 161, January, 1973.

Tennessee Valley Authority, "Monitoring of Water Temperatures in Wheeler Reservoir to Determine Compliance of Browns Ferry Nuclear Plant with Water Temperature Standards," TVA Division of Water Control Planning, Browns Ferry Nuclear Plant Advance Report No. 21, Norris, Tennessee, May, 1974.

APPENDIX A

EQUATIONS TO COMPUTE NET HEAT FLUX

The basic equation used is:

$$\phi_n = \phi_r - \left\{ 4 \times 10^{-8} (T_s + 460)^4 + f(w_2) \left[(e_s - e_a) + 0.255 (T_s - T_a) \right] \right\} \quad \text{(A-1)}$$

where ϕ_n = net heat flux, BTU/ft^2-day

ϕ_r = net solar plus atmospheric flux, BTU/ft^2-day

T_s = water surface temperature, °F

T_a = ambient air temperature, °F

e_s = saturated vapor pressure (mm Hg) at the temperature of the water surface given by:

$$e_s = -2.4875 + 0.2907T_s - 0.00445T_s^2 + 0.0000663T_s^3$$

e_a = vapor pressure of ambient air, mm Hg, given by:

$$e_a = \left(\frac{RH}{100}\right) \times (-2.4875 + 0.2907T_a - 0.00445T_a^2 + 0.0000663T_a^3)$$

where RH = relative humidity in %

$f(W_2)$ is a wind function based on a virtual temperature difference and the wind speed at 2 meters, W_2, (in miles per hour) above the water surface given by either:

$$f(w_2) = 22.4 (\Delta\theta_v)^{1/3} + 14w_2 \quad \text{(A-2)}$$

$$f(w_2) = 14w_2 \quad \text{(A-3)}$$

The choice of A-2 or A-3 depends on :

$$\Delta\theta_v = T_{sv} - T_{av}$$

where $T_{sv} = (T_s + 460)/(1 - 0.378\ e_s/p)$

$T_{av} = (T_a + 460)/(1 - 0.378\ e_a/p)$

p = ambient air pressure, mm Hg

If $\Delta\theta_v < 0.0024W_2^3$, use A-3

Else use A-2

Work reported in this document was sponsored by the Department of Energy under contract No. EY-76-S-02-4114.A001. This report was prepared as an account or work sponsored by the United States Government. Neither the United States nor the United States Department of Energy, nor any of their employees, makes any warranty, express or implied, or assumes any legal liability or responsibility for the accuracy, completeness, or usefulness of any information, apparatus, product or process disclosed or represents that its use would not infringe privately owned rights.